Investigation of E-cadherin dynamics in Cancer Cell Adhesion and Metastasis

Zahra Erami Rud-Majani

This thesis is submitted to the University of Glasgow towards the

Degree of Doctor of Philosophy

The Beatson Institute for Cancer Research

College of Medical, Veterinary & Life Sciences

University of Glasgow

April 2014

Abstract:

E-cadherin is a cell adhesion protein required for epithelial tissue integrity. In many cancer cells mis-regulation of E-cadherin adhesions causes increased progression and invasion of cancer. Alteration in E-cadherin dynamics could therefore serve as an early molecular biomarker of metastasis. In this project, I used E-cadherin FRAP to asses real time dynamics of cadherin junctions in a pancreatic cancer mice model of in a variety of micro-environments. My data showed that p53 mutation drives metastasis through mobilizing E-cadherin in junctions. Also, I used FRAP as a pharmaco-dynamic marker to assess the effect of an anti-invasive drug (dasatinib) in pancreatic tumours in vivo. Moreover, my E-cadherin FRAP data along with cross-linking experiments and disruption of E-cadherin interactions by mutation provided a comprehensive framework for understanding E-cadherin dynamics at cell-cell. Here, I have identified four distinct populations of E-cadherin within regions of cell-cell contact and characterized the interactions governing their mobility using FRAP. These pancreatic cancer cells had the immobile fraction (Fi) of E-cadherin-GFP comprised adhesive and non-adhesive populations. The remaining mobile fraction (Fm) also comprised of non-adhesive and adhesive populations, one population moves at the rate of pure diffusion, and therefore represents free E-cadherin monomers. The other population moves more slowly, and represents E-cadherin monomers turning over within immobile complexes. Inclusion of E-cadherin into either adhesive population requires cis-, trans-, and actin interactions. The signaling pathways in cells dramatically affect the fractions of these cadherin components. I showed that understanding the dynamics of these four populations of E-cadherins could be used to design or interpretation of future pharmacological and genetic experiments to probe the function of E-cadherin in development, disease progression, and response to therapy.

Table of Contents:

List of Figures:

List of tables:

Acknowledgment:

Author's declaration:

I declare that this thesis represents my own work except where acknowledge to others. No part of this work has been submitted for consideration as part of any other degree.

Abbreviations:

AJC	Apical Junctional Complex
BM	Basement Membrane
BRCA2	Breast Cancer 2, Early Onset Protein
CBD	Catenin Binding Domain
CDM	Cell Derived Matrix
cre	Cre Recombinase
ECM	Extracellular Matrix
EMT	Epithelial Mesenchymal Transition
Fi	Immobile Fraction
Fm	Mobile Fraction
FRAP	Fluorescence Recovery After Photobleaching
GFP	Green Fluorescent Protein
GFP-f	GFP With Farnesylation Signal From C-Ha- Ras
JMD	Juxta-Membrane Domain
KRAS	Kirsten Rat Sarcoma Viral Oncogene Homolog
LEF	Lymphoid Enhancer Factor (Transcription Factor)
MMPs	Matrix Metallo-Proteinases
OT	Optical Tweezers
PanIN	Pancreatic Intraepithelial Neoplasm
PDAC	Pancreatic Ductal Adenocarcinoma
ROI	Region Of Interest
SPT	Single Particle Tracking
Ras	Rat Sarcoma Viral Oncogene Homolog
RTK	Receptor Tyrosine Kinases
T1/2	Half Time Of Recovery
TCF	T-Lymphocytes Enhancer Factor (Transcription Factor)
TGF-β	Tranforming Growth Factor-Beta
VEGF	Vascular Endothelial Growth Factor
VH3	Vinculin Homology Domain 3

1. Introduction

1.1. Understanding cancer cell metastasis.

1.1.1. Cancer

Each year 10.9 million people are diagnosed with cancer globally and 7.5 million die from it (Jemal 2011). Therefore, Cancer is a key global health and economic issue. Cancer is an extremely complex disease. Each organ can have diverse tumour types which originated from different cell types. Moreover, each tumour includes various cell clones, where each clone evolves by different set of random mutations in their genome (Nowell 1976).

It has been observed pathologically in several cancer types, that invasive cancer cells evolve from normal cells in multiple steps of premalignant lesions. Each step reflects different genetic mutations (Thiery 2002, Foulds 1954). These genetic alterations vary from single point mutations to large chromosomal deletions which affects many genes. Therefore, there is cascade of random genetic alteration which transforms normal calls to cancer cells. Genomic instability in cancer cells generates genetic diversity that leads to acquisition of biological capabilities during cancer progression. These "hallmarks of cancer" include sustaining proliferative signalling, evading growth suppression, resisting cell death, enabling replicative immortality, inducing angiogenesis, reprogramming of energy metabolism, escaping immune system inhibition and activating invasion and metastasis (Hanahan 2011). Also, it's not only the cancer cells that acquire physiological changes, but also other cell types in a tumour site create a specific "tumour microenvironment" which exceedingly affects progression of cancer (Figure 1.1) (Hanahan 2011). In early steps of tumour formation, hypoxia occurs which favours the selection of cells with up-regulated glycolysis and resistance to acidosis in tumours. This adaptation in cells reduces their sensitivity to extracellular acidosis and resistance to acid-mediated apoptosis through mutations in p53 or other pro-apoptotic pathways. This resistance to apoptosis and cell cycle checkpoints and defective DNA repair mechanisms dramatically increase genomic instability in hypoxic cells. This genetic instability accelerates the genetic alterations which will give the cancer cell a new growth advantage, and leads to transformation of normal cells to cancer (Gillies 2007).
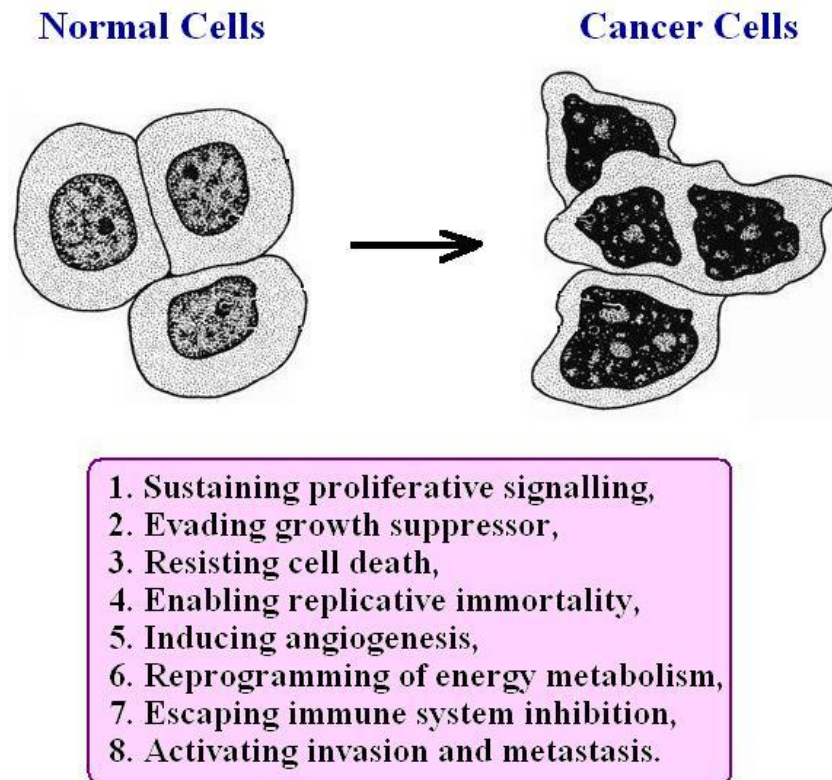
Figure 1. 1. Genomic instability in cancer cells let them evolve different biological capabilities. (adapted from Hanahan 2011)

1.1.2. A hallmark of epithelial cancer is loss of cell polarity.

The majority of human cancers are carcinomas derived from epithelial tissues. Carcinomas represent about 85% of cancers (Jemal 2011). Based on histological features of the tumour, carcinoma can be divided in to several subtypes. More common types are Squamous cell carcinoma (flat, surface covering cells called squamous cells) and Adenocarcinoma (of glandular cells).

Epithelial tissues cover the external and internal surfaces of the body and have many characteristic functions or structures. In all epithelial tissues retaining the integrity of the architecture is essential for proper function. Commonly, epithelial cells are polarized and their plasma membrane is divided into apical and baso-lateral domains. The apical-basal polarisation is crucial for maintaining cell-cell adhesion, communication, transport and permeability through epithelial layer (Dow 2007).

Loss of epithelial characteristics of tissue and the appearance of more mesenchymal-like cells is one of the important hallmarks of evolving invasive tumours. Studies in Drosophila melanogaster have shown there are several tumour-suppressor genes

involved in establishing and maintaining a correct apical-basal polarity, suggesting that a link exists between disruption of epithelial polarity and the control of cell proliferation (Wodartz 2007, Bilder 2000, Humbert 2003).

The tumour suppressive function of polarity complexes has been extensively studied in Drosophila. Many studies showed that proteins that maintain polarity in human epithelia are also cellular targets of human oncogenes, and several tumour suppressors have been shown to regulate polarity pathways. However, there are not strong evidences that loss of polarity is directly causing tumorigenesis (Royer 2011). In epithelial cells apical-basal polarity proteins hinder progression of cancer through two mechanisms. First is control of asymmetric cell division, which affects regulation of stem cell numbers and the differentiation of daughter cells. Therefore, disruption of asymmetric cell division of epithelial stem cells disrupts cells differentiation. Consequently, disrupting the asymmetric cell division could promote formation of tumours (Royer 2011).

Moreover, baso-lateral polarity in epithelial cells also regulates formation of AJC (Apical Junctional Complex). Adherens and tight junctions form AJC adhesion complexes which hinder invasion and metastasis in epithelial cells. In several human cancers, components of Adherens and tight junctions are mutated. Loss of E-cadherin, which is a key component of adherens junctions, in later stages of tumourigenesis is one of the essential steps of epithelial mesenchymal transition (EMT). This transition strongly enhances cancer metastasis.

1.1.3. Pancreatic cancer

Pancreatic ductal adenocarcinoma (PDAC) has an extremely poor prognosis. It has one of the highest fatality rates of all cancers. While it forms only 2.5% of occurrence of cancer, pancreatic cancer is responsible for 6% of cancer related death (Anderson 2006). 80% of patients die in the first year after the time of diagnosis of tumour because the disease is already advanced and the tumours are metastatic and surgically unresectable (Jemal 2011). Because of this high failure rate for therapies it is very important to have a better understanding of this cancer, to develop more effective strategies and discover better targets for new drugs. One approach is to study mouse models of PDAC. In this section, first the genetic alterations in

pancreatic cancer are described; then the mouse model of pancreatic cancer which is used in this study is introduced.

1.1.3.1. Genetic background

PDAC occurs from pre-invasive lesions called pancreatic intraepithelial neoplasms (PanINs). PanINs are microscopic papillary or flat, noninvasive epithelial lesions that are usually in the smaller (<5 mm) pancreatic ducts. The progression of cancer from low-grade PanIN, then to high-grade, and to invasive carcinoma is associated with the accumulation of mutations in several oncogene and tumor suppressor genes.
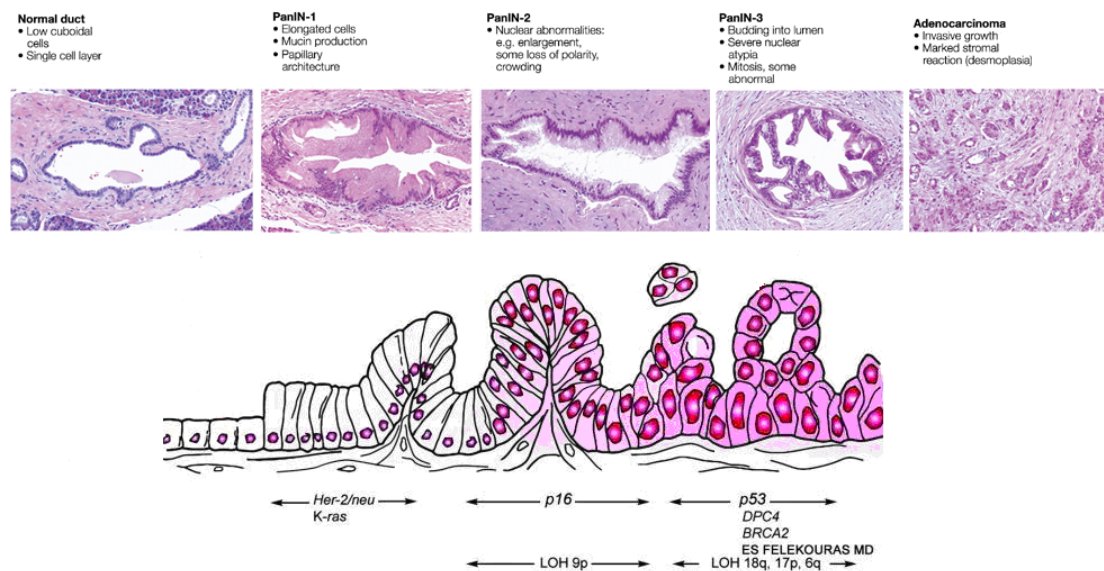
Figure 1.2. PDAC develops from PanINs. From left to right, progression of ductal adenocarcinoma from normal epithelium to low-grade PanIns, to high-grade PanIN, to invasive carcinoma. Accumulation of several genetic mutations drives the progression of the disease. In early stage mutation in the oncogene KRAS is happens in 90% of PanIns. In later stages the most important mutations happens in the tumor suppressors CDKN2, TP53, SMAD4/DPC4 and BRCA2. (adapted from Bardeesy 2002 and Hezel 2006)

Activating point mutations in the KRAS oncogene are the most important genetic alteration in pancreatic cancers. In 90% of pancreatic tumours KRAS is mutated. This mutation happens early and plays an important role for formation of human PanINs (Almoguera 1998). Inactivation of cell cycle inhibitor p16 (CDKN2/INK4A locus) happens in similar frequencies and leads to progression of early PanIns to high grade PanIns. Moreover, TP53 tumor suppressor is mutated in 50-75% of pancreatic

cancers (Scarpa 1993). Most of these mutations are mis-sense mutations which often result in accumulation of mutant p53 protein. Around 80% 0f genetic alterations in TP53 in cancer are mis-sence mutations not deletion. This suggests the gain-of-function or dominant-negative properties of the mutant p53 are more important than loss of its expression in cancer progression. Mutated p53 could provide tumor cell growth advantages. Commonly mutant p53 have a dominant–negative effect to disrupt wild-type p53 function mostly by forming mixed tetramers that are unable to bind to DNA. Moreover, many mutant p53 isoforms could bind and inactivate the p53-related tumour suppressor proteins p63 and p73 (Weisz 2007).

In addition, in 55% of pancreatic tumors SMAD4 is mutated. BRCA2 mutations are also reported in 10% of sporadic pancreatic cancers and around 19% of familial cases (Hruban 2000).

Despite of all advances in understanding the genetic alteration in progression of pancreatic cancer, there has been no significant improvement in the survival rate of clinical treatments. Therefore, it is important to investigate the molecular mechanisms of PDAC progression to find new targets for therapy.

1.1.3.2. P53 is a tumour suppressor protein.

P53 is a member of the p53-family of transcription factors. It is a well known tumour suppressor protein and has a vital role in DNA repair and induction of apoptosis and senescence in damaged cells. P53 is activated by cellular stresses like DNA damage or over activated oncogenes and then p53 activates its transcription targets that can mediate a various responses, as an example cell cycle arrest, DNA repair, anti-angiogenic effects, senescence and apoptosis. Therefore, p53 prevents the accumulation of malignant cells.

Mostly tumour cells escape the control of p53 by either disruption upstream and downstream of p53, or by mutating p53 itself. Loss of p53 inhibits senescence and apoptosis in tumor cells; moreover it disrupts cell-cycle checkpoints. These cells continue to divide regardless of their DNA damage and it results in accumulation of additional mutations in their DNA.

1.1.3.2.1. Mutant p53 drives invasion in many cancer models.

In vivo studies in mouse cancer models showed that expression of mutant p53 is not similar to p53 loss, and that mutant p53 can acquire new functions to drive cell migration, invasion, and metastasis. However, p53 null mouse tumors do not metastasize frequently (Muller 2011, Attardi 1999). Commonly *Tp53* mutations are mis-sense mutations in exons 4–9, which encode the DNA binding domain of the protein. 30 % of these mutations are in six residues: R175, G245, R248, R249, R273, and R282. Genetically engineered mouse with expression of R175H or R273H mutant p53 have increased occurrence of highly metastatic tumours (Lang 2004, Olive 2004).

These mutant proteins are found at high concentrations in tumor cells relative to WT p53 (Yu 2012) and are not able to bind to DNA and their function as tumour suppressor is disrupted. However, these mutations give mutant p53 a gain of function property to drive invasion in tumour cells (Muller 2011). These mutations disrupt DNA binding function therefore this gain of function in promoting metastasis is due to non-transcriptional functions of p53. It is possible that mutant p53 exert their effects by modifying the function of other proteins, including the p53 family members p63 and p73 (Muller 2011). Mutant p53 drives cell invasion by inhibiting p63 function. One suggested mechanism is that that oncogenic RAS and TGF-β cooperate with mutant p53 to form a mutant p53/p63 complex that serves to inhibit the function of p63 and targets two metastasis suppressors: Sharp-1 and cyclin G2 (Adorno 2009)

1.1.3.2. Mouse PDAC model

Here I used a mouse model of Pancreatic ductal adenocarcinoma, in which activation of oncogene KRAS by G12D mutation initiates the formation of PanINs similar to the three stages found in human pancreatic cancer. Occasionally, mice with PanINs spontaneously developed locally invasive adenocarcinoma (Morton 2010). However, KRAS^{G12D} mutation is only an initiating step in PDAC and p53 mutation is also needed for formation of the malignant tumours. Therefore, to develop a pancreatic mouse model endogenous expression of KRAS^{G12D} and p53^{R172H} were targeted to the mouse pancreas by expression of cre recombinase under control of the Pdx1

pancreatic progenitor cell gene promoter. This results in the formation of pre-invasive PanIN neoplasms that later developed into invasive and metastatic pancreatic tumours. In this model tumours appear in mice after around 10 weeks (Hingorani 2005).

In addition, mice with KRAS mutation and a loss of P53 (instead of mutant p53) developed PanINs and tumours later. However, these tumours were not invasive. In this model, mice with KRAS^{G12D} and p53^{R172H} genetic background develop metastatic pancreatic cancer; in contrast, mice that have a KRAS^{G12D} and Trp53 null allele, despite similar kinetics of primary tumor formation, rarely develop metastasis. In other words, activation of KRAS and loss of p53 function is sufficient for development of tumours. However, these tumours are not invasive. Only tumours with expression of mutant p53 developed metastasis.

The p53 gain of function mutant accumulates in PDAC cells and promotes metastasis. Two PDAC cell lines were derived from these primary pancreatic tumours of KPC mouse model. PDAC cell with loss of p53 expression (here called PDAC^{fl}) are not invasive in an in vitro invasion assay. On the other hand, PDAC cells from tumours with p53^{R172H} mutation (here called PDAC^{R172H}) are more progressive and highly invasive than PDAC^{fl} cells (Morton 2010). Moreover, expression of human mutant p53 protein (p53^{R175H}) in PDAC^{fl} cells is sufficient to activate cell invasion in PDAC^{fl} cells. PDAC^{fl} and PDAC^{R172H} are cell lines derived from mice tumours, consequently these cells could have gained random mutations in their genome during progression of tumours. However, PDAC^{fl} cells transfected with p53^{R175H} mutant (here called PDAC^{fl}R175H) are genetically similar to PDAC^{fl} cell line and the only difference is mutant p53 mutation.

Therefore, in this model one genetic alteration (loss of p53 in contrast to mutation) determines either the tumors are metastatic or not. This gives us a very good tool to study metastasis; as this model recapitulates the human disease in many features, it provides an excellent system to study the disease progression and metastasis in vitro and in vivo.

1.1.4. Metastasis

Tumours can be classified depending on the degree of aggressiveness. Those which grow at the site of origin without invading the surrounding tissue are classed as

benign tumours, whereas tumours which have infiltrated the nearby tissue or spread to distant organs are classified as malignant. (Weinberg 2007).

Metastasis is the process by which cancer cells leave the primary tumour and spread to distant sites where they proliferate and form secondary tumour mass. These secondary tumours are the most usual cause of death in cancer. Because of this significance in clinical outcome of cancer treatment, it is important to have a complete understanding of the mechanisms of metastasis.

1.1.4.1. Metastasis is a complex process.

Metastasis is a complex and multi-step process, comprising many steps such as alterations in cell adhesion, acquisition of invasive abilities, entry into the circulation and transfer to distant tissues, followed by exit into new sites and ultimately colonisation of secondary tumour (figure 1.3).

Metastasis can happen in many different forms, but commonly there are several critical steps in metastasis from primary tumour to formation of secondary mass (reviewed in Brooks 2010). Initially, before metastasis starts new bloods vessels should develop at the primary tumour (angiogenesis). Next step is dissociation of tumour cells from the primary tumour mass. Down-regulation of cell-cell adhesion in tumour cells through Epithelial-to-mesenchymal transition (EMT) is a key process in this step. However, sometimes collective migration enables cancer cells to migrate in a group, without going through EMT transition and loosing cell-cell adhesions.

Then the detached mesenchymal cells invade and migrate through the basement membrane and extracellular matrix (ECM) surrounding the tumour epithelium, and subsequently invade through the basement membrane of the endothelium of local blood vessels. Basement membrane is a dense meshwork of glycoproteins and proteoglycans (such as type IV collagen and laminins). For penetrating through this structure matrix-degrading proteases such as matrix metallo-proteinases (MMPs) are needed. Normal epithelial cells have very low activity of these proteases. However, during the progression of cancer, malignant cells down-regulate matrix protease inhibitors. At the same time cells upgrade integrin expression to mediate adhesion to the ECM. The process of penetration of tumour cells into tumour-associated vasculature is referred to as intravasation. Following intravasation, tumour cells travel to secondary sites through the circulatory system (Brooks 2010).
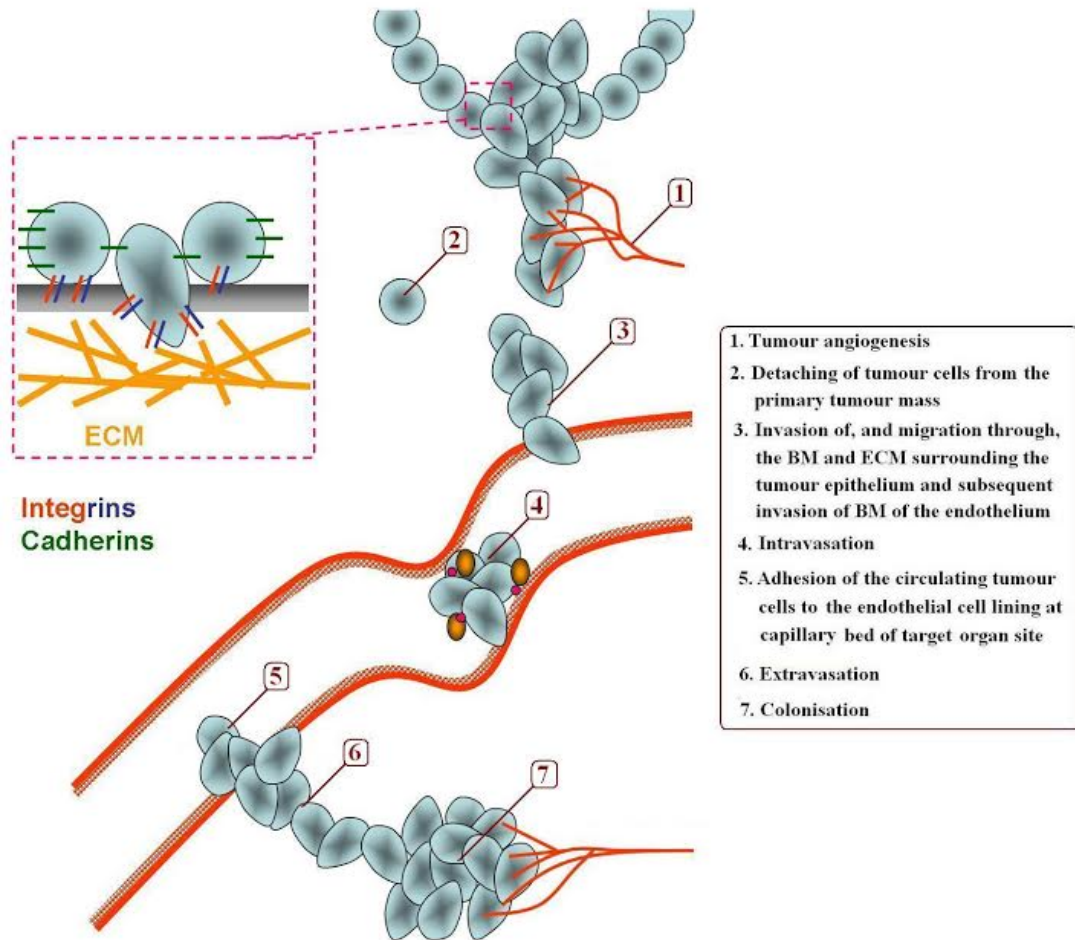
Figure 1.3. There are several critical steps in metastasis from primary tumour to formation of secondary mass. 1. Tumour angiogenesis, 2. EMT and dissociation of tumour cells from the primary tumour mass, 3. Invasion through the BM and ECM surrounding the tumour epithelium and subsequent invasion through the BM of the endothelium, 4. Intravasation of the tumour cells prior to hematogeneous dissemination, 5. Adhesion of the circulating tumour cells to the endothelial cell lining at the capillary bed of the target organ site, 6. Extravasation (invasion of the tumour cells through the endothelium, surrounding BM and target organ tissue), 7. Colonization (the development of secondary tumour foci at the target organ site.) (adapted from Alexander 2011)

After arriving at a secondary site, tumour cells form cell-cell adhesion to endothelial cells through selectins, integrins and members of the immunoglobulin superfamily. Then tumour cells invade through the endothelial cell layer (extravasation) (Brooks 2010).

Vascular endothelial growth factor (VEGF) released by metastatic cells is thought to increase vascular permeability by activating Src family kinases in the endothelial cells and thus disturbing endothelial cell- cell junctions. This in turn can facilitate extravasation of circulating tumour cells and metastatic spread (Criscuoli 2005).

In the final stage of metastasis, cancer cells colonize as a secondary tumour at the target organ tissue.

1.1.5. Dissociation of cell-cell adhesions is necessary for tumour cells metastasis

As explained above, loss of cell-cell adhesion in primary tumour cells is critical for their dissociation and permits their initial dissemination. As the cancer progress, epithelial cells lose their cell-cell adhesion and polarity and undergo a developmental switch to highly invasive cells having a fibroblastoid or mesenchymal phenotype. This process is called epithelial-mesenchymal transition (EMT).

1.1.5.1. EMT (Epithelial-to-mesenchymal transition)

Strong cell-cell adhesion is necessary for maintaining epithelial structure. This includes tight junctions, cadherin based adherens junctions, gap junctions and desmosomes. Epithelial cells also have cell-ECM (extracellular matrix) adhesions mediated by integrins. During EMT cell-cell and cell-ECM adhesions are disrupted to release the epithelial cells from the surrounding tissue. These cells loose their polarity. Then by reorganization of the actin cytoskeleton these cells gain the ability to migrate. Moreover, expression of matrix degrading metallo-proteinases (MMPs) allows the cells to invade through a three-dimensional ECM.

Several oncogenic signalling pathways induce the process of EMT such as TGF-β, Receptor Tyrosine Kinases (RTK)/Ras signalling, integrin, Wnt/ β-catenin, Notch, Hedgehog and NF-kB-dependent pathways (Polyak 2009).

However, 'EMT' includes a broad range of changes in epithelial plasticity. In each cellular model, activation of different pathways, or their combinations, can induce or repress the progression of the epithelial cell's gene expression program towards a mesenchymal phenotype to a varying extent, which creates some subtypes of EMT.
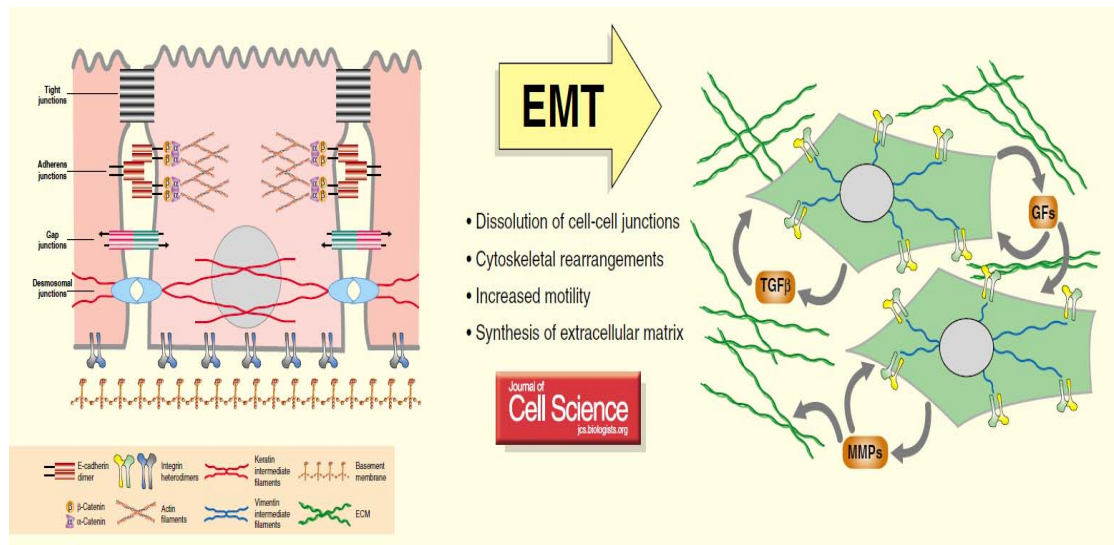
Figure 1.4. The epithelial-mesenchymal transition (EMT). The epithelial-mesenchymal transition is associated with disruption of cell-cell adhesions adhesion, down-regulation of E-cadherin expression and increased cell mobility. (Radisky 2005)

1.1.5.2. De-regulation of E-cadherin mediated cell-cell adhesion is a key step during the EMT process:

Inhibition of E-cadherin function is a critical step driving EMT (Yap 1998-2, Birchmeier 1994). During tumor progression, E-cadherin expression can be down-regulated or it can be functionally inactivated by different mechanisms. These mechanisms include post-translational control, somatic mutations, and down-regulation of gene expression through promoter hypermethylation, histone deacetylation and transcriptional repression (Huber 2005). Several EMT-inducing developmental regulators, for example snail and slug, repress E-cadherin transcription. Up-regulation of Snail correlates with metastasis and poor prognosis, whereas silencing of Snail can reduce tumour growth and invasiveness. Slug has also been shown to induce EMT and metastasis through the repression of E-cadherin (Huber 2005).

However, it is not always necessary for epithelial cells to undergo EMT and loose E-cadherin expression to migrate. Cells which have retained their epithelial phenotype, keep their adhesions while they migrate as a group. This is called collective migration. One of examples of collective migration happens during wound healing. As the barrier function of the epithelial sheet is very essential, cells migrate while

cell-cell adhesions are kept. Signalling pathways (particularly the pathways which play a role in EMT) and interactions with ECM have been shown to effect either the cell migrate collectively or individually (Rorth 2009). It has been shown that cadherin adhesions play a role in collective migration probably through coordinating traction forces (Li 2012). Moreover, catenins which associate with cadherins for formation of adhesions are important for regulation of actin reorganization (Hidalgo 2010, Rorth 2009).

In summary, the ability of tumour cells to invade and metastasize requires modulation of cell-cell adhesions. Disruption of cell-cell adhesion occurs not just through down-regulation of E-cadherin levels, but also through mis-regulation of its dynamics and interaction with other proteins (Gumbiner 2000). Moreover, EMT is not an all or nothing process and in different cells represents various level of mesenchymal phenotype. Therefore although loss of E-cadherin is on of key mark of EMT process, not all the cells undergoing EMT completely lose E-cadherin expression (Hollestelle 2013). Many forms of metastatic cancers retain E-cadherin expression (Gaida 2012). This suggests that, alteration in E-cadherin dynamics can be used as a marker for metastasis. In the next section, the basis of cadherin mediated cell-cell adhesion in epithelial cells is introduced.

1. 2. Cadherin mediated cell-cell adhesions

1.2.1. Adherens junction structure

The ability of cells to stick to one another is a crucial property in the evolution of multi-cellular organisms. Classical cadherins are a family of trans-membrane proteins that mediate cell-cell adhesion at adherens junctions. In epithelial cells, intercellular adhesion is primarily mediated by E-cadherin, one of members of this family; other members of this family include N-, P, and R-cadherin (Takeichi 1990). Cadherin adhesions play a critical function for cell recognition and cell sorting during development and morphogenesis (Takeichi 1995). Retaining of adherent junctions is crucial for maintaining tissue homeostasis, resistance to mechanical force and sheer stress. Moreover, cell-cell adhesions are important for regulation of permeability and barrier function of epithelia (Niessen 2007).

Cadherin molecules cluster by homophilic interaction of their extracellular domains with molecules from neighbouring cells (trans) and on the same cell (cis). In addition, the intracellular domain of cadherins interacts with two catenin proteins, p120 and β-catenin. Interaction of β-catenin with α-catenin and other actin binding protein mediate anchoring cadherin complexes to actin cytoskeleton (Aberle1994). Moreover, formation of acto-myosin and contractile ring stabilizes cadherin adhesions at mature cell-cell junctions (Vasioukhin 2000).

Adherens junctions show huge variation in their morphology and protein composition. As an example cadherin forms two different adherens junctions in epithelial cells: apical adherens junctions (zonulae adhaerentes) and spot-like adherens junctions (puncta adhaerentia) present on the lateral cell surfaces. The apical adherens junctions typically associate with a group of cytosolic actin-binding proteins such as vinculin, VASP, and EPLIN. Also, another trans-membrane adhesion receptor, nectin, interacts with cadherins (Meng 2009). In contrast, spot-like lateral junctions do not exhibit association with these proteins. These lateral junctions still interact with actin and this interaction results in their basal to apical flow in many cells (Kametani 2007).

Although homophilic interaction of cadherin and their anchoring to actin is the basis of formation of adherens junctions the details of these structures are not completely understood. Moreover, adherens junctions are very dynamic structures which continuously loose and gain cadherin. The assembly and disassembly are regulated by diverse intracellular signalling pathways which affect endocytosis, recycling and degradation of cadherins.
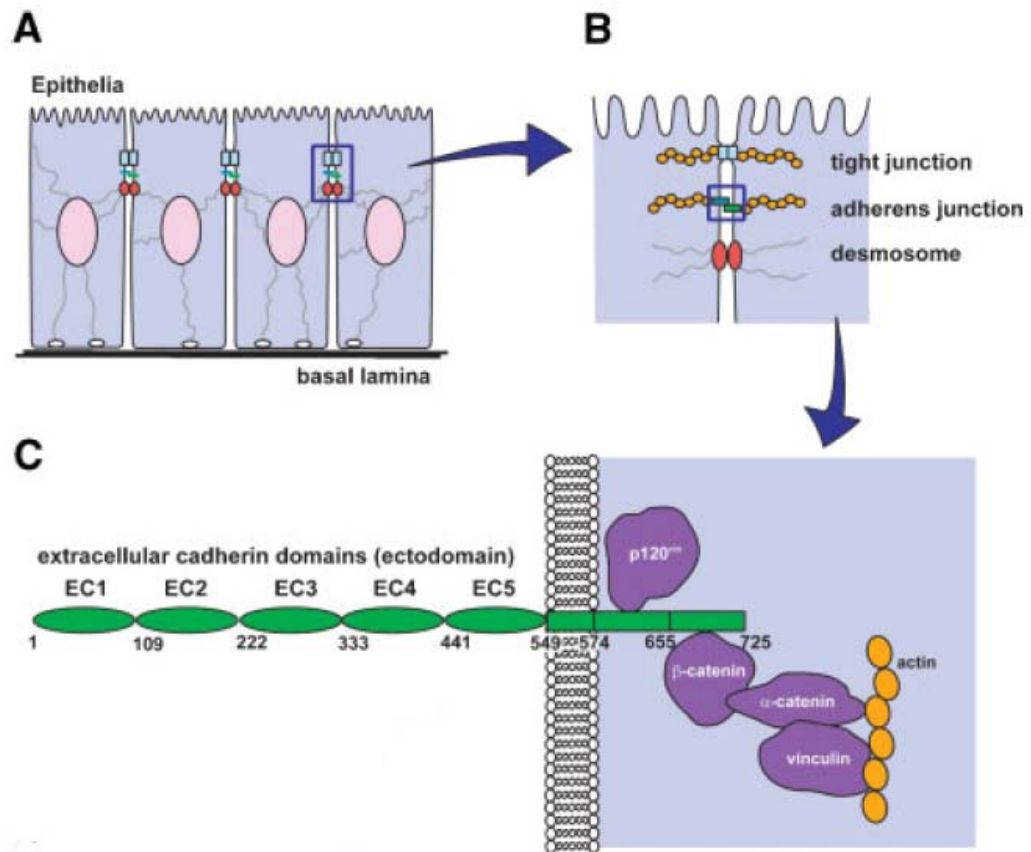
Figure 1.5. Adherens junction structure: A) Cell-cell adhesion in epithelial cells is a crucial and tightly controlled process. The integrity of cell-cell contacts is essential for the regulation of paracellular permeability. B) In polarized epithelial cells Adherens Junctions, Tight Junctions and desmosomes are responsible for the establishment of contacts between neighbouring cells. The Adherens Junctions consist of Cadherin and Nectin cell adhesion molecules. C) E-Cadherin is a Ca^{2+} dependent cell adhesion molecule at Adherens Junctions. The intracellular domain of cadherin is anchored to the Actin cytoskeleton through interaction with α-catenin and β-catenin (Gooding 2004).

1.2.2. Cadherin-catenin complex is the main component of adherens junctions

1.2.2.1. E-cadherin molecular structure

After protein translation, a 130 amino acid prodomain is cleaved from the E-cadherin protein precursor. The mature 728 residue mature protein includes an extracellular domain, a short trans-membrane domain and a 150 amino acid cytoplasmic domain (figure 1.6) (Nagafuchi 1987). E-cadherin structure is highly conserved during evolution. The 550 residue extracellular domain has 5 repeated domains (EC1-EC5). These EC repeats are present in all cadherin superfamily proteins. Binding of Ca2+ to each EC domain is required for the correct conformational organization of the

cadherin extracellular domain (Pokutta 1994). The cytoplasmic domain of E-cadherin is divided into two domains, the juxtamembrane domain (JMD) that binds p120-catenin (Yap 1998-1), and the β-catenin binding domain (CBD) (Aberle 1994).
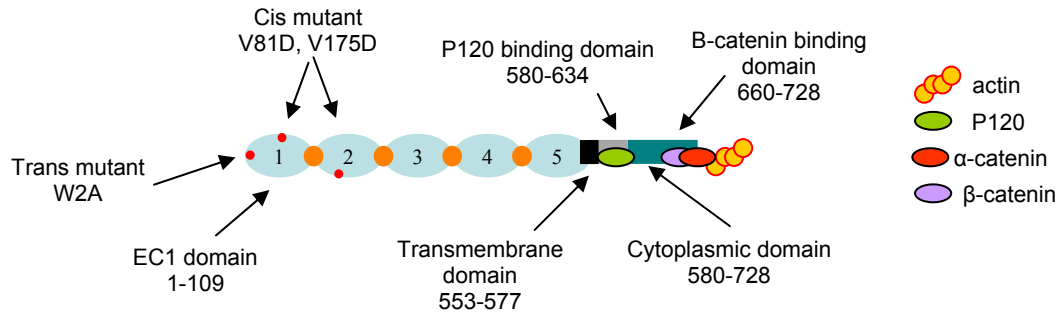
Figure1.6. E-cadherin molecular structure and domains map.

1.2.3. Extracellular domain of cadherin forms several homo-dimer interactions

In this section the structure of extracellular domain of E-cadherin is described. The E-cadherin forms three interactions through extra-cellular domain: strand-swapping, X-dimerization and cis interaction.

1.2.3.1. Strand swapping

The basis of cadherin adhesions is the homophilic interactions of extracellular domain of E-cadherin molecules. Nose et al, showed that expression of a chimera consisting of P-cadherin with EC1 domain of E-cadherin, results in aggregation of the cells with E-cadherin expressing cells (Nose 1990). The interaction of EC1 domains was confirmed by more advanced technique as electron microscopy (Tomschy 1996, Zhang 2009, Kim 2011). Point mutations provided more information about the adhesive site of cadherins (Kitagawa 2000; Laur 2002).

Moreover, cross-linking experiments confirmed that exchange of N-terminal β strands of the EC1 domains (A*) between two cadherin molecules is the basis of strand-swap cadherin dimerization. The amino-terminal amino group stabilizes strand swapping by the salt bridge with Glu89 so proteolytic removal of the prodomain is essential for strand swapping as (Troyanovsky 2003, Troyanovsky 2005, Zhang 2009, Kim 2011). The A*-A strand contacts the B and G strands of the

seven β strands that form the core of the EC1 domain. The N-terminal segment of the A*-A strand (A*), which include 1 to 3 residue (including Trp2) forms hydrogen bonds with the B strand. Trp2 is inserted in the core of the EC1 domain where it forms several hydrophobic bonds. In monomeric cadherin all of these contacts are intra-molecular. To form strand swap dimers, the A* strand is swapped to another molecule EC1 domain and forms exactly the same contacts (Fig. 1.4) Although strand swap dimerization is the stronger than other cadherin–cadherin interactions, it is still a weak interaction, and corresponds to a KD of 100mM in solution (9–11kT) (Vendome 2011). However, force measurements using atomic force microscopy showed that single cadherins adhere strongly, indicating that cadherin trans dimers are stabilized in the presence of a pulling force (Rakshit 2012).

Cross-linking experiments on E-cadherins in cell culture showed that strand swapping can form both lateral (cis) and adhesive (trans) dimers on the cell surface (Chitaev 1998, Harrison 2005). Although, there is no evidence that these strand-swapped cis dimers are necessary for adhesion.
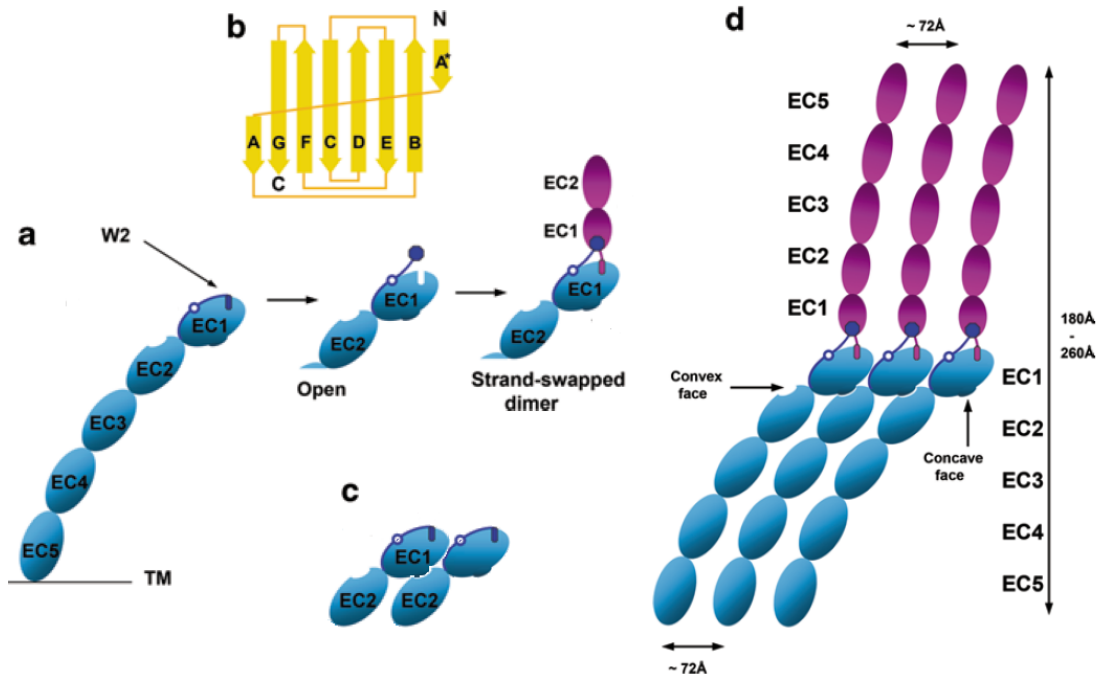
Figure.1.7. Cadherin molecules cluster through strand swap (trans) and cis interactions. a) The strand swap dimerization forms by insertion of the Trp2 residue (dark blue rectangle) from A* strand (dark blue line) in to a pocket in the core of EC1 domain which can be intra- or inter-molecular. The intra molecule interaction (or closed form) need to be opened in order that the free A* strand form a strand swap interaction with another molecule. b) The topology diagram of the seven β strands in EC1 domain of E-cadherin. The first strand is divided into two strands A* and A. in strand swapping A* forms a contact with strand B. c) Schematic representation of cis interaction between two cadherin molecules in same membrane. Only EC1 and EC2 domains are shown. d) Formation of cis and trans dimers clusters cadherin molecules. Cadherin molecules shown with blue colour formed a linear array by cis interactions (periodicity 72 Å). Each molecule in this array forms a strand swap trans interaction with a cadherin molecule on opposite cell membrane (shown in magenta), which belong to the cell. Each of the magneta molecules is part of its own cis array of cadherin molecules which are placed in a 90˚ angle compared to neighbouring membrane cis arrays. (Harris 2012)

1.2.3.2. X dimerization

Nagar et al showed that two-domain (EC1-EC2) E-cadherin fragments can form dimers through another interaction other than strand-swapping (Nagar 1996). The dimerized molecules contact each other via calcium binding interfaces which forms an X shaped structure of two molecules. Initially, the X dimerization was considered as a crystal-packing artefact (Häussinger 2004). However, recently more data revealed that this dimerization happens in cells and it probably plays a role in

formation of cadherin clusters (Hong 2011). X dimers are very unstable (KD~ 900 μM) and are transient intermediate to formation of strand-swap dimers. Disruption of X dimer formation by point mutations leaded to a very slow kinetics of strand-swap formation. Moreover, dissociation of strand swapped dimers is extremely slow in this mutant (Harrison 2010; Vunnam 2001). However, expression of the X dimer mutant in A431 cells showed that although adhesions formed in these cells have slower association/dissociation rates, they still form functional junctions (Hong 2011).

1.2.3.3. Cis dimerization clusters cadherin molecule.

In order to form clusters from individual strand swapped trans dimers probably some form of cis interactions is necessary. Computational analyses also suggested that cadherin clusters are formed by formation of cis interactions between linear arrays of trans dimers (Wu 2011). Cis interactions are too weak to be detected in solution, and not able to produce clusters in the absence of trans interactions. Therefore, biochemical approaches including cross-linking or co-immunoprecipitation assays are not able to show formation of such cis interactions (Harrison 2011, Shapiro 1995, Troyanovsky 2007, reviewed in De Beco 2012). However, Structural analysis in the E-, N-, and C-cadherin crystals showed formation of cis interaction was (Harrison 2011). These cis dimers are formed by a nonsymmetrical interaction between the concave face of the EC1 domain of one molecule and the convex face of the EC2 domain of the other cadherin. The EC1 cis binding surface is oriented 90˚ compared to the trans dimer interface. Each cadherin molecule can form two cis interaction in its concave EC1 and convex EC2 surfaces simultaneously. This could arrange the cis dimerized molecules into a linear array.

Each cadherin molecule in the linear array of cis interacting molecules could also form a trans strand swapped dimer with a cadherin located at the opposing plasma membrane. Moreover, since trans dimerized cadherin molecules are in a 90˚ angle to each other, the cis dimerized linear arrays of cadherin molecules on the opposing surfaces crisscross at right angles (Figure. 1.7).

Disruption of cis interaction by (V81D/L175D) mutations, which destroy the hydrophobic core of the cis interface, inhibits cadherin junction assembly. These cadherin mutants can form trans interactions, and they are localize into cell–cell contacts. However, the junctions formed by the cis mutant cadherin adhesions are

transient and unstable (Harrison 2011). Although the cis interactions are too weak to be detected in solution, in cooperation with trans interactions, they produce stable and ordered adhesive clusters of E-cadherins (Harrison 2011).

1.2.4. E-cadherin Cytoplasmic interactions

E-cadherin molecule has a 150 residue cytoplasmic domain which interacts with actin through catenins and several other cytoplasmic proteins. The cytoplasmic domain is divided into the juxtamembrane domain (JMD) that binds p120-catenin and the β-catenin binding domain (CBD).

1.2.4.1. β-Catenin

β-catenin protein sequence include 13 repeats of the 42 amino acids armadillo domain that form a triple α-helix structure (Huber 1997) (Fig 1.8.). The armadillo domains in β-catenin interact with the CBD domain of cadherin. Association of β-catenin to E-cadherin is necessary for transportation of the E-cadherins from the endoplasmic reticulum to cell membrane and E-cadherin is normally found to be linked to β-catenin in plasma membranes (Chen 1999).

The N-terminal domain of β-catenin interacts with α-catenin and this interaction anchors cadherin to the actin cytoskeleton. How this interaction with β- and α-catenin clusters the cadherins and stabilize the junctions will be explained in next section. In addition, β-catenin plays an important role in cell signalling pathways. Free β-catenin moves from the cytoplasm to nucleus and where it binds to the TCF/LEF transcription factor to activate the expression of numerous genes involved in proliferation and development (Klaus 2008).

1.2.4.2. Interaction of E-cadherin to actin cytoskeleton through β-catenin and α-catenin

The cytoplasmic domain of E-cadherin binds to the central armadillo domain of β-catenin (Aberle 1994) and β-catenin binds to α-catenin by interaction of their N-terminal domains (Rimm 1995) (figure 1.8). Figure 1.5.C shows the commonly accepted model for cadherin-catenin-actin interaction based on these data. E-

cadherin binds to β-catenin. β-catenin attaches to α-catenin. α–catenin simultaneously interacts with β-catenin and actin. Also vinculin homology domain 3 (VH3) of α-catenin binds to vinculin which is an actin binding protein. These interactions anchor the E-cadherin clusters to actin cytoskeleton (Rimm 1995).
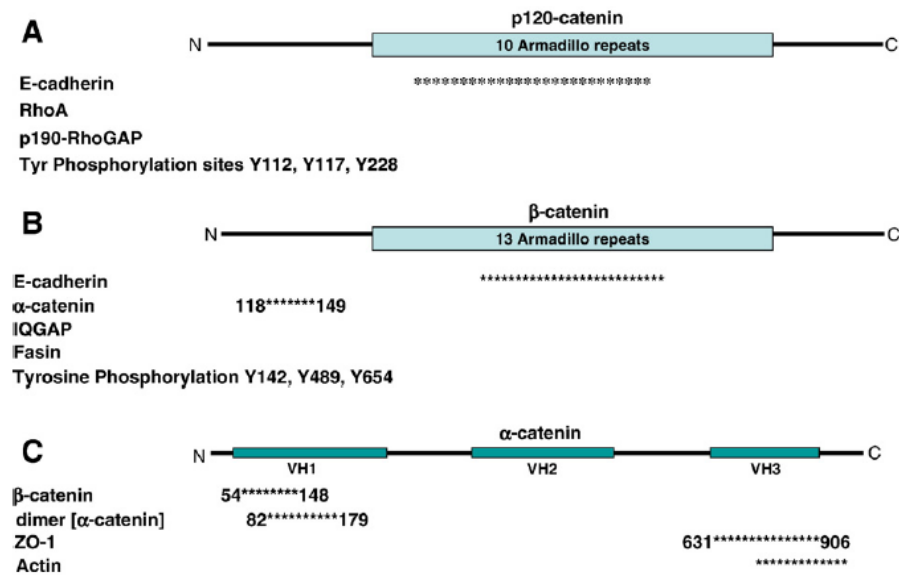
Fig. 1.8. Catenin molecules structures and interactions. (A) p120-catenin, (B) β-catenin, and (C) α-catenin. All three proteins interact with additional proteins which regulate actin cytoskeleton. (Hartsock 2008)

Recently the Nelson group proposed a different model: α-catenin does not bind to actin and β-catenin simultaneously (Yamada 2005). α-catenin exists in either a monomeric or homo-dimeric state. The β-catenin binding domain and the α-catenin homodimerization domains overlap within amino acids 57–143 on α-catenin (Pokutta 2000), consequently, only monomeric α-catenin binds β-catenin. On the other hand, homo-dimeric α-catenin binds actin filaments but not β-catenin (Yamada 2005). Although experimental data showed there is a direct physical link between E-cadherin\β-catenin complex and actin, this may happen through interaction of other actin binding proteins with α-catenin (Desai 2013). Based on these data a new model proposed that α-catenin shifts between inactive homodimer formats bound to actin and active monomeric form which binds to β-catenin-E-cadherin complex (Yamada 2005).

In vitro studies showed that dimerization of α-catenin occurs at a 10-fold higher concentration than that of the monomeric pool of α-catenin in the cytoplasm of

epithelial cells, which suggests that α-catenin must be locally concentrated prior to dimerization probably through binding to the cadherin–catenin complex during cell–cell adhesion. In other words, binding to the cadherin–catenin complexes at cell-cell junctions increases the local concentration of α-catenin. This local increase in α-catenin concentration drives α-catenin dimerization. α-catenin dimers would locally inhibit Arp2/3 and thereby the formation of branching networks of actin filaments characteristic of lamellipodia of migrating cells. At the same time, α-catenin dimers bind to and bundle existing actin filaments, resulting in actin reorganization from branched to bundled arrays (Drees 2005).
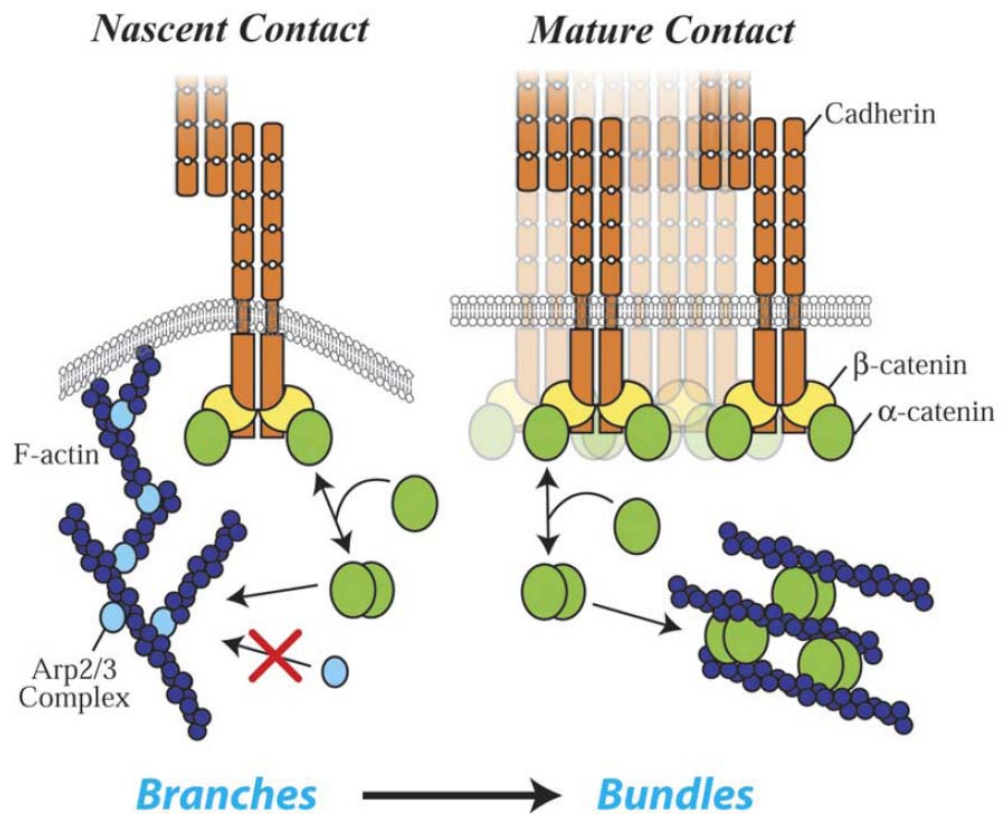
Figure 1.9. Regulation of actin organization by α-catenin. Clustering of cadherins at the growing newly formed contacts leads to accumulation of cadherin-catenin complexes. This leads to a high local concentration of α-catenin as it dissociates from these complexes. α-catenin is present both in monomer or homodimer forms. The α-catenin dimers compete with Arp2/3 complex for binding to actin filaments. This interaction disrupts Arp2/3-mediated actin assembly that drives lamellipodia formation (the monomeric form are less potent to interact with actin than dimers). α-catenin also bundles actin filaments, which may contribute to the reorganization of actin in the mature contact. (Drees 2005).

1.2.4.2.1. Phosphorylation of β-catenin regulates its function

The interaction of E-cadherin with β-catenin is regulated by phosphorylation (Daugherty 2007). CKII and GSK-3β kinases phosphorylate E-cadherin at three serine residues in the cytoplasmic domain (S684, S686, S692). This phosphorylation enables formation of additional interactions which leads to increase in affinity of E-cadherin and β-catenin interaction. Expression of E-cadherin molecules with mutations in putative CKII sites reduced cell-cell adhesion (Lickert 2000).

In the other hand, phosphorylation of β-catenin at Y489 by Abl kinase and at Y654 by Src or EGF receptor weakens interaction with cadherin (Lilien 2002, Rhee 2002, Roura 1999, Hoschuetzky 1994). The structural basis for these effects is due to β-catenin Y654 forming a hydrogen bond with E-cadherin Asp 665, which stabilizes the interaction of the cadherin region 2 helix with the last two armadillo repeats of β-catenin (Huber 2001); phosphorylation of Y654 would prevent this interaction thereby eliminating binding of this region of cadherin and sharply reducing the cadherin/β-catenin affinity. Moreover, Tyrosine phosphorylation of β-catenin at Y142 by Fer kinase weakens its binding to α-catenin (Piedra 2003). Phosphorylation at this site increases β-catenin cytoplasmic level and its interaction with BCL9-2, a transcription factor involved in inducing EMT (Brembeck 2004).

1.2.4.3. P120 catenin

P120 was originally discovered as a Src substrate and later classified as a cadherin binding catenin through its sequence homology to the armadillo domain of β-catenin (Reynolds 1992). P120 has a short C-ter and N-ter domain and in the middle there is an ARM domain which consists of 10 arm repeats. These Arm repeats interact with cadherin juxtamembrane domain (Anastasiadis 2000). The juxtamembrane domain is a 22 AA domain proximal to membrane with a conserved sequence motif, YDEEGGGEED. Mutation in this motif results in unbinding of p120 catenin from the E-cadherin complex (Yap 1998-1). Expressing this mutant in E-cadherin null cells is not adequate to restore cell-cell adhesion in contrast to wild type E-cadheirn (Thoreson 2000, Yap 1998-1). P120 binding inhibits endocytosis and subsequent degradation of E-cadherin molecules. Therefore, loss of this interaction destabilizes cadherin localization to the membrane and inhibits its accumulation at cell borders

(Yap 1998-2). This indicates that, interaction of cadherin with P120 is essential for maintaining cadherin adhesion.

In the E-cadherin sequence there is an YYY sequence adjacent to the p120 binding motif which can be phosphorylated by kinases such as Src. Phosphorylation of this site disrupts p120 and E-cadherin interaction which leads to interaction of E-cadherin with Hakai, a c-Cbl-like E3 ubiquitin-ligase. Ubiquitination of E-cadherin results in endocytosis and degradation of E-cadherin molecules (Fujita 2002). Although interaction with p120 enhanced cell-cell adhesion, it is not necessary for localization of E-cadherin to cell-cell junctions. However, disruption of this interaction increases the turnover of E-cadherins on cell-cell junctions (Davis 2003). P120 binding to E-cadherin stabilizes E-cadherins junctions. It has been shown that loss of p120 function disrupts cell-cell adhesions and increases tumor progression and invasion in cancer (Conacci-Sorrell 2002).

1.2.4.4. Additional proteins in adherens junctions regulate the dynamics of cadherin-catenin-actin interactions.

While the basic structure of cadherin junctions are cadherin-catenin complexes, many other proteins are reported to be present at adherens junction. For example formin, an actin nucleator binds α-catenin (Kobielak 2004) and cortactin, an actin assembly regulator, binds p120-catenin (Boguslavsky 2007). Both formin and cortactin are necessary for the formation of linear actin bundles in mature cell–cell contacts (Kobielak 2004, Helwani 2004).

In addition, Ankrin-G binds to the juxtamembrane domain of E-cadherin and recruits beta-2 spectrin to E-cadherin/β-catenin complexes providing another potential link to the actin cytoskeleton (Kizhatil 2007).

Moreover, the interaction of other transmembrane receptors has been shown to affect cadherin junctions. The interaction of cadherin with γ-secretase, a large transmembrane proteolytic enzyme, excludes cadherin molecules from junction assembly. A complex consisting of E-cadherin and γ-secretase is mostly present within the extrajunctional lateral surface of epithelial cells (Kiss 2008). Another transmembrane protein which has been studied extensively is nectin. Nectin is a cell-cell adhesion molecule which can form adhesion clusters in the absence of cadherins. When cadherin is present, nectin colocalizes with cadherin molecules. Although this

interaction is not necessary for formation of individual junctions, several studies showed disruption of this interaction can affect cadherin junction organization (Takahashi 1999, Takai 2008).

1.2.5. Cadherin clusters to mature junctions.

Linear arrays of Cis and trans interacting E-cadherin molecules are the basis of clustering of E-cadherin molecules at cell-cell junctions. Tailless mutant cadherin molecules are still able to form these clusters (Troyanovsky 2006, Hong 2010). Upon formation of cell-cell contacts, cadherin molecules cluster at contact sites and the newly formed puncta junctions spread laterally to form mature linear junctions (Adams 1998, Vaezi 2002). In cell culture, the initial junction contact is established by lamellipodia of two adjacent cells (in MDCK cells McNeill 1993, Adams 1998-2) or the initial contact is made by crosssing filopodia that form transient point contacts, which then zipper into a continuous mature junction (in mouse keratinocytes, Vasioukhin 2001). Also, catenin interactions are required for formation of mature junctions (Yap 1998-1). The catenin bindings are also responsible for regulation of actin cytoskeleton. When junctions start to expand laterally from initial contact point of two lamellipodia, the branched organization of actin cytoskeleton in the lamellipodia reorganizes to bundles of actin fibers in mature junctions. Formation of acto-myosin contractility is necessary for organization of actin cytoskeleton and maturation of junctions (Cavey 2008, Vasioukhin 2000).

1.2.6. Adherens junctions continuously exchange cadherins.

Cadherin-mediated adherens junctions are not static structures. During development or wound healing cells require to dissociate from each other, to migrate or to form new junctions and dynamic structure of the junctions enables the cell to remodel adhesions in respond cell signalling. They are constantly remodelled to be able to respond to developmental growth, cell renewal, cell migration and wound healing. FRAP (fluorescence recovery after photobleaching) analysis of dynamics of fluorescent tagged cadherin molecules showed that junctions continuously exchange cadherins (E-cadherins FRAP experiment are explained in detail in section 1.4). It is commonly assumed the recovery of bleached molecules is duo to association and

dissociation of extrajunctional cadherin molecules from junctional complexes (Kusumi 1999, Serrels 2009). Some experiments show that dissociation of cadherins from junctions is an active process and ATP depletion decreases mobile cadherins at junctions (Troyanovsky 2006, Hong 2010). However, it is not clear that what the active mechanisms that remove cadherins from membranes are. One possible mechanism is that catenin interactions induce conformational changes needed for dissociation of cadherins. Also, endocytosis plays a role in physically removing cadherin from the membrane.

1.2.6.1. Endocytosis

Endocytosis is one of the mechanisms that direct remodelling of adherens junctions. It has been shown that regulation of E-cadherins endocytosis by signalling pathways during development, wound healing or cancer metastasis controls assembly, disassembly and stabilization of adherens junctions. (Gumbiner, 2000). Inhibition of clathrin mediated endocytosis (by 0.4 M sucrose in A431 cells (Troyanovsky et al. 2006; Hong et al. 2010) or by dynasore or MiTMAB, in MDCK cells (de Beco 2009)) is shown to stabilise cadherin at junctions

However, the process that unlocks cadherin and removes it from the junctions is more complex. For example, point mutations of cadherin endocytic motifs to inhibit endocytosis do not stop the release of cadherin from junctions in A431 cells (Hong 2010). Or the same inhibitors, dynasore and MiTMAB that blocked cadherin junctional turnover in MDCK cells produce little effect in MCF7 cells (de Beco 2009).

1.3. E-cadherin dynamics as marker for metastasis

1.3.1. E-cadherin dynamics are related to cell migration.

As mentioned before, de-regulation of E-cadherin junctions is a critical step during metastasis. Disruption of cell-cell adhesions happens not just through down-regulation of E-cadherin levels, but also through mis-regulation of its dynamics and interaction with other proteins (Gumbiner 2000). Many forms of metastatic cancer retain E-cadherin expression (Gaida 2012), and recent evidence supports the

hypothesis that mis-regulation of E-cadherin dynamics can also drive metastasis (Serrels 2009).

Consequently, alteration in E-cadherin dynamics could serve as an early molecular biomarker of metastasis. Serrels et al used photo-bleaching and photo-activation to quantify GFP-E-cadherin dynamics in vitro and in vivo. They showed that E-cadherin is mobilized in cell-cell junctions between migrating cells. Their in vitro experiments showed that E-cadherin mobility in cell-cell junctions is related to cell migration. Moreover, they measured E-cadherin dynamics in vivo in xenograft tumours and their data showed E-cadherin has significantly different dynamics in cells in the tumour 3D environment compared to cells in cell culture (Serrels 2009).

1.3.2. In vivo imaging is critical for investigating metastasis.

Metastasis is greatly affected by the cancer cell local micro-environment (niche) and its interaction with the extracellular matrix (ECM). Cancer de-regulates biochemical and biomechanical properties of the tumour ECM. For example, the tumour ECM changes stiffness which affects the interaction of cells with ECM and affect cell invasion (Pathak 2013). Moreover, the tumour micro-environment and interaction of tumour associated macrophages (TAMs) affects cell invasion. Therefore, cell migration and invasion show different patterns in vivo compared to in vitro situations. For example, cancer cells move more quickly in vivo than in vitro, by tracking along ECM fibres, and this could affect to predicting metastatic properties of cells (Condeelis 2003). In vivo studies are therefore required to completely understand the metastatic process.

The use of new in vivo imaging techniques has greatly enhanced our understanding of how this process occurs (reviewed in Nobis 2013). Initial in vivo imaging studies used cytoplasmic fluorescent proteins (for example GFP) to label whole cell and then the migration of these labelled cells was observed in vivo (Naumov 1999, Ito 2001).

Tracking of fluorescent labelled cell migration in tissues revealed several aspects of cancer cell metastasis such as "cell morphology changes, track cell movement and velocity, or gauge vector-based persistence over time or interactions with ECM" (Nobis 2013). These fluorescently-labelled cells were also used to study circulating tumour cells to analyse later stages of metastasis in colonization, extravasation or tumour dormancy. (Condeelis 2003)

Although it is important to understand cellular dynamics, we also want to understand protein dynamics within cells. One approach which has been widely used in the study of cell adhesion is a family of techniques known as FRAP including fluorescent recovery after photo-bleaching (FRAP) (this methods is explained in section 1.4.1), photo-activation or photo-switching.

Moreover, these techniques can be applied to study real-time disease in an in vivo setting (Timpson 2011, Lippincott-Schwartz 2003). The functional and physiological properties of surrounding tissue micro-environment significantly affect protein kinetics. Consequently, imaging disease processes in an in vivo setting is therefore critical to accurately understand disease aetiology and develop effective treatment strategies.

1.4. Studying dynamics of E-cadherin mediated cell-cell adhesion by FRAP

Here, I first introduce the FRAP technique and basis of data analysis, then explain in more detail FRAP of GFP-E-cadherin.

1.4.1. Fluorescence Recovery After Photobleaching: FRAP

Fluorescence Recovery After Photobleaching (FRAP) is commonly employed to study protein mobility in live cells. Initially this technique was used to measure the diffusion rate of lipophilic or hydrophilic fluorophores, like fluorescein, coupled to proteins and lipids especially in cellular membranes (for example Axelrod 1976). With the development of fluorescent protein technology and advanced confocal microscopy, FRAP has become widely used to study protein mobility in living cells. Green fluorescent protein (GFP) can be attached to virtually any protein of interest. GFP protein chimaeras provided excellent tools to understand the dynamics of many cellular proteins. FRAP can be used to quantify the mobility of proteins in the cytoplasm, nucleus, organelle lumens and membranes of living cells. In addition to the study of mobility and diffusion rates, FRAP has also been extensively utilized to address protein interactions (Reits 2001, Carrero 2003, Kimura 2004).

1.4.2. How FRAP is performed?

FRAP involves irreversibly bleaching fluorophores in a small region of a cell, then monitoring the recovery of fluorescence molecules into the bleached region as surrounding non-bleached molecules diffuse into bleached region over time while bleached molecules move out of region (Figure 1.10). FRAP analysis can be used to estimate kinetic parameters of a protein, including diffusion rate, mobile fraction, or binding/ dissociation rate from other proteins (Reits 2001, Sprague 2005).

Developing the FRAP technique on the laser-scanning confocal microscope has made this technique widely available. Confocal microscope obtain the image by scanning a focused laser beam across the specimen, then the emitted fluorescence is collected through a pinhole in front of light detector. The same laser beam in higher power can be utilized to irreversibly bleach the fluorescent molecules in the region of interest (ROI) (Lippincott 2003). Accurate analysis of FRAP data requires that the bleach event is much shorter than the recovery time, preferably as short as possible. In analysis of FRAP data the duration of the bleach time is assumed to be zero. However, in practice, it is satisfactory that bleach time is much smaller than the recovery time.

Moreover, the accurate quantification of the immobile fraction requires that the recovery must be monitored until a recovery plateau is achieved.

1.4.3. Analysis of FRAP data: Quantifying recovery curve by T1/2 and Fi

FRAP recovery curves can provide information about the mobility of a fluorescent protein in living cells. Two values are derived from a FRAP recovery curve: half time of recovery (T1/2) and immobile fraction (Fi%) (Figure 1.10. B).

(1) The "half time of recovery" (T1/2) is the time it takes for fluorescence intensity to return to half of its recovered value. The rate of fluorescence recovery provides a measure of how quickly fluorescent molecules move in and out of the bleached region. If motion is not due to active transport or directional flow, then this 'mobility' is determined, in part, by the rates of diffusion and transport for the fluorescent molecule through the cell membrane. Mobility can also be influenced by

binding interactions, which detain molecules that would otherwise diffuse freely (Reits 2001).

(2) The immobile fraction (Fi%) refers to the unrecovered fraction of fluorescence intensity in a FRAP recovery curve. The immobile fraction can be determined by comparing the fluorescence in the bleached region after full recovery (F_∞) with the fluorescence before bleaching (F_{t0}) and just after bleaching (F_B). The mobile fraction Fi is defined as: Fi% = $(F_\infty-F_B)/(F_i-F_{t0})\times100$

The rate of mobility of molecules could be affected by rate of association and dissociation of transient binding of fluorescently labelled proteins with other molecules or membranes. Membrane barriers and micro domains in the membrane can also affect the mobile fraction. These discontinuities can prevent, or temporarily restrict, the free diffusion of membrane molecules.
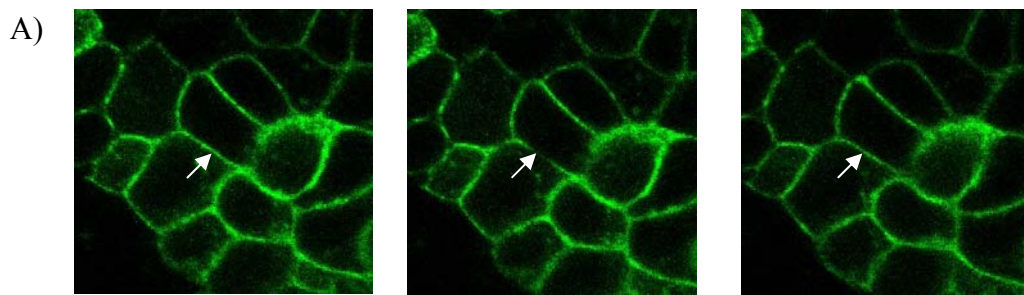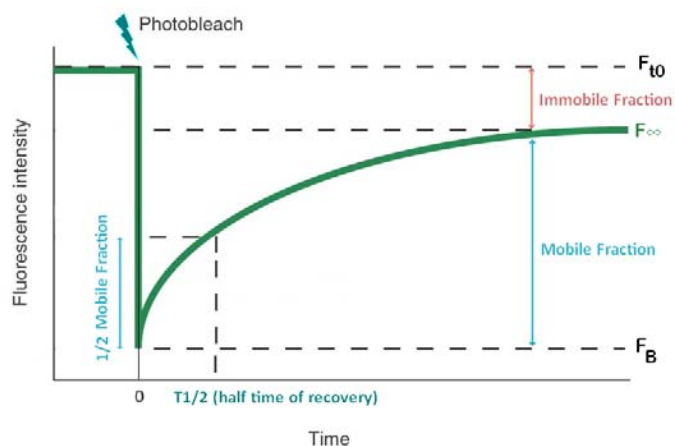
Figure 1.10. Schematic diagram of FRAP curve. (A) FRAP involves bleaching a small region of a cell with high laser power, then monitoring recovery of fluorescence molecules over time. (B) Two values are derived from a FRAP recovery curve. The "half time of recovery" (T1/2) is the time it takes for half of the affected molecules to recover. The immobile fraction (Fi%) refers to the unrecovered fraction of fluorescence intensity in a FRAP recovery curve .

1.4.4. Analysing FRAP recovery of free molecules without binding

Recovery which occurs in the absence of binding/dissociation, active transport or unidirectional flow, is due to Brownian motion. In this case, the mobility can be expressed as the diffusion coefficient D, which is related to the half time of recovery T1/2. Generally the two-dimensional diffusion equation described by Axelrod et al (Axelrod 1976) is used to calculate D:

$$T1/2 = \beta\omega^2/4D$$

Where ω is defined as the radius of the focused circular laser beam and β is a function of the degree of bleaching. This equation assumes unrestricted two-dimensional diffusion in a circular bleached area, with no recovery from above and below the focal plane. This is the case expected in the plasma membrane.

However, diffusion can be hindered by cellular structures, such as cytoskeleton networks, that trap the random movements of a freely diffusing molecule. These 'molecular sieving' effects, which depend on the molecular size, are more significant in cell membrane compared to cell cytoplasm (Edidin 1994, Saxton 1999).

1.4.4.1. Transmembrane proteins do not diffuse freely in the plasma membrane.

Diffusion coefficients measured for transmembrane proteins in the plasma membrane are generally much smaller than D (diffusion coefficient) calculated for transmembrane proteins in an artificial lipid bilayer. Several different factors affect the free diffusion of trasmembrane proteins. One is the presence of membrane microdomains with high viscosity such as lipid rafts. Big protein complexes also hinder free diffusion. Moreover, the cytoskeleton network underneath the plasma membrane acts as a fence which obstructs the lateral movement of molecules (Kusumi, 1996).

This process strongly affects the free diffusion of trans-membrane proteins. To understand the effect of molecular sieving on diffusion, more complicated models are required. More importantly, in the presence of hindered diffusion it is important to distinguish between the contribution of obstructed diffusion and the contribution

of protein binding to a FRAP recovery. To understand if a fluorescent molecule has interactions with other molecules or not (which will respectively retard its recovery), FRAP should be measured on an inert molecule of the same size as the GFP-fusion molecule. This will set the base line for free diffusion. When binding interactions are present, they retard FRAP recovery in relation to what would be observed for free diffusion of an inert molecule.

Analyzing FRAP recovery curves is more complicated when a molecule undergoes binding and dissociation from intracellular structures, or exists as a monomer and multimeric forms. In addition, the molecule movement might not be just diffusing but be affected by movement driven by molecular motors or membrane tension flow and endocytosis.

1.4.5. Analysing FRAP recovery in the presence of binding interactions

If the fluorescent molecules associate\dissociate from stationary complexes during FRAP, the interpretation of data is more complicated. In this case the recovery curve is slower, recovers partially (an immobile fraction presents) or may have several components with different slopes (as different association\dissociation reactions have different rates) (Sprague 2004, Sprague 2005)

To analyse these complicated FRAP recovery curves Kinetic modelling methods and computer simulations can be used. Initially biophysical parameters of the reaction like association\dissociation rates and diffusion constants are used to define a kinetic model. Then the model is simulated with a computer program to calculate different values to find the parameters that best fit the experimental data. Then the model can be tested against experimental data (Phair 2001).

However, to analyse a FRAP recovery curve in the presence of binding, the first step is to determine the relevant role of diffusion and binding to the recovery curve. FRAP recovery is either 'diffusion-uncoupled' or 'diffusion-coupled' depending on whether the diffusion time can be ignored relative to association rate or not (Figure 1.11) (reviewed in Sprague 2005). The time required for a freely diffusing molecule to move across the bleached region, is diffusion time. The association rate is the rate of binding multiplied by the concentration of available binding sites at equilibrium. The next section will describe how the relative magnitude of these two parameters creates two distinctive FRAP recovery regimes.
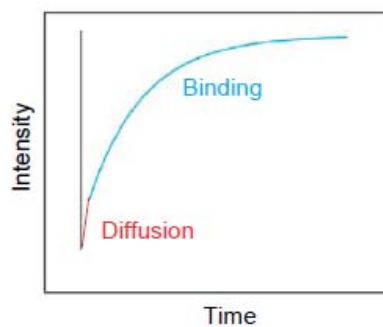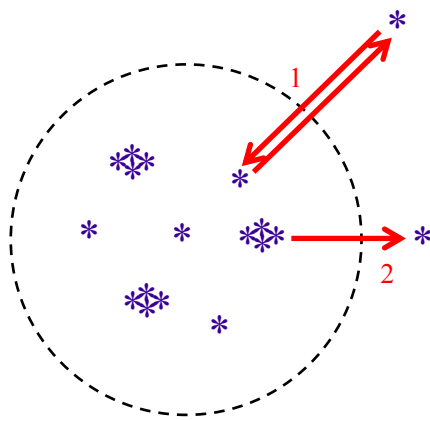
A) Diffusion Uncoupled Recovery   B) Diffusion Coupled Recovery
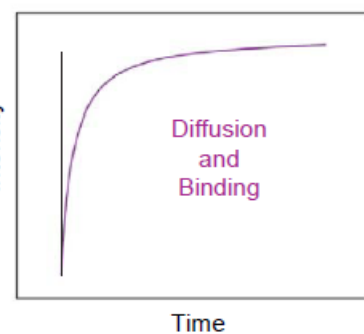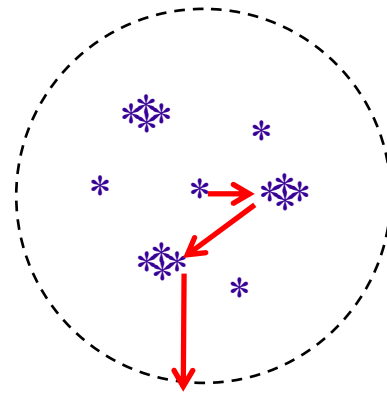
Figure 1.11. Diffusion coupled and diffusion uncoupled recovery. A) Diffusion-uncoupled FRAP. Initially free bleached proteins rapidly diffuse out of ROI. The bound bleached proteins which were bound to stationary complexes remain in the ROI. The dissociation\association of molecules from binding sites gradually releases the bleached molecules and they rapidly leave the ROI and Fluorescent molecules replace them in clusters. The diffusion-uncoupled FRAP recovery curve consists of two separable fragments: in the first part (in red) the recovery is fast and it is due to diffusion and in the second part (in blue) recovery is slower and it is because of binding\unbinding of fluorescent proteins from binding sites. B) Diffusion-coupled FRAP. The association of free molecules to binding sites is faster than the time for diffusion of free bleached molecules out of ROI. so the bleached molecules associate with another cluster before diffusing out of ROI. In a diffusion-coupled FRAP curve (purple) diffusion and dissociation happens at same time, so it cannot be separated into distinct segments (Sprague 2005).

1.4.5.1. Diffusion-uncoupled FRAP recoveries

If diffusion of fluorescent molecules in the ROI is much faster than association with binding sites, the recovery is diffusion uncoupled (Figure 1.11). This means that the recovery due to diffusion happens first, and is followed by dissociation of bleached molecules and binding of unbleached molecules. Consequently, the recovery curve can be separated in two phases. The first part is due to diffusion of free unbleached

molecules into the ROI and happens over timescale of few seconds. However, exchange at stationary binding sites is much slower. Therefore most of recovery curve reflects dissociation/binding rates rather than diffusion rates. So, longer recovery rate indicate that binding interactions are stronger, and in this case the recovery rate can be used to determine binding strength. Moreover, if the recovery curve can be separated into components with different slopes, it indicates that the fluorescent molecules engage in different binding reactions. The location of each shoulder in curve gives an estimate of fraction of molecules in each binding reaction (Phair 2004).

In many studies, particularly in the case of a single binding reaction, the FRAP recovery curve has been used to calculate k_{on} and k_{off} of binding reactions. The recovery is modelled by a single component exponential curve (Sprague 2004)

$F(t) = 1 - C_{eq} \exp(-k_{off} t)$

Once this equation has been fit to a FRAP recovery curve K_{off} can be calculated. In this equation C_{eq} is the equilibrium concentration of the bound state. In the case that concentration of binding sites can be assumed constant, C_{eq} can be used to calculate k_{on} of the binding reaction (Sprague 2004).

1.4.5.2. Diffusion-coupled FRAP recoveries

If the diffusion time for fluorescent molecules across the ROI is longer than the time needed to form new binding, the FRAP recovery is said to be diffusion coupled. In this case, the fluorescent molecules may bind and unbind several times as they move across the bleached region. Since diffusion and binding are mixed through recovery, the FRAP curve cannot be separated into a diffusive phase and a binding phase.

As a result, to be able to calculate binding parameters from FRAP recovery, it is important to study diffusion baseline by looking at an inert free diffusing molecule of the same size. Because this baseline diffusive behaviour must be included, the equations describing diffusion-coupled FRAP are, in most cases, more complex than those used to describe diffusion-uncoupled FRAP.

In addition, as diffusion is not separated from binding and continues during recovery, it affects recovery more significantly. So, analysis of binding reactions in diffusion-coupled FRAP recoveries is more complicated and requires a number of assumptions to ensure proper analysing of diffusion, which are not significant in diffusion

uncoupled recoveries. For example, the bleach time should be very fast in relation to the diffusion rate, or the binding site should have a homogeneous distribution that is assumed to be immobile during the fluorescence recovery (Sprague 2005).

1.4.5.3. Distinguishing diffusion-coupled from diffusion uncoupled FRAP

In order to be able to estimate the biophysical characteristic of binding reactions of fluorescent molecules from FRAP recovery curves, it is necessary to distinguish between diffusion coupled and uncoupled recovery first. One approach is to measure fluorescent intensities in different sub-regions of bleached ROI. In diffusion uncoupled recovery, the diffusion of free molecules in the ROI is much faster than dissociation\association from binding sites. Therefore, if the recovery is diffusion uncoupled different regions of the bleached ROI will have similar fluorescent intensity (Phair 2004). Another approach is to perform FRAP using different sizes of bleached region. In the diffusion-uncoupled mode, there is almost no change in the recovery rate with bleach spot size because diffusion happens approximately instantly and there would be a negligible difference by changing bleach size. However, in the diffusion-coupled mode, diffusion and binding/dissociation happen simultaneously during measured recovery phase, and there will be a detectable change in recovery time (Sprague 2004, reviewed in Sprague 2005).

1.5. FRAP on GFP-E-cadherin molecules reveals the factors which influence E-cadherin mobility.

Cadherin-mediated cell-cell adhesions are very dynamic structures which allow rapid modification of junctions in response to signalling during processes such as morphogenesis or wound healing. FRAP has been used to study the dynamics of cadherins in cell-cell adhesion. It is generally believed that there are two populations of E-cadherin molecules on the membrane: the free defusing monomers and the molecules clustered together in junctions. And the recovery of photo-bleached fluorescent molecules probably indicates the exchange of cadherin molecules between these two populations (Kusumi 1999, Adams 1998). Previous FRAP experiments on VE-cadherin junctions showed that different ROI sizes recovered at

similar rates, suggesting that recovery is diffusion uncoupled (Nanes 2012); In other words, the VE-cadherin recovery rate is not limited by diffusion rate of monomers but instead by dissociation\association of monomers from clusters.

It is not clear which E-cadherin interactions drive diffusible molecules into clusters. Photo-switching experiments on a tailless E-cadherin mutant showed that formation of cis and trans dimmers is enough for formation of clusters (Klingelhöfer 2002, Hong 2010). Disruption of either cis (by V81D/V175D mutation (Harrison 2011)) or trans (by W2A mutations (Klingelhöfer 2002)) dimer formation inhibits formation of E-cadherins clusters. In these studies a slower (or no difference in) recovery rate is reported for the tailless mutant compared to intact molecules, however, they just measured the initial recovery rate of fluorescent intensity in the junctions and their recovery curve does not measure if there is any difference in immobile fraction or not (Hong 2010).

On the other hand, other photo-bleaching experiments reported that interaction with actin stabilizes cadherin clusters (Cavey 2008, Hong 2013). Disruption of α-catenin interaction with cadherin also inhibits assembly and maintenance of adherens junctions (Vasioukhin 2000, Pappas 2006, Kwiatkowski 2010).

Moreover it has been reported that interaction of E-cadherin molecules with actin cytoskeleton cooperates with formation of cis interactions and enhances cluster formation (Hong 2013)

Interaction with actin not only stabilizes spot like E-cadherin clusters on cell-cell junctions, it is also responsible for movement of these clusters toward apical surface in A431 cells (Kametani 2007, Hong 2010).

The recovery of E-cadherin-GFP FRAP is an active process and ATP depletion decreases mobile cadherins at junctions (Troyanovsky 2006, Hong 2010). However, it is not clear what are the active mechanisms that remove cadherins from membrane. One of possible mechanisms is that interactions with catenins or modification of catenin interaction with phosphorylation of E-cadherin or catenins induce conformational changes needed for dissociation of cadheins. Also, there is evidence to suggest that endocytosis has an important role to physically remove cadherin from membrane. It has been shown that inhibition of clathrin mediated endocytosis stabilizes cadherin at junctions (Troyanovsky 2006; Hong 2010, de Beco 2009).

Moreover, p120 regulates endocytosis of cadherins. Disruption of interaction of VE-cadherin with p120 (by mutation in p120 binding domains) stabilizes VE-cadherin

junctions and inhibits induction of cell migration by vascular endothelial growth factor (Nanes 2012).

Finally, E-cadherin FRAP recovery is also affected by non-specific trapping in membrane (Kusumi 2005). Single particle tracking (SPT) and optical tweezers (OT) studies on both wild-type and tailless mutant E-cadherin on dorsal surface of cells also showed that movement of a population of E-cadherin molecules is hindered by trapping in membrane corrals by the cortical actin cytoskeleton (Sako 1998).

1.6. Aims:

The first aim of this thesis is to understand E-cadherin cell-cell adhesion dynamics using the FRAP technique. I want to understand how E-cadherin interactions and organization of cadherin molecules in junctions affects FRAP parameter Fi% and T1/2. Although FRAP has been used extensively for investigating E-cadherin dynamics, it's not clear how interpretation of FRAP results can informs us about molecular interactions of cadherin molecule. So, I want to use this data to have a better understanding of organization of cadherin molecules in adherent junctions.

In second part of this thesis, I will use the information from first section to understand how FRAP on GFP-E-cadherin molecules can be used as a method to evaluate the metastatic capability of tumour cells in vivo in a mouse pancreatic cancer model.

Then I will use FRAP to assess how mutant p53 affects E-cadherin dynamics, in order to understand how mutant 53 drives metastasis in this model.

2. Materials and Methods

2.1. Materials

2.1.1 General reagents

The sources of all chemicals, reagents and enzymes mentioned in this work are listed.

Table 2.1. Chemicals and reagents.

Material:	Source:
35 mm glass-bottomed dishes	MatTek
6×DNA loading dye	Fermentas
10X T4 DNA Ligase Buffer	Invitrogen
12 well transwell supports	costar
Agar	Beatson Central Services
Agarose	Sigma-Aldrich
Ampicillin	Sigma-Aldrich
Antibody (horse anti-mouse IgG) HRP-linked	NEB (Cell Signaling)
Anti-E-cadherin antibody	BD Transduction Laboratories
ATP (adenosine-5'-triphosphate)	Roche
BglII	Invitrogen
Bromophenol blue	Sigma-Aldrich
BSA (bovine serum albumin)	Sigma-Aldrich
BS3	Thermo Scientific
Cell Line Nucleofactor® Kit V	Amaxa
CDM glass bottom dish	Beatson Molecular Services
cOmplete Protease inhibitor cocktail	Roche
DAPI (4',6-diamidino-2-phenylindole)	Sigma-Aldrich
Dispase II	Sigma
DMEM (Dulbecco's modified Eagle medium)	Life Technologies
DMSO (dimethyl sulfoxide)	Sigma-Aldrich
DNase	Roche
dNTPs	Invitrogen
DMEM	Gibco

EDTA	Sigma-Aldrich
Ethanol	Thermo Fisher Scientific
Ethidiumbromide solution	Sigma
Fetal Bovine Serum	Healthcare
G148	Sigma
Glutamine	Life technologies
Glycerol	Sigma-Aldrich
HBS buffer	Biacore
HindIII enzyme	Invitrogen
Kanamycin	Sigma-Aldrich
L-Glutamine	Gibco
Neomycin	Sigma
Nitrocellulose membranes	Perkin Elmer
Not I enzyme	NEB
NuPage Tris-acetate gradient gels	Life Technologies
NuPAGE Tris acetate running buffer (20x)	Life Technologies
O'GeneRuler 1kb	Fermentas
Paraformaldehyde 16% Solution	Electron microscopy sciences
Pen-Strep	Gibco
PonceauS	Sigma-Aldrich
Protease inhibitor cocktail	Roche
Puromycin	Sigma-Aldrich
QIAquick®Gel Extraction Kit	Qiagen
QIAprep® Spin Miniprep Kit	Qiagen
QIAquick® PCR Purification Kit	Qiagen
Quick Change® Site-Directed Mutagenesis Kit	Stratagene
Spectra multicolor high range protein ladder	Thermo Fisher Scientific
T4 DNA Ligase	Invitrogen
Tris-HCL	Sigma-Aldrich
TritonX-100	Sigma-Aldrich
Trypsin 2.5%	Life technologies

Tween-20	Sigma-Aldrich
β-Mercaptoethanol	Sigma-Aldrich
Xho enzyme	Roche
Xba enzyme	Roche

2.1.2 Solutions and buffers

The buffers and solutions used in this study are listed with the composition of buffers.

Table 2.2. Buffers composition.

Buffer	Composition
Culture medium:	450ml DMEM (Gibco)
	50ml Foetal Bovine Serum (PAA laboratories)
	5ml of 200mM L-Glutamine solution (Invitogen)
	5ml of PenStrep (10000U/ml) (Gibco)
Tris-Buffered Saline (TBS)	25mM Tris-HCl pH 7.4
	137mM NaCl
	5mM KCL
Phosphate Buffered Saline (PBS)	170mM NaCl
	3.3mM KCl
	1.8mM Na_2HPO_4
	10.6mM KH_2PO_4
	pH 7.4
Lysogeny broth (LB)	1% Bacto-tryptone
	86mM NaCl
	0.5% yeast extract
	1.5% agar
Tris-EDTA (TE)	10mM Tris-HCl pH 8
	1mM EDTA
SDS-PAGE (polyacrylamide gel	125mM Tris pH 6.8

electrophoresis) sample buffer	4% SDS
	10% β-mercaptoethanol
	15% glycerol
	0.01% bromophenol blue
SDS-PAGE running buffer	0.1% SDS
	192mM glycine
	25mM Tris-HCl pH 8.3
Electroblotting buffer	192mM glycine
	25mM Tris
	20% methanol
Laemmli sample buffer	62.5 mM Tris-HCl pH6.8,
	10% Glycerol, 2% SDS,
	5% Mercaptoethanol,
	0.0025% Bromphenol Blue
Blocking solution (Western blotting)	5% milk powder in TBS-T
Blocking solution (immunostaining)	1% BSA in PBS
Fixing solution (cells or tissue)	4% PFA in PBS
Cross-linking buffer (HEPES/PBS)	20 mM HEPES, pH7.6,
	1 mM $CaCl_2$,
	150 mM NaCl
Quenching buffer (cross-linking)	20 mM Tris-HCl, pH7.5

2.2 Methods

2.2.1. Plasmids

The pAcGFP1-F plasmid (referred here as the GFP-f plasmid) was obtained from Clontech. This plasmid encodes a fusion protein consisting of a 20-amino-acid farnesylation signal from c-HRas fused to the C-terminus of AcGFP1. Post-translation of this farnesylation signal targets AcGFP1-F to the inner leaflet of the plasma membrane. pAcGFP1-F is designed for use as a plasma membrane marker, as well as a cotransfection marker, because it remains attached to the plasma membrane and it can be detected by fluorescence microscopy. Here, GFP-f FRAP recovery time is used for analysis of diffusion rate in plasma membrane.
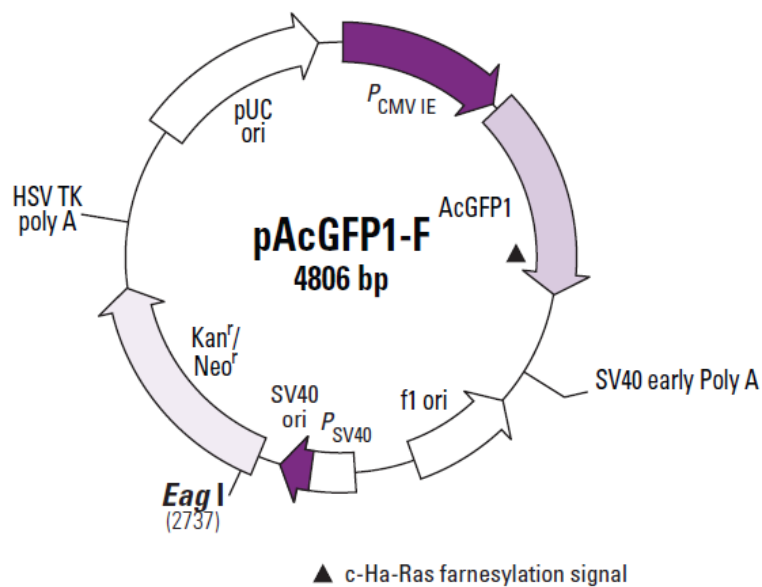
Figure 2.1. GFP-F (pAcGFP1-F) plasmid map.

The GFP-E-cadherin plasmid was a gift from Jennifer Stow (Serrels 2009). As this plasmid map showed in figure 2.1, the EGFP sequence is fused to C-terminal of E-cadherin. So, the GFP protein is fused to the cytoplasmic domain of E-cadherin. Moreover, the neomycin resistance gene allows stably transfected eukaryotic cells to be selected using G418.
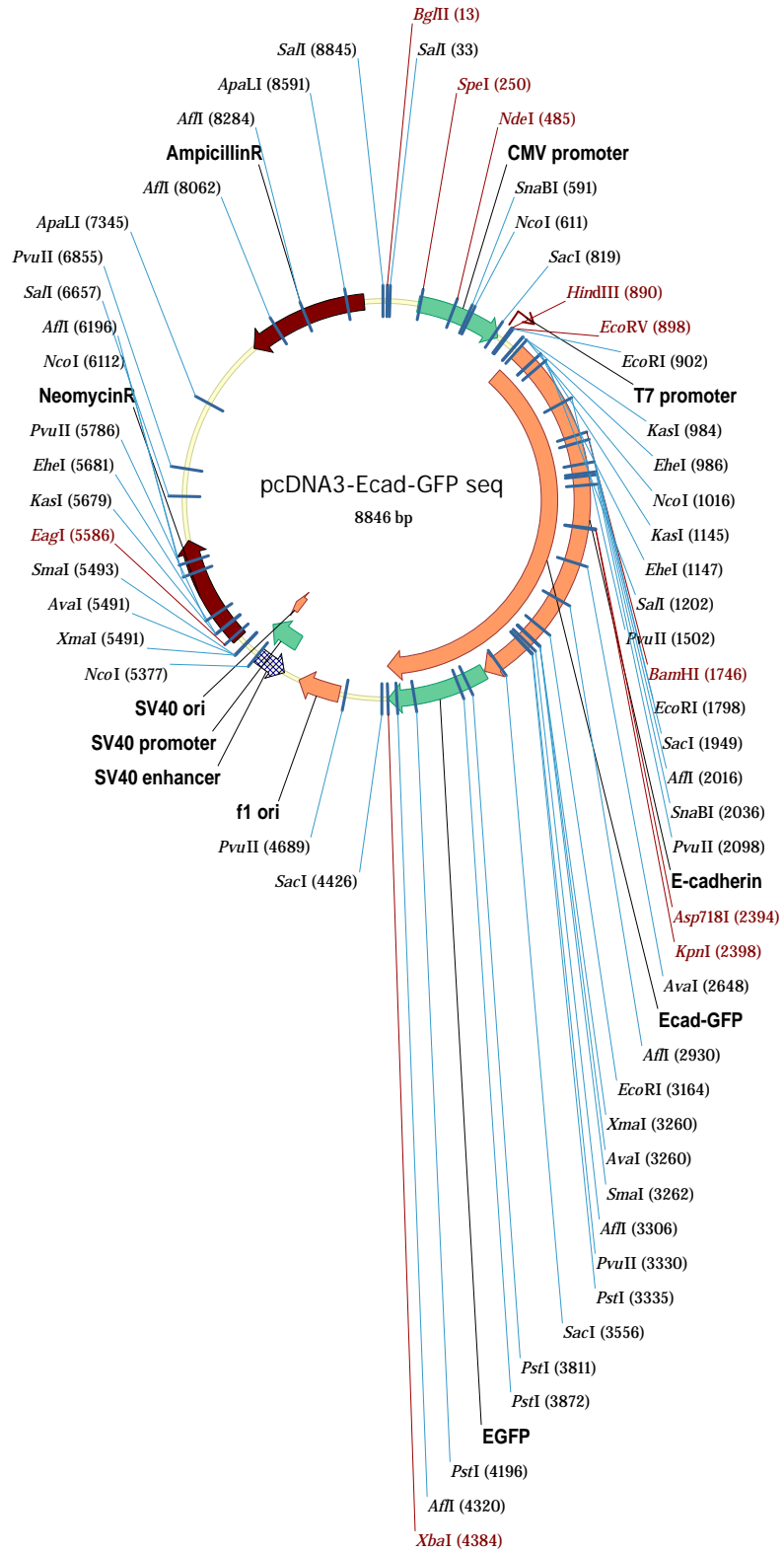
Figure 2.2. GFP-E-cadherin plasmid map.

2.2.2. Mutant GFP-E-cadheirn plasmids

All mutant E-cadherin-GFP plasmid used in this study are cloned from the wild type GFP-E-cadherin plasmid described above. Site directed mutagenesis was used for cloning each mutants.

For disrupting the trans interaction the W2 residue (Laur 2002) was mutated by Quick Change Lightning site directed mutagenesis kit (Agilent technologies) according to manufacturer's protocol.

Primers for W2A mutation:

Sense primer: 5'-CAG AAG ACA GAA GAG AGA CGC GGT TAT TCC TCC CAT CAG C-3'

Antisense primer: 5'-GCT GAT GGG AGG AAT AAC CGC GTC TCT CTT CTG TCT TCT G-3'

For disrupting the cis interaction V81D, V175D mutations were used as previously reported in Harrison et al. (Harrison 2011).

Primers for human sequence mutation:V81D,V175D mutation:

T402A antisense primer: 5'-CCA GCC CAG TGG TGT CCA CAC TGA TGA CT-3'

T120A G121C antisense primer: 5'-GCA TTC CCG TTG GAT GAG TCA GCG TGA GAG AAG AGA-3'

T402A sense primer: 5'-AGT CAT CAG TGT GGA CAC CAC TGG GCT GG-3'

T120A G121C sense primer : 5'-TCT CTT CTC TCA CGC TGA CTC ATC AAC GGG AA TGC-3'

For deletion of the cytoplasmic domain (Δcyt mutant) the Quick Change Lightning site directed mutagenesis kit was used to introduce two new NotI restriction sites on each side of cytoplasmic domain. Then NotI restriction enzyme (NEB) was used to cut out the residues 580 to 726.

For Deletion of the EC1 domain, two XhoI (Roche) sites were introduced in the same way to excise the region encoding residues 2 to 109.

In the following section the cloning method used for making these mutants is explained in more detail.

2.2.2.1. Mutagenesis PCR reaction with quick change lightning kit

Total reaction volume	50μl
DNA Template (0.1μg/μl)	1 μl
10x Buffer	5 μl
dNTP mix	1 μl
Quick solution	1.5μl
Primer Sense (0.1μg/μl)	5 μl
Primer Antisense (0.1μg/μl)	5 μl
Polymerase	1 μl
H_2O	ad 50 μl

PCR program:

1x   95°C 2 min
18x   95°C 20 sec
        60°C 10 sec
        68°C 30 sec per kb plasmid DNA
1x   68°C 5 min

The PCR mix was then treated with DpnI restriction enzyme to remove the template DNA.

2.2.2.2. Restriction digest reaction

Treatment 150 minutes at 37°C	50μl (Total volume)
DNA /PCR Prod.	5 μl (~1μg)
10 x RE-Buffer	5 μl (~1μg)
R-Enzyme 1	1 μl (10-20U)
R-Enzyme 2	1 μl (10-20U)
H_2O bid. (sterile)	ad 50 μl

2.2.2.3. Agarose gel electrophoresis

Agarose gel electrophoresis was used for the analysis of DNA from PCR and also for separation of band after restriction digests. 1% agarose gels in 1×TAE buffer was boiled in the microwave, allowed to cool and poured into the casting tray. The DNA was mixed with 6×DNA loading dye (Fermentas) and loaded into the gel. O'GeneRuler 1kb (Fermentas) was used as size marker. The gel was run for 30 min at 100V and after the electrophoresis the gel was incubated in EtBr bath for 15 Min. the stained bands were visualized by the Syngene Genius Bio imaging system.

2.2.2.4. Gel extraction

After cutting the band from the gel, QIAquick gel extraction kit (Qiagen) was used to extract each plasmid segment from the gel.

2.2.2.5. Ligation reaction

Treatment 150 min at Room Temp.	10μl (Total volume)
10x Ligase buffer	1 μl
vector DNA	1 μl
insert DNA	7 μl
ATP (25mM)	0.4 μl
Ligase enzyme	0.6 μl

2.2.2.6. Transformation of E.coli and DNA preparation

For DNA preparation of mutant plasmid DNA E. Coli DH5α competent cells were thawed on ice. Then 0.5 μg of DNA plasmid (or 5 μl of ligation reaction) was added to 50 μl of bacteria and incubated on ice for 20 min. For heat shocking the bacteria were heated at 42°C for 45 seconds then immediately cooled on ice. Then the bacteria were incubated in 0.5 ml LB for 1 hour at 37°C with shaking at 450rpm. Cells were spread on agar plates with ampicillin or kanamycin and grown upside down at 37°C overnight. The next day the colonies were inoculated in 3 ml LB with appropriate antibiotic and grown overnight at 37°C whilst shaking. Then QIAprep spin kit (Qiagen) was used to extract DNA from culture according to manufacturer's protocol.

2.2.2.7. DNA sequencing

DNA sequencing was carried out by the Molecular Technology Service at the Beatson Institute using the BigDye® Terminator v3.1 Cycle Sequencing Kit (Applied Biosystems).

2.2.3. Cell culture methods

2.2.3.1. L cells

L cells (ATCC® CRL-2648) are mouse fibroblast cells which do not express E-cadherin molecule endogenously. The cells were maintained in DMEM supplemented with 10 % FCS/2 mM L-glutamine / 1% penicillin/streptomycin solution (Gibco).

2.2.3.2. PDAC cells

PDAC^{R172H} cells are primary mouse cells with KRAS mutation and p53^{R172H} mutation. These cells are derived from pancreatic tumors harvested from Pdx1-Cre, LSL-KRAS$^{G12D/+}$, LSL-Trp53$^{R172H/+}$ mice (Morton 2010). I have also used PDAC^{fl} cells, mouse tumour cells isolated from Pdx1-Cre, LSL-KRAS$^{G12D/+}$, Trp53$^{LoxP/+}$ mice (Morton 2010).

PDAC^{fl}R175H and PDAC^{fl}vector cells are PDAC^{fl} cells which were transfected stably with p53^{R175H} or empty vector respectively. In FRAP experiments reported in this thesis all this cell lines are stably transfected with GFP-E-cadherin plasmid.

PDAC cells were cultured in Dulbecco's Modified Eagle Medium (DMEM) supplemented with 10% FBS, 2 mM L-glutamine (Invitrogen) and 1 % penicillin/streptomycin solution.

2.2.3.3. Passaging cells

After the cells had got to confluency an aliquot of the cells was passaged to a new flask to continue cells growth. For passaging the cells in T75 flasks (both PDAC and L cells), the media was first aspirated from the cells and they were washed with 10 ml of 37°C PBS. Then 1 ml of 1% trypsin in PBS was added to the flask. The flask was kept at the 37°C incubator until the cells had detached form the plate. Once detached, 10 ml of fresh pre-warmed cell culture media was added to the cells to inactivate the trypsin. An aliquot of this cell suspension was then added to a new flask containing fresh media. Then the cells were kept in incubator and allowed to adhere again and start to grow.

2.2.3.4. Counting the cells

Cells were counted using the automated Casy® Cell Counter and Analyser System (Innovatis). The appropriate dilution of cells following trypsinisation was automatically counted by the machine set to exclude debris from the calculation.

2.2.3.5. Cryogenetic preservation of cell lines

For long term storage of cells, cell culture flasks which were not yet reach to 70% confluency and they were still in the log phase of growth, were trypsinised and then re-suspended in complete media+10% DMSO (Sigma-Aldrich) and divided into 1 ml aliquots in 1.5 ml cryovials (Thermo-scientific). Initial freezing was carried out in a Mr Frosty container (Fisher Scientific) (containing isopropanol) at -70°C to give a cooling rate of 1°C /minute. Once a temperature of -70°C was reached the cells were transferred to storage in liquid nitrogen tanks at -180°C.

To grow cell from frozen vials, they were quickly warmed by submerging in a 37°C water bath. Then the thawed cells were added to pre-warmed culture media and let to adhere overnight. The next day the cells were passaged (or the media was changed if the cells were not confluent).

2.2.3.6. Transfection

Both cell lines were transfected with either wild-type or mutant GFP-E-cadherin plasmid using the Amaxa cell line nucleofector Kit V (Cell Line Nucleofactor® Kit V Lonza) according to manufacturer's protocol. Prior to transfection the plasmid was linearized with transfected cells were selected by G418 sulphate at 0.7 mg/ml (Formedium) and stable pools generated.

2.2.3.7. Cell sorting

After selection of stably transfected cells by G148, cells were harvested with trypsin-EDTA, and then washed in PBS three times to obtain a single cell suspension. The cells were suspended in 1% trypsin in PBS. Then cells were sorted by FACS into two

populations of low and high GFP expressing cells using a FACS Vantage Cell Sorter (BD Biosciences). The sorted cells were kept cultured in G418 solution.

2.2.3.8. Organotypic assays

Organotypic assays were done as described previously (Tipmson 2011-2). Initially, the 3D collage matrixes with fibroblast cells were made. ~7.5×10^4/ml primary human fibroblasts were mixed with rat tail tendon collagen to polymerize the gel at 35 mm petri dishes. Rat tail tendon collagen solution was prepared by the extraction of tendons with 0.5 M acetic acid to a concentration of ~2 mg/ml. the polymerized gels were detached from dish and allow to contract for approximately 6 days in complete media until the fibroblasts had contracted the matrix to ~1.5 cm diameter. The media on the matrixes was changed every 2 days.

Next, PDAC cells were seeded on top of these matrixes and allowed to invade. 4 × 10^4 cells were plated on the matrix and allowed to grow to confluence for 5 days in complete media. The matrix was then mounted on a metal grid and raised to the air/liquid interface resulting in the matrix being in contact to media just from below. the culture media that was changed every 2 days. After 8–12 days, the cultures were fixed using 4% paraformaldehyde and processed by standard methods for staining with Hematoxylin & Eosin (H&E), which marks the nucleus, cytoplasm and connective tissue in sections, was carried out by Histology Service of Beatson Institute.

2.2.3.9. Cross linking

PDAC cells were seeded confluently in 35 mm glass-bottomed dishes (MatTek), then cells were washed three times with HEPES/PBS buffer (20 mM HEPES, pH 7.6, 1 mM CaCl$_2$, 150 mM NaCl). Then the buffer aspirated and 100 μM BS3 cross linker (Thermo Scientific) freshly solved in water was added to the cells for 10 or 20 minutes. For quenching the cross linker the cells were incubated for 10 minutes in 20 mM Tris-HCl, pH 7.5. Cells were imaged for FRAP in cell culture media for 2 hours, and then the cells were lysed for western blotting.

2.2.3.10. SDS-PAGE electrophoresis and western blotting

The cells were scraped and lysed in Laemmli sample buffer (62.5 mM Tris-HCl pH6.8, 10% Glycerol, 2% SDS, 5% Mercaptoethanol, 0.0025% Bromphenol Blue). Next the cell lysate was sonicated 5×15 seconds. Then the cell lysates in sample buffer were heated to 95ºC for 5 minutes. After a short spin, samples were loaded on appropriate SDS-polyacrylamide gels (3-8% NuPage Tris-acetate gradient gels, Life Technologies). Electrophoresis was performed in SDS-PAGE buffer at 180V for 90 minutes using Power Pac Basic (Biorad)

By Western blotting protein was transferred to nitrocellulose membrane (Nitrocellulose Protran BA 83 0.2μm, Perkin Elmer) at 250 mA for an hour. Staining with PonceauS was used to check protein load (0.1 % (w/v) in 5% acetic acid solution Sigma-Aldrich). After imaging the protein staining the membrane was washed with water to remove the PonceauS solution. Then the membranes were blocked in 5% milk powder in TBS-T for one hour and incubated with primary antibodies over night at 4ºC. Anti-E-cadherin antibody (BD Transduction Laboratories™, Cat. No.610182) was used for western blots.

Membranes were then washed three times in TBS-T and incubated for 1 hour with secondary antibodies (horse anti-mouse IgG HRP-linked at 1:10,000 dilutions). Proteins were visualized by Pierce ECL reagent, using Fuji X-Ray Film Super RX on an AGFA classic E.O.S film processor.

2.2.3.11. Cell adhesion measurement

2.2.3.11.1. TEER measurement

Before measuring TEER, the 12 well transwell supports (costar) were treated for 30 min with DMEM. Then $3x10^5$ PDAC cells (or $6x10^5$ in L cells case) were seeded overnight on transwells. TEER was measured using an EVOM2 epithelial voltohmmeter with an STX2 electrode (World Precision Instruments). The results were reported as percentage of control cell resistance.

2.2.3.11.2. Dispase

For Dispase assays, a confluent cell monolayer in a 6 well dish was treated with 6 mg/ml dispaseII (Sigma) in PBS, the detached monolayer was broken up by pipetting up and down, and single cells were counted after passing through a cell strainer (BD Falcon, 40 um nylon) using a hemocytometer. The single cell number was reported as percentage of the total cell number which was counted after treating a control well with trypsin.

2.2.4. In vivo models

The PDAC mice models which used for in vivo experiments or for establishing cell lines were already described (Morton 2010). Pdx1-Cre, LSL-KRAS$^{G12D/+}$, Trp53$^{LoxP/+}$ mice have KRAS mutation and loss of p53 expression. Pdx1-Cre, LSL-KRAS$^{G12D/+}$, LSL-Trp53$^{R172H/+}$ mice have both KRAS and p53^{R172H} mutation. These mice get more malignant tumours.

In order to investigate E-cadherin dynamics in the context of pancreatic tumours, I used a mouse engineered to express E-cadherin-GFP from the Rosa26 locus under the control of cre-recombinase which was generated by D. Strathdee and colleagues in the Beatson Transgenic Production facility. This mouse crossed with mice expressing cre recombinase under control of PDX1 promoter which lead to expression of E-cadherin-GFP in the pancreas.

2.2.4.1. Breeding strategy and colony maintenance

All mice were bred and maintained in the Beatson Institute for Cancer Research animal facility and in accordance with UK Home Office guidelines and regulations. The experiments are done Under Project Licence Number (PPL): 60/4264. Experimental cohorts and breeding stocks were maintained for defined periods of time. The animals were checked at least two times weekly. Animals were culled according to Schedule 1 techniques as addressed in our project licence. Mouse ear notching and general maintenance (food, water and housing) was carried out by the Biological Services Unit at the Beatson Institute.

2.2.4.2. Animal genotyping

All animals were ear clipped at weaning and samples sent to Transnetyx for genotyping (Transnetyx, Cordova, TN, US). Transnetyx analyses samples using real time PCR.

2.2.4.3. Preparation and administration of cell suspension for xenografts

PDAC cells for subcutaneous injection into CD1 nude mice were grown in DMEM cell culture media up to ~70% confluency. Then the cells were trypsinized and counted using the Casy cell counter. The cells were then washed in PBS 3 times and the resuspended in required amount of PBS for injection. For each mouse 10^6 cells/100µl of PBS was injected.. The mice subcutaneous injections were done by Biological Services Unit at the Beatson Institute.

2.2.4.4. Tissue fixation

The tissue samples were fixed in 4 % paraformaldehyde (Electron microscopy sciences) in PBS for 24 hours after sample collection. They were paraffin embedded and tissue sections cut and fixed onto slides by the Histology Service at the Beatson Institute. Staining with Hematoxylin & Eosin (H&E), which marks the nucleus, cytoplasm and connective tissue in sections, was also carried out by Histology Service.

2.2.4.12. Dasatinib treatment in vitro and in vivo

Dasatinib (Bristol-Myers Squibb, Princeton, NJ) was administered daily by oral gavage in 80 mM citrate buffer (10 mg/kg) (or 100 nM in vitro). After pancreatic tumours were observed in mice, the animals were dosed three times, and after third treatments the tumours were imaged (Morton 2010-2).

2.2.5. FRAP and data analysis

2.2.5.1. FRAP in cell line:

For performing FRAP on cell line, $2.5x10^6$ PDAC cells were plated onto glass-bottomed dishes. The cells were left to adhere overnight. For L cells $4x10^6$ cells were seeded in dishes. The cells monolayer should be completely confluent. The glass bottom dishes maintained at 37 ℃ on a heated stage during FRAP.

2.2.5.2. FRAP in tissue

For performing the FRAP on xenograft the PDAC cells were injected subcutaneously into the flank of nude mice and then allowed to grow the tumour until it was reached the length between 1-1.4 mm. then while the mice was kept under anesthesia, small incisions in the skin surrounding xenograft tumors are made and a skin flap is created, allowing images to be acquired at a distance from the body of the mouse. The blood flow was kept through a skin flap attached to the body. The tumour is placed on a glass bottom dish on the heated microscope stage. A small amount of DMEM was added to prevent the tissue from drying. After FRAP the tumour was fixed and stained with H&E. performing the FRAP in xenograft ex vivo, the skin flap was cut before starting the imaging.

Ex vivo FRAP on pancreatic tissue (from the tumour or normal pancreas) performed on the freshly dissected tissue which was cut through with a clean edge and placed on a glass bottom dish on the heated microscope stage.

2.2.5.3. Performing FRAP and analysis

Photo-bleaching experiments were performed using an Olympus FV1000 confocal microscope with SIM scanner. Cells were imaged using the following settings: 4 μs pixel dwell time, 512 x 512 pixel resolution, 2% 488 nm laser power. For bleaching, a circular ROI with 30 pixel diameter (3 μm) was bleached to approximately 50% of its initial intensity using 35% 405 nm laser power, 20 μs/pixel dwell time for one frame. Images were captured every 1.6 seconds for 5 minutes. Individual recovery curves were exported into SigmaPlot (Systat Inc, London, UK) for exponential curve

fitting. Data were fit to the exponential equation $I(t) = I(0) + a \times (1-exp(-b \times t))$, where $I(t)$ denotes the percentage of recovered fluorescence intensity at time t after bleaching, $I(0)$ is percentage of fluorescent intensity after bleach and a and b are extracted by fitting the curve. The half-time of recovery was then calculated using the formula $T1/2 = ln(2)/b$, and the immobile fraction (Fi) was calculated (as a percentage) using the formula $Fi = 100*(1-a/(1-I(0)))$.

2.2.5.1. Statistical analysis

Statistical significance ($p < 0.05$) of differential findings between each pair of experimental groups was determined by a two tailed unpaired Student's t-test. In cases that the Kolmogorov-Smirnov normality test or the Equal Variance test failed, a Mann-Whitney Rank Sum test was used to test for statistical difference between groups of T1/2 and Fi.

3.   Cis, trans and actin interactions form adhesive E-cadherin clusters.

3. Cis, trans and actin interactions form adhesive E-cadherin clusters.

In this chapter I employed FRAP to understand the dynamics of E-cadherin in cell-cell junctions. I studied the effect of disrupting each interaction of E-cadherin (cis, trans and actin binding) on E-cadherin mobility and the strength of cell-cell adhesions. Moreover, I want to investigate the effect of expression level of E-cadherin-GFP molecules on their E-cadherin dynamics and the cell-cell junctions adhesiveness.

3.1. Localization of E-cadherin-GFP molecules in PDAC^{fl} cells

Initially, I wanted to study FRAP parameters of wild-type E-cadherin molecules in PDAC^{fl} cells. These cells are pancreatic cancer cells isolated from Pdx1-Cre, LSL-KRas$^{G12D/+}$, Trp53$^{LoxP/+}$ mice which do not express p53 (Morton 2010). PDAC^{fl} cells express endogenous E-cadherin and they were stably transfected with GFP-chimeras of wild-type E-cadherin or mutants. After drug selection, the transfected cells were FACS sorted into two groups of high expression and low expression (figure 3.1).
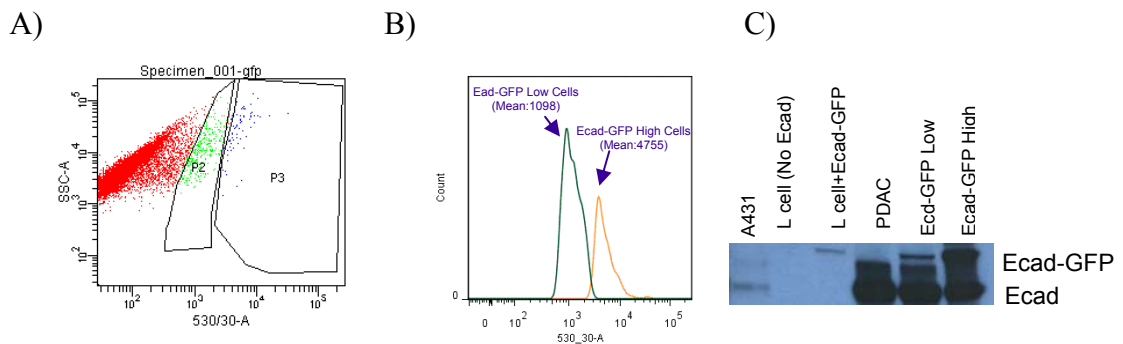
Figure 3.1. The expression levels of E-cadherin and E-cadherin-GFP in high and low expressing PDAC^{fl} cells. A) PDAC^{fl} cells were sorted by FACs, after transfection with E-cadherin-GFP plasmid. B) A FACS report demonstrating how high and low expressing cells are sorted C) western blot showing the difference between expression levels of E-cadherin (Ecad) and E-cadherin-GFP (GFP-Ecad) in PDAC^{fl} cells.

In order to understand the effect of expression level of wild-type or mutant E-cadherin-GFP on FRAP results, each experiment was carried out separately on low and high expressing cells.

Before performing the FRAP experiment; I examined the localization of E-cadherin-GFP in cell junctions. In order to visualize the 3-dimensional structure of junctions in PDAC[fl] cells expressing high E-cadherin-GFP level and the extent of photo bleaching, I fixed the cells and then imaged the cells by serial confocal sections acquired before and after photo bleaching. Figure 3.2.A shows the 3-dimensional structure of junctions in high expressing cells. These images showed a relatively homogeneous distribution of E-cadherin-GFP in the plasma membrane, unlike the punctuate localization of E-cadherin reported elsewhere (Hong 2010, Ozaki 2011, Harrison 2011) When viewed *en face*, the photo-bleached region appeared as a column of reduced fluorescence intensity (Figure 3.3.B).
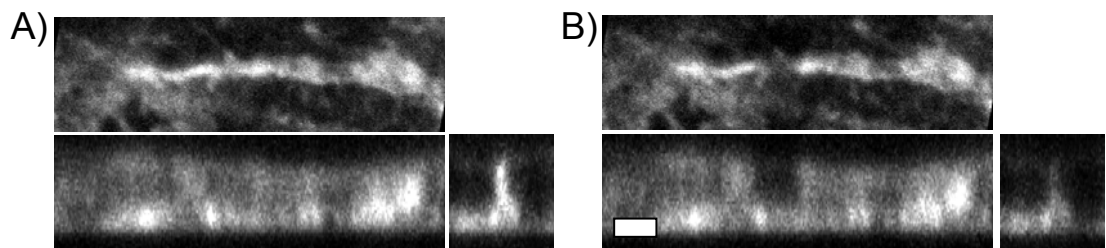
Figure 3.2. Localization of wild-type E-cadherin-GFP in high expressing PDAC[fl] cells. PDAC[fl] cells expressing E-cadherin-GFP were fixed and serially sectioned before (A) and after photo-bleaching (B) using confocal microscopy. Data sets were reconstructed to produce top-down (top), en face (bottom), and cross-section views (side) of the junction. Bar = 2 μm.

Next, FRAP was performed on wild-type E-cadherin-GFP in PDAC[fl] high expressing cells. To perform FRAP a small region in the membrane was bleached with high laser power and the recovery of fluorescent intensity was monitored for 5 minutes. The measured fluorescent intensity of the bleached ROI was divided by the fluorescent intensity of the ROI before the bleach and plotted against time. Then several individual FRAP recovery curves were averaged to get a representative recovery curve (Figure 3.3.B) For quantification of the results, Fi% and T1/2 were extracted from each single recovery curve, then averaged from all the recovery curves. To calculate Fi% and T1/2 recovery curve for each bleached point were fit by the exponential equation $I(t) = I(0) + a(1-\exp(-bt))$, where $I(t)$ is the percentage of recovered fluorescence intensity at time t after bleaching. The values a and b are calculated from the fitted curve. The half-time of recovery was then calculated using the formula $T1/2 = \ln(2)/b$, and the immobile fraction (Fi%) was calculated (as a

percentage) using the formula Fi =100*(1-a /(1-I(0))). Then t test have been used to analyse if the difference between each pair of data is statistically significant or not (See methods section 2.2.5).

Quantification of the FRAP result on PDAC^{fl} cells expressing high level of wild-type E-cadherin-GFP showed that these cells have 58.6% immobile fraction and 41 seconds T1/2 value (FRAP data for all experiments and t test values are summarized in Table 3.1 and 3.2)

A)
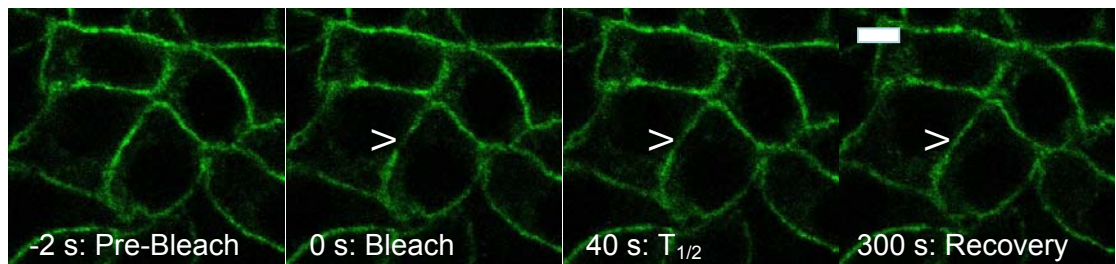
B)
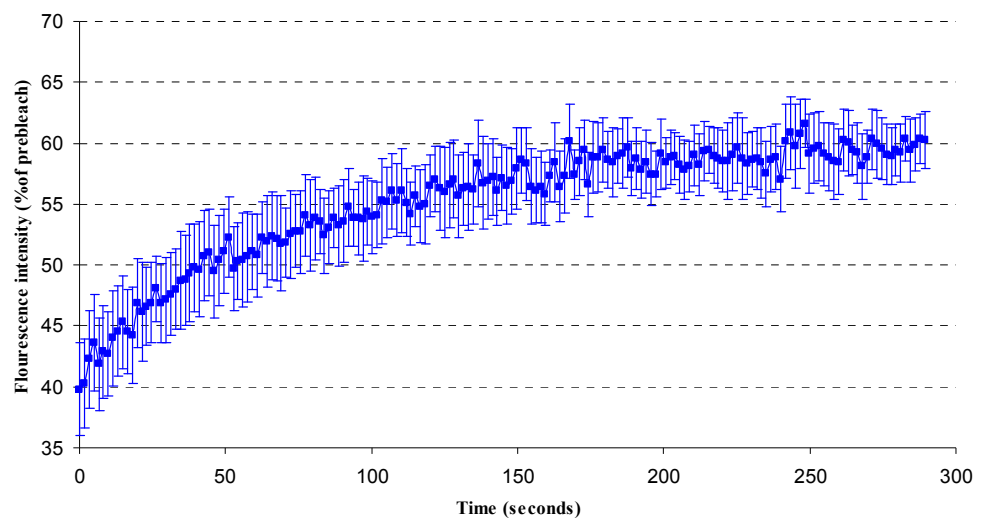
Figure 3.3. FRAP on high expressing wt-E-cadherin-GFP in PDAC^{fl} high cells. A) PDAC^{fl} cells expressing wild-type E-cadherin-GFP before bleaching, immediately after bleach, at T1/2 and after complete recovery. These cells are PDAC^{fl} with High E-cadherin-GFP expression. Bar = 5 μm. B) The averaged fluorescent recovery curve of wt-E-cadherin-GFP. The measured fluorescent intensity of the bleached ROI was divided by fluorescent intensity of the ROI before the bleach and the plotted against time. Ten individual FRAP recovery curves were averaged. Error bars show SEM. (n=10)

3.2. ΔEC1Δcyt-E-cadherin-GFP is non-specifically immobilized in the plasma membrane structure.

FRAP results for wild-type E-cadherin-GFP in PDAC[fl] cells revealed that both high and low cells had the same Fi% (58% immobile fraction). The immobile fraction determined by FRAP is typically used to estimate the amount of E-cadherin immobilized in cell-cell junctions. However, single particle tracking experiments at the free cell surface have previously shown that a fraction of E-cadherin is immobilized within the plasma membrane by non-specific trapping (Kusumi 1993, Sako 1993). In order to estimate the amount of E-cadherin non-specifically trapped in PDAC[fl] cell-cell junctions, an E-cadherin-GFP molecule with deletion of both EC1 and cytoplasmic domains was made. This mutant (abbreviated ΔEC1Δcyt in short form) is unable to form cis, trans, or actin interactions and therefore does not form any interactions with other E-cadherins or the cytoskeleton. ΔEC1ΔCyt-E-cadherin-GFP has approximately similar molecular weight and geometry as E-cadherin-GFP and should therefore report the rate at which wild-type E-cadherin moves by diffusion alone. Consequently, I used this mutant as a control for free diffusion of trans-membrane protein in these cells. The FRAP data from PDAC[fl] ΔEC1Δcyt-E-cadherin-GFP High cells showed that this mutant has significantly lower Fi and T1/2 compared to WT E-cadherin-GFP high expressing cell (p values for Fi and T1/2 are 0=<0.001 and 0=<0.001 respectively). However, the ΔEC1Δcyt mutant still had 31% immobile fraction (Figure 3.4).

Consistent with single particle tracking experiments of Kusumi et al, our FRAP results showed a high immobile fraction for ΔEC1Δcyt-E-cadherin-GFP which is an inert molecule (Kusumi 1999, Sako 1998). Moreover, as a control, I analyzed GFP targeted to the inner leaflet of the plasma membrane via the 20 amino-acid farnesylation signal from HRas (GFP-F). The immobile fraction for GFP-f in PDAC[fl] cells was also close to immobile fraction of ΔEC1Δcyt-E-cadherin-GFP (GFP-f Fi=26.3%). These data suggest that approximately half of E-cadherin trapped in cell-cell junctions (58%) were immobilized through non-specific interactions (31%).

In order to examine if endogenous wild-type E-cadherin affects the recovery of mutant E-cadherin-GFP, the FRAP recovery of ΔEC1Δcyt-E-cadherin-GFP was examined in a different cell line. L cells are mouse fibroblasts cells, which do not express endogenous E-cadherin. These cells were transfected with the E-cadherin-

GFP constructs and the sorted to high and low expressing cells. Figure 3.5 shows the FRAP results for wild-type, ΔEC1Δcyt and GFP-f in L cells. ΔEC1Δcyt-E-cadherin-GFP has 34.9% immobile fraction in L cells expressing high levels of E-cadherin-GFP, which is similar to the Fi% of ΔEC1Δcyt in PDAC^{fl} cells. ΔEC1Δcyt mutant Fi% and T1/2 are significantly lower than WT molecules (p values for Fi% and T1/2 compared in high expressing cells are 0=<0.001 and 0=<0.001   respectively).

A)
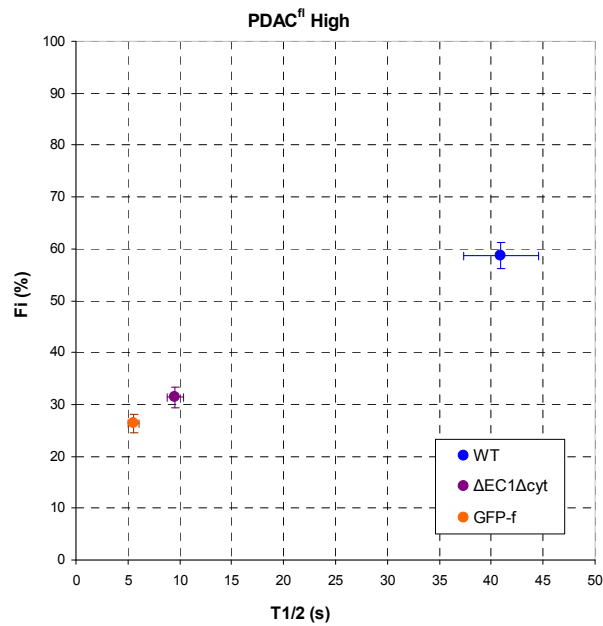
B)
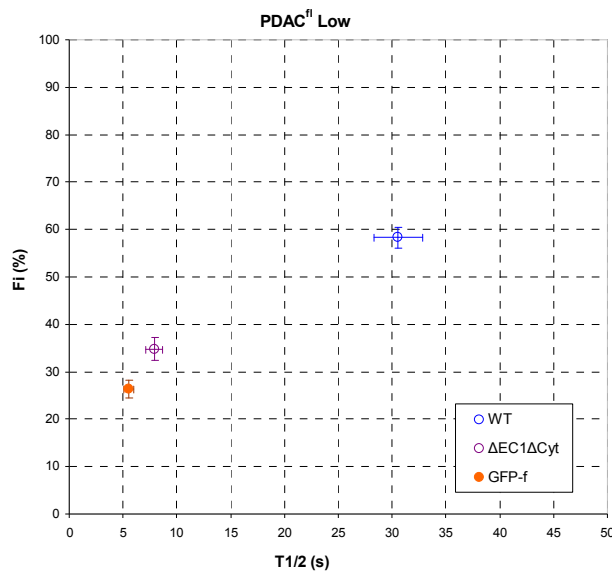
Figure 3.4. FRAP data for ΔEC1Δcyt-E-cadherin-GFP and GFP-f compared to wild-type E-cadherin-GFP in PDAC^{fl} cells. Immobile fraction (Fi%) is shown on y-axis and T1/2 on x-axis. A) FRAP results for high expressing cells (N_{wt}=24 $N_{ΔEC1Δcyt}$=39 N_{GFP-f}=9). B) Data for low expressing cell (N_{wt}=32 $N_{ΔEC1Δcyt}$=23 N_{GFP-f}=9). Error bars show SEM.

A)

B)
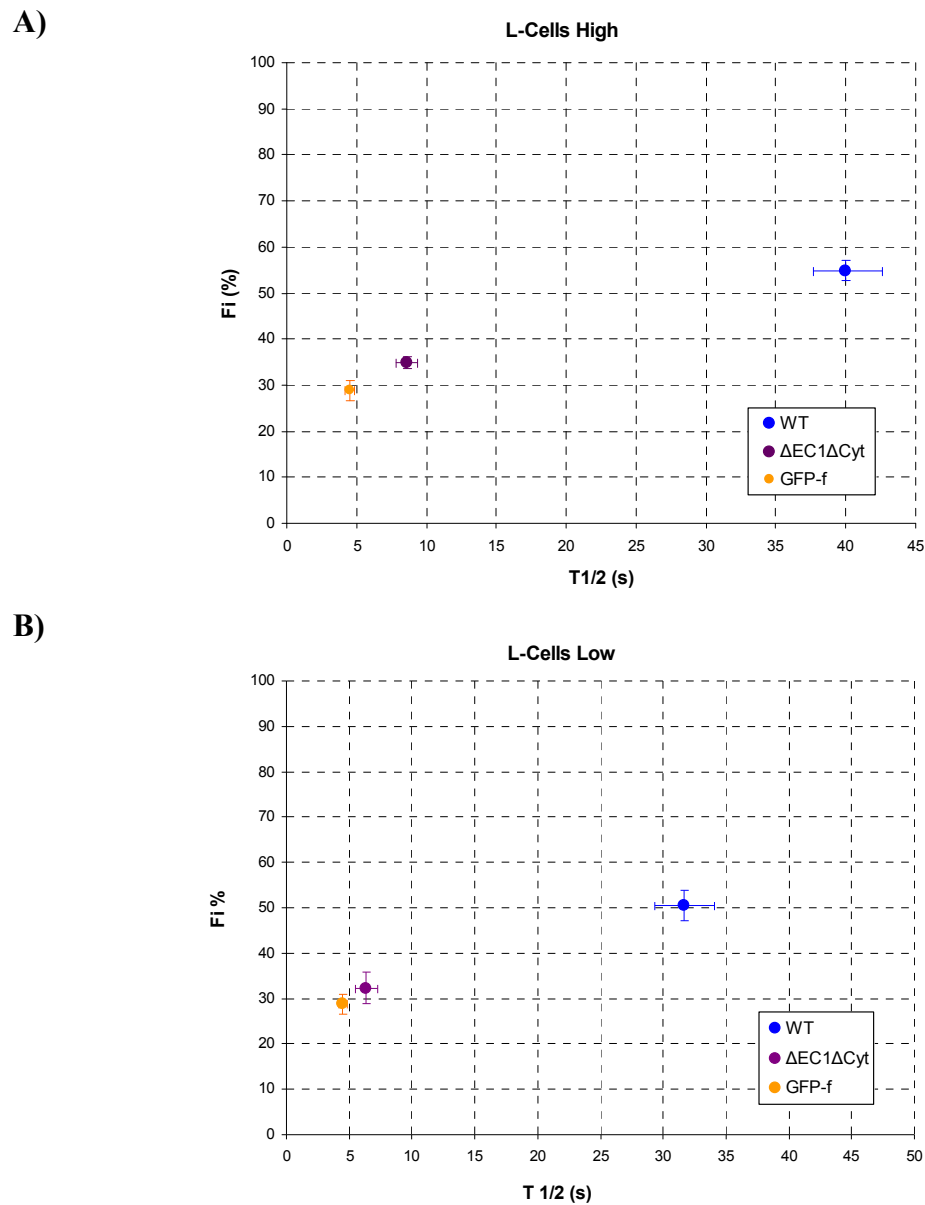
Figure 3.5. FRAP data for ΔEC1Δcyt-E-cadherin-GFP and GFP-f compared to wild-type E-cadherin-GFP in L cells. A) FRAP results for high expressing cells (N_{wt}=19 $N_{ΔEC1Δcyt}$=15 N_{GFP-f}=26. B) Data for low expressing cell (N_{wt}=19 $N_{ΔEC1Δcyt}$=11 N_{GFP-f}=26). Error bars show SEM.

As expected, there was a significant difference in the immobile fraction and T1/2 between wild-type E-cadherin-GFP and the non-interacting ΔEC1Δcyt E-cadherin-GFP mutant both in PDAC^{fl} and L cells. Disruption of E-cadherin cis, trans and actin interactions dramatically mobilized these molecules. The difference between the immobile fractions of wild-type E-cadherin and mutant demonstrates that around 30% of E-cadherin-GFP molecules are stably clustered to stationary complexes. Disruption of these three interactions dissociated the molecules from these complexes and decreased the mobile fraction. Moreover, the significant reduction in

T1/2 between wild-type E-cadherin-GFP and ΔEC1Δcyt E-cadherin-GFP mutant indicates that the recovery of E-cadherin-GFP molecules is restrained by transient binding to E-cadherin clusters which are relatively stationery in junctions in our FRAP experiment.

Therefore, E-cadherin is immobilized at cell-cell junctions through two mechanisms: by specific interactions mediated by the EC1 and/or cytoplasmic domain, and by non-specific interactions such as the cortical membrane fence. It is also apparent that the recovery rate of E-cadherin-GFP is much slower than would be expected for a process limited by the rate of diffusion only, suggesting that transient interactions with stationary binding partners slowed down its recovery.

3.3. Expression level of wild-type E-cadherin-GFP affects T1/2 but not Fi

The FRAP results from both PDAC^{fl} and L cells showed that E-cadherin dynamics are different in high and low expression levels of wild-type GFP-E-cadherin (In figure 3.6.A and B, FRAP results from figure 3.4 and 3.5 for high and low expression of wild-type and ΔEC1Δcyt E-cadherin-GFP are put together in one figure).

T test analysis of the result illustrated that there is no statistical difference between Fi% of high and low expression level of wild-type E-cadherin-GFP (p values for PDAC^{fl} and L cells are P=0.916 and P=0.281 respectively). This indicates that the amount of E-cadherin immobilized in cell-cell junctions was the same for different expression levels in each cell type. However, high expressing cells have significantly slower recovery rate of E-cadherin-GFP molecules than low cells in both PDAC^{fl} and L cell lines (p values for PDAC^{fl} and L cells are P=0.014 and P=<0.001 respectively). Moreover, there was no difference between Fi% and T1/2 of high and low ΔEC1Δcyt E-cadherin-GFP in either PDAC^{fl} or L cells (P values for Fi% and T1/2 in ΔEC1Δcyt mutant in high expressing PDAC^{fl} cell are P=0.284 and P=0.153. P values for Fi and T1/2 in ΔEC1Δcyt mutant in high expressing L cells are P=0.449 and P=0.133 respectively). This indicates that the level of non-specific trapping does not change by increasing expression level of the mutant E-cadherin-GFP.

A)
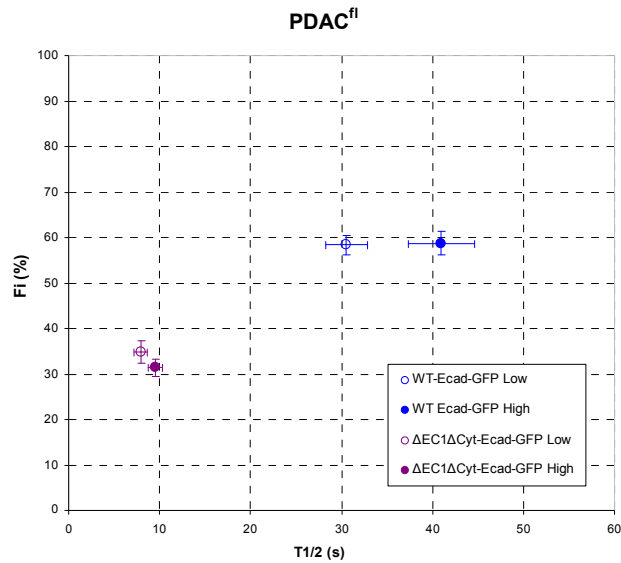
B)
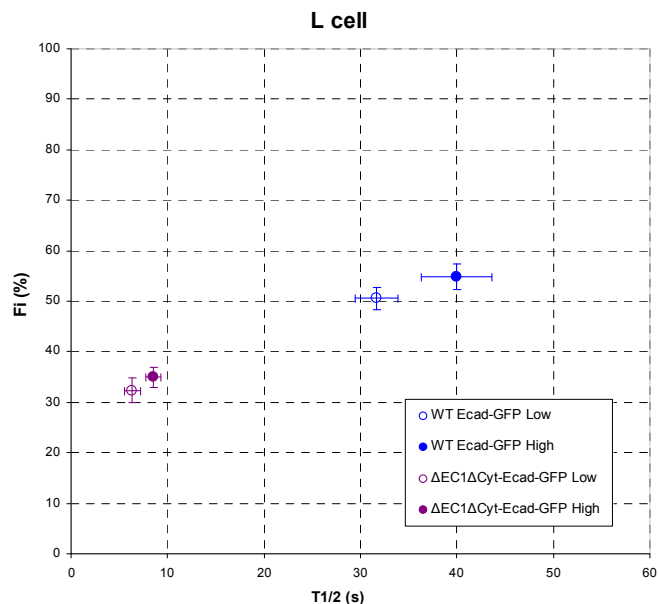
Figure 3.6. FRAP data for high and low expression of wild-type E-cadherin-GFP compared to high and low expression of ΔEC1Δcyt-E-cadherin-GFP. High expressing cells have significantly higher t1/2 values for wild-type E-cadherin-GFP. In both PDAC^{fl} and L cells there is no significant difference between Fi% of high and low E-cadherin-GFP cells. A) FRAP results in PDAC^{fl} cells. B) Data for L cells. Error bars show SEM. The data are duplicated from figure 3.4 and 3.5.

3.3.1. The level of E-cadherin-GFP expression influences cell-cell adhesion strength:

The FRAP data showed there is no difference in the proportion of E-cadherin molecules immobilized in cell-cell junctions between E-cadherin-GFP high and low expressing cells. However, previous work has demonstrated that the level of E-

cadherin influences cell adhesion strength (Steinberg 1994). To asses the effects of expression level on cell-cell junctions strength, I used two techniques: Dispase assay and TEER.

In the dispase assay, the cell monolayer was treated with dispase enzyme, which digests fibronectin, collagen IV and to a lesser extent collagen I, until it was separated from substrate. The detached cell layer was then broken up by mechanical force and the number of single cells was counted. For comparison, the number of single cells in high and low expressing cell lines was normalized to the number of single cells for PDAC^{fl} cells. In this assay, cells with stronger cell-cell adhesion show a lower number of single cells.

Comparison of cell-cell adhesions between parental PDAC^{fl} cells with PDAC^{fl} cell with high and low level of E-cadherin-GFP expression with dispase assay showed that PDAC^{fl} cell have significantly higher number of single cells than PDAC^{fl} E-cadherin-GFP low cells (p=<0.001) and cells with low expression have significantly higher number of single cells than high expressing cells (p=<0.001) (figure 3.7.A). These data indicate that by increasing the expression level of E-cadherin from PDAC^{fl} cells to PDAC^{fl} cells with low and high cells cell adhesion became stronger.

Similar results were obtained in L cell with high and low expression levels of E-cadherin-GFP (figure 3.8.A). L cell have significantly higher number of single cells than E-cadherin-GFP low cells (p=0.026) and cells with low expression have significantly higher number of single cells than high expressing cells (p=0.014). therefore, high expressing cells showed significantly higher cell-cell adhesion in both cell types.

In order to assess the effects of E-cadherin expression level on junctional integrity, I measured Trans-Epithelial Electrical Resistance (TEER) using an EVOM2 epithelial ohm-meter. TEER was measured for PDAC^{fl} cells expressing high and low levels of wild-type E-cadherin-GFP and high expression of ΔEC1Δcyt-E-cadherin-GFP (figure 3.8.B). The numbers are normalized to TEER in PDAC^{fl} cells. Statistical analysis of the results showed that, there is a significant difference between high and low expressing cells (p=<0.001). In addition, even low expression of E-cadherin-GFP in addition to endogenous protein increased TEER in comparison to PDAC^{fl} cells (p=<0.001). Furthermore, expression of the ΔEC1Δcyt-E-cadherin-GFP mutant decreased the junctional integrity compared to PDAC^{fl} cells alone (p= 0.013).

A)
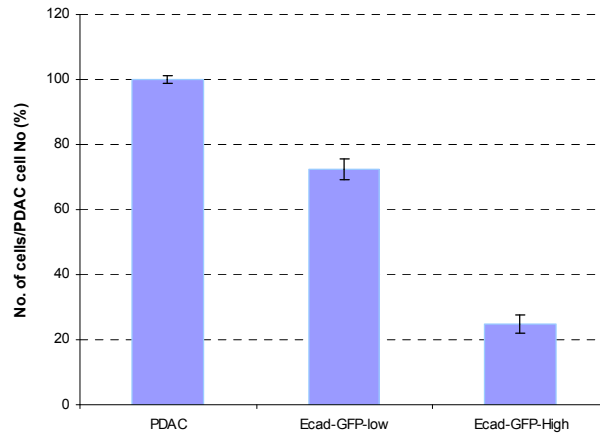
B)
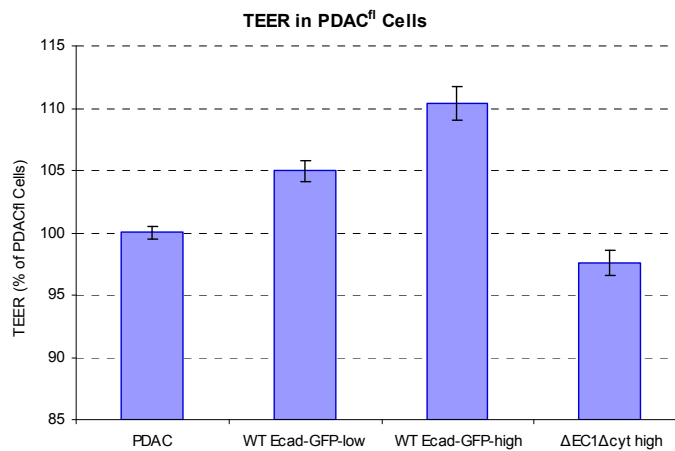
Figure 3.7. Cell-cell adhesion and junctional integrity in high and low expressing PDAC^{fl} cells.
A) Measuring cell-cell adhesion with dispase assay in PDAC^{fl} cells and cells expressing high and low
level of wild-type E-cadherin-GFP. PDAC^{fl} cells transfected with E-cadherin-GFP have significantly
lower number of single cells than PDAC^{fl} cells indicating that Cell-cell adhesion in high expressing
cells is significantly higher than low cells. B) Trans-Epithelial Electrical Rresistance (TEER)
measured in PDAC^{fl} cells expressing high and low level of wild-type E-cadherin-GFP and high
expression of ΔEC1Δcyt-E-cadherin-GFP. N=3. Error bars show SEM.

Subsequently, TEER was used to measure junctional integrity in L cells expressing
high and low levels of E-cadherin-GFP in comparison to L cell with no E-cadherin
expression, and L cells expressing high levels of ΔEC1Δcyt-E-cadherin-GFP. These
measurements revealed a significant difference in barrier function between high and
low expressing cells (figure 3.8.B). In addition, expression of ΔEC1Δcyt-E-cadherin-
GFP in L cells did not affect junctional integrity in these cells compared to L cells
with no E-cadherin expression.

A)
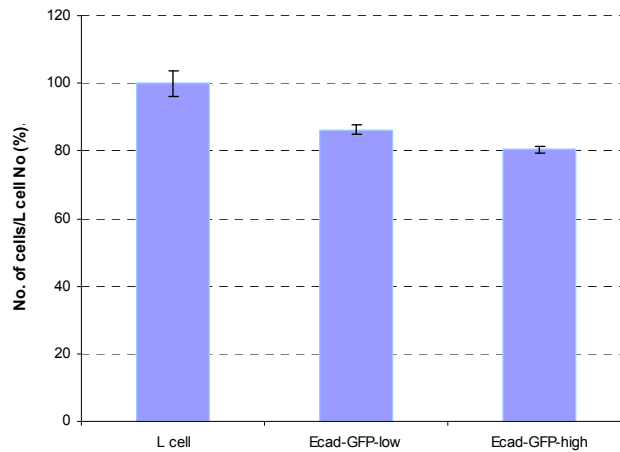
B)
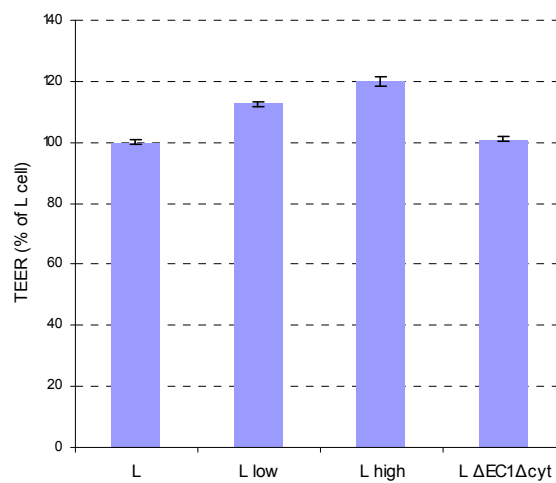
Figure 3.8. Cell-cell adhesion and junctional integrity in high and low expressing L cells measured. A) Measuring cell-cell adhesion with dispase assay in L cell expressing high and low level of wild-type E-cadherin-GFP. Expression of high or low expression levels of E-cadherin-GFP in L cells significantly decreased the number of single cells compared to L cells. Cell-cell adhesion in high expressing cells was significantly higher than low cells. B) Trans-Epithelial Electrical Resistance (TEER) is measured in cells expressing high and low level of wild-type E-cadherin-GFP and high expression of ΔEC1Δcyt-E-cadherin-GFP. N=3. Error bars show SEM.

In summary, these results showed that increasing the cadherin expression level enhanced cell-cell adhesion, although there was no difference in the fraction of E-cadherin immobilized in cell-cell junctions in high and low expressing cells. This implies that although the high-expressing cells engage more E-cadherin in cell adhesion than the low-expressing cells, the proportion of E-cadherin molecules engaged in junctions remains constant at both expression levels. Therefore, by itself, the immobile fraction does not represent an absolute measure of cell-cell adhesion

strength. Similar expression level of E-cadherin is necessary to use immobile fraction as an indicator of cell-cell adhesion strength.

In contrast, the recovery rate was significantly affected by expression level of E-cadherin-GFP. Although there was no significant difference between T1/2 of high and low expression of ΔEC1Δcyt-E-cadherin-GFP mutants (both in PDAC^{fl} and in L cells), increasing the expression level of wild-type E-cadherin-GFP significantly increased the recovery time of E-cadherin FRAP.

3.4. Trans dimers are essential for immobilizing E-cadherin-GFP:

In order to investigate the relative contributions of cis-, trans-, and actin interactions to immobilizing E-cadherin within cell-cell junctions I made mutants defective for each interaction and analyzed those using FRAP to establish the influence of each interaction on mobility and recovery rate.

3.4.1. The Availability of E-cadherin on the neighbouring cell membrane affects FRAP data.

In order to determine how different expression levels of E-cadherin on adjacent membrane affects Fi% and T1/2, I mixed high expressing E-cadherin-GFP PDAC^{fl} cells with PDAC^{fl} cells with no E-cadherin-GFP cells. Then, I performed FRAP at the junctions between a green cell and a non-GFP cell (see figure 3.9).

As shown in figure 3.1 by western blot analysis, high expressing E-cadherin-GFP PDAC^{fl} cells express more E-cadherin that parental PDAC^{fl} cells. Therefore, mixing these cells results in formation of junctions, which do not have same level of E-cadherin on two neighbouring membranes (here referred to Hi-No junctions between PDAC^{fl} cells just express endogenous E-cadherin and no E-cadherin-GFP).

The FRAP data in Hi-No junctions showed that there is a significant reduction in both Fi% and T1/2 compared to Hi-Hi junctions (High expression level of E-cadherin-GFP on both sides of junction) (figure 3.9.B). T test p values for Fi% and T1/2 are P=0.005 and P=<0.001. This indicates that reducing trans dimer formation because of limitation in availability of E-cadherin on parental PDAC^{fl} cell (P), reduced Fi% in high E-cadherin-GFP expressing cells (Hi).

Next, the FRAP experiment was done at the free cell edge in PDAC^{fl} cells expressing high level of E-cadherin-GFP (Hi-Bo). For stabilizing the free cell edge in order to perform FRAP, high expressing E-cadherin-GFP PDAC^{fl} cells are mixed with L cells. L cells do not express E-cadherin and do not form any contact with PDAC^{fl} cells. FRAP at a free cell edge (Hi-Bo) showed that Fi% and T1/2 are significantly reduced compared to Hi-Hi junctions (T test p values for Fi% and T1/2 are P=<0.001 and P=<0.001). E-cadherins at a free cell edge is able to form cis and actin interactions, which indicates that cis interaction and binding to the actin cytoskeleton are not enough to immobilized E-cadherin in the membrane.

Moreover, FRAP for E-cadherin-GFP molecules at free-cell edge which are unable to form trans dimers have the same immobile fraction as ΔEC1Δcyt mutant. These data indicate that trans dimer formation is necessary for immobilizing E-cadherin in the membrane. To confirm this idea, I disrupted trans dimer formation with point mutation and measured how it affects FRAP recovery.

A)

B)

C)
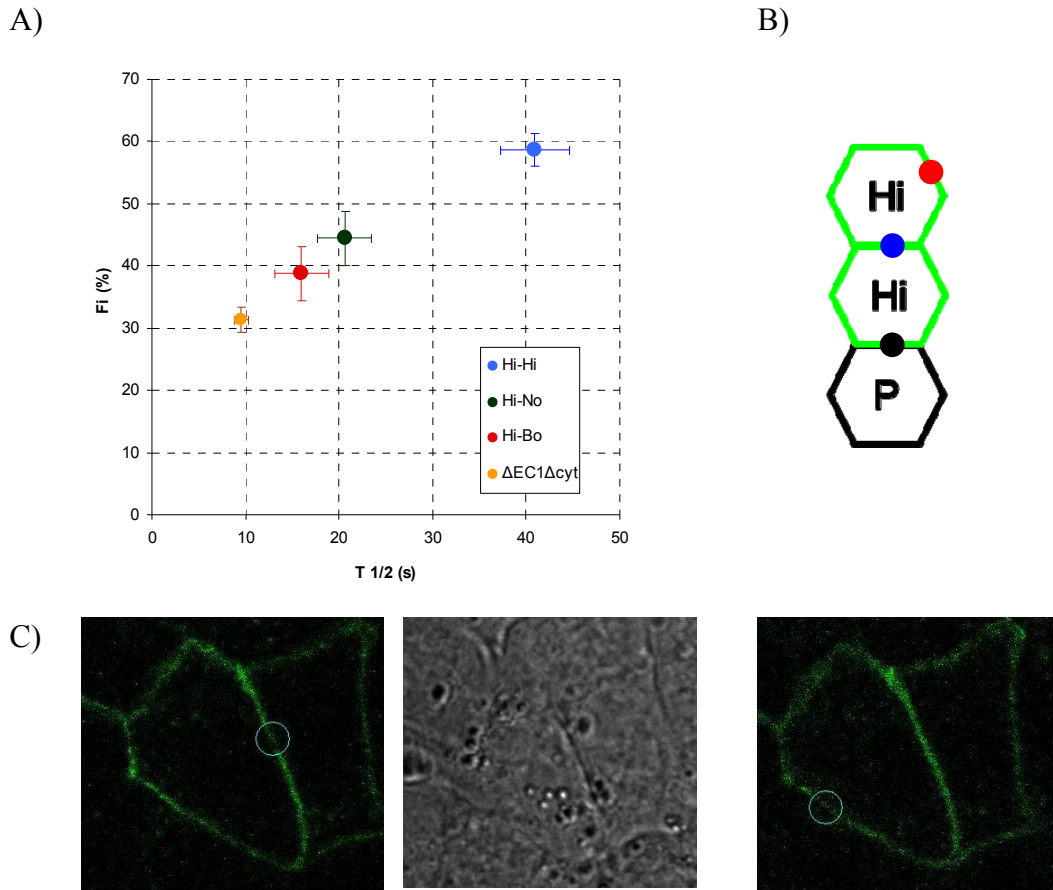
Figure 3.9. E-cadherin mobility is affected by availability of E-cadherin in the neighbouring plasma membrane. A) FRAP data for two high expressing cells (Hi-Hi) is shown as a blue dot. The FRAP data is from figure 3.4.A. Black dot (Hi-No) represents data for FRAP at a contact between a Hi cell and a PDAC[fl] cell (P). Red dot (Hi-Bo) is FRAP at free edge of a cell. The FRAP data for ΔEC1Δcyt mutant is from figure 3.4.A. B) schematic drawing of cell-cell contacts which are used for FRAP experiments in A. C) microscopic image showing how FRAP is performed at contact of a green cell and a non-GFP cells (Hi-No dot) compared to FRAP of membrane between to high expressing cells or two green cells (Hi-Hi dot). $N_{Hi-No}=16$, $N_{Hi-Bo}=14$. Error bars show SEM.

3.4.2. Disruption of trans interaction by W2A mutation:

In order to investigate the effects of specifically disrupting trans dimers on E-cadherin mobility, I performed FRAP on E-cadherin-GFP with W2A mutation. This mutation disrupts the β strands needed for strand swapping (Laur 2002). Therefore, the W2A mutant is unable to form trans dimers. I expressed this mutant in PDAC[fl] cells which also express wild-type endogenous E-cadherin and sorted the cells to high and low expression similar to wild-type E-cadherin-GFP and ΔEC1Δcyt-E-cadherin-GFP expressing cells.

Analysis of E-cadherin mobility by FRAP showed that reduction of trans dimer formation reduces immobilized E-cadherin to 36% and the recovery rate to around 20 seconds in PDAC^{fl} cells with high expression of W2A-E-cadherin-GFP, compared to 60% Fi and 40 seconds T1/2 for wild-type E-cadherin-GFP in PDAC^{fl} cells (figure 3.10.A). (T test p values for Fi% and T1/2 are P=<0.001 and P=<0.001). The data for wild-type E-cadherin-GFP and ΔEC1Δcyt mutant are duplicated from figure 3.4. PDAC^{fl} cells expressing low level of the W2A mutant showed similar decrease in both Fi% and T1/2 (T test p values for Fi% and T1/2 are P=<0.001 and P=0.009).

The W2A mutation significantly decreased the amount of E-cadherin immobilized at cell-cell junctions. This is in agreement with the data from the previous section and confirms that formation of strand swapped trans dimers is necessary for inclusion of E-cadherin into adhesive clusters of E-cadherin on membrane.

Moreover, W2A mutant recovered significantly more slowly than ΔEC1Δcyt-E-cadherin-GFP but there is no significant difference between their immobile fractions. (T test p values in high expressing cells for Fi% and T1/2 are P=0.075 and P=<0.001). The W2A mutant can form cis dimers and bind to the actin cytoskeleton. This slower recovery rate of the W2A mutant compared to the non-binding mutant indicates that cis dimerization or binding to actin are responsible for slowing down the recovery of W2A-E-cadherin-GFP molecules.

A)
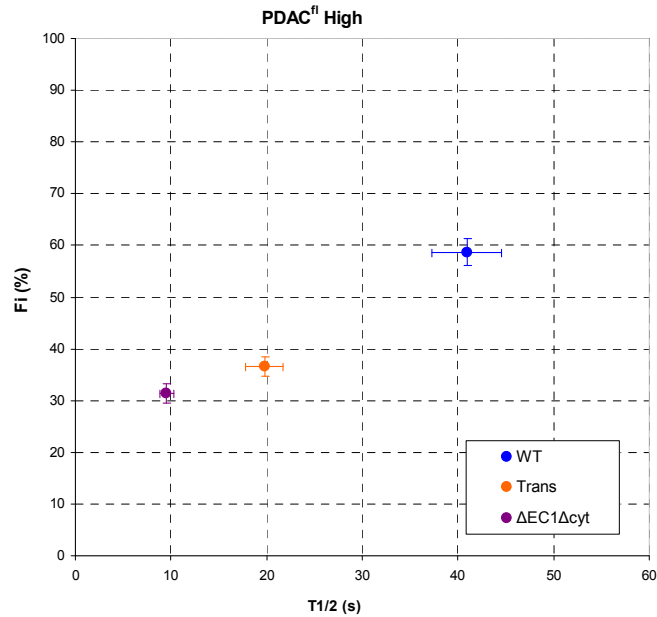
B)
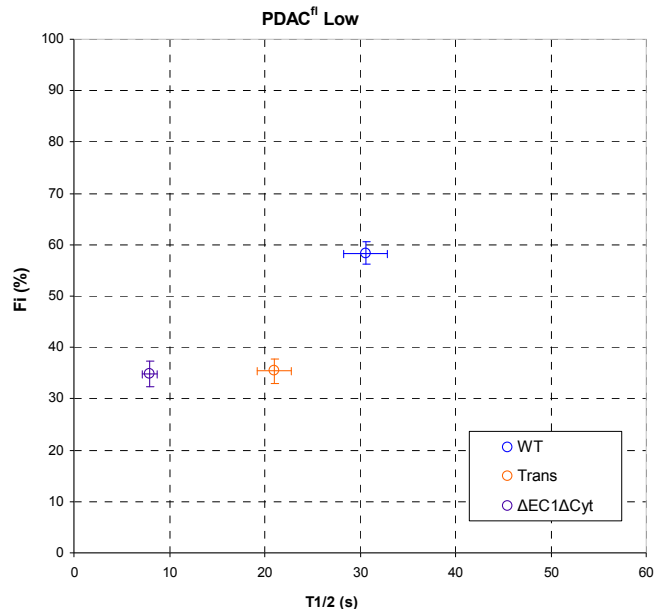
Figure 3.10. FRAP data for GFP-W2A-E-cadherin (trans interaction mutant) compared to WT E-cadherin-GFP and ΔEC1Δcyt-E-cadherin-GFP in PDAC^{fl} cells. The data for wild-type E-cadherin-GFP and ΔEC1Δcyt mutant are duplicated from figure 3.4. There is a significant decrease in both T1/2 and Fi% between wild-type and trans mutant (W2A-E-cadherin-GFP). Although W2A mutant and ΔEC1Δcyt-E-cadherin-GFP have the same Fi%, T1/2 is significantly higher in W2A mutant. A) FRAP results for high expressing cells. $N_{trans\ Hi}$=24. B) Data for low expressing cell. $N_{trans\ Low}$=20. Error bars show SEM.

Next I examined whether the presence of endogenous wild-type E-cadherin affects the recovery of W2A-E-cadherin-GFP in PDAC^{fl} cells. To do this, I transfected L cells with trans mutant (W2A-E-cadherin-GFP) construct and sorted for high and low

expression. L cells with W2A mutant expression do not express any wild-type E-cadherin. I analysed FRAP in both high expressing and low expressing cells (figure 3.11). The results showed that, similar to PDAC^{fl} cells, in L-cells the W2A mutant had the same immobile fraction as the non-binding $\Delta EC1\Delta cyt$ mutant, but the rate of mobility was significantly reduced in W2A mutant. (T test p values in high expressing cells for Fi% and T1/2 are P=0.890 and P=<0.001).

A)
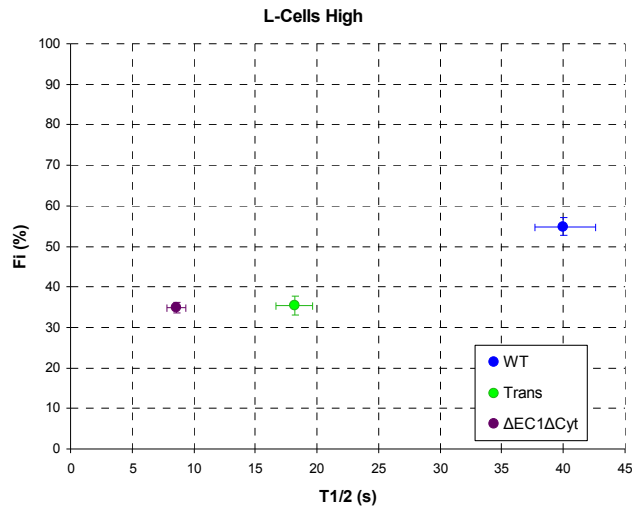
B)
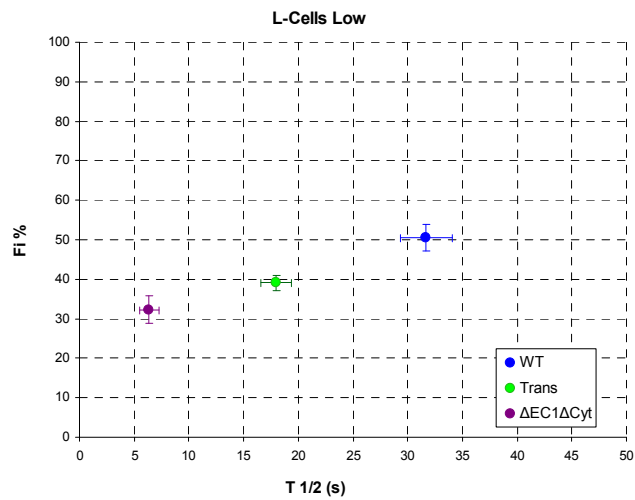
Figure 3.11. Mobility of for GFP-W2A-E-cadherin (trans interaction mutant) compared to Wild-type E-cadherin-GFP and ΔEC1Δcyt-E-cadherin-GFP in L cells. The data for wild-type E-cadherin-GFP and ΔEC1Δcyt mutant are duplicated from figure 3.5. There is significant decrease in both T1/2 and Fi% between wild-type and trans mutant (W2A-E-cadherin-GFP). Although, W2A mutant and ΔEC1Δcyt-E-cadherin-GFP have same Fi%, but T1/2 is significantly higher in W2A mutant. A) FRAP results for high expressing cells $N_{trans\ Hi}$=41. B) Data for low expressing cell $N_{trans\ Lo}$=33. Error bars show SEM.

The FRAP data showed a significant decrease in E-cadherin immobilized in W2A mutant cells. This suggests that W2A mutant E-cadherin affects cell-cell adhesion. Therefore, I analysed how this mutant affects cell-cell adhesion in PDAC^{fl} cells expressing the W2A mutant using the dispase assay (Figure 3.12). The data showed that expression of GFP-W2A-E-cadherin in significantly increased the number of free cells following dispase treatment compared to the PDAC^{fl} cells (P=0.003) or PDAC^{fl} cells with high expression of wild-type E-cadherin-GFP (P = <0.001). Therefore, W2A-E-cadherin-GFP molecules not only were not able to increase the cell-cell adhesion like wild-type E-cadherin-GFP molecules but these molecules significantly weakened the cell-cell adhesion compared to parental PDAC^{fl} cells as well.
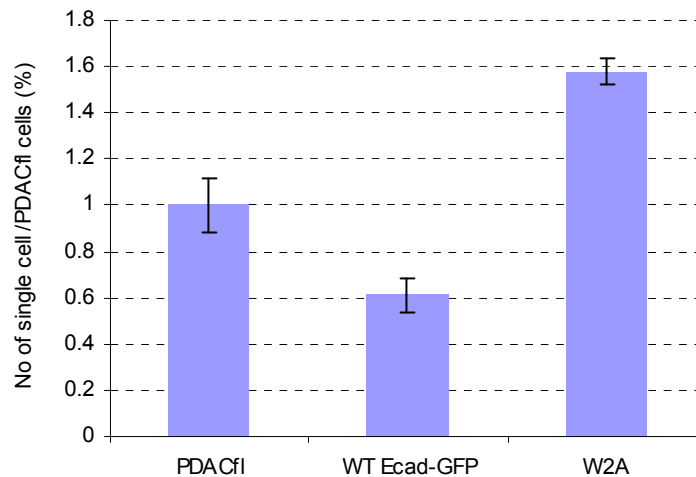
Figure 3.12. Cell-cell adhesion measurement by Dispase assay. Measuring cell-cell adhesion with dispase assay in PDAC^{fl} cell and PDAC^{fl} cells expressing high level of wild-type E-cadherin-GFP and trans mutant (W2A-E-cadherin-GFP). For each case, the number of single cells is normalized to PDAC cell number. PDAC^{fl} cells transfected with E-cadherin-GFP have significantly fewer cells following dispase treatment than PDAC^{fl} cells. Expression of W2A-E-cadherin-GFP in PDAC^{fl} cells significantly increased single cells number indicating reduced cell-cell adhesion strength. N=3. Error bars show SEM.

Moreover, measurement of cell-cell adhesion by dispase assay in L cells showed that W2A mutant expressing L cells have same number of single cells as L cells (figure 3.13) (P = 0.188). Which confirms that W2A mutant E-cadherin-GFP is not capable of forming adhesive complexes and increasing cell-cell adhesion in L cells. In

summary, W2A-E-cadherin-GFP was unable to form junctions in L-cells and disrupted formation of junctions in PDAC^{fl} expressing endogenous E-cadherin.
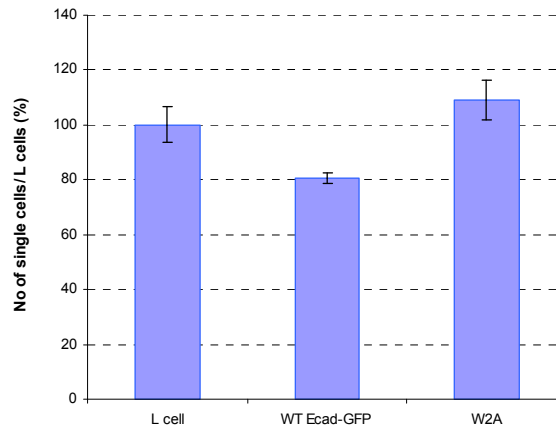
Figure 3.13. Cell-cell adhesion measurement by Dispase assay. Measuring cell-cell adhesion with dispase assay in L cell and L cells expressing high level of wild-type E-cadherin-GFP and trans mutant (W2A-E-cadherin-GFP). For each case, the number of single cells is normalized to L cell number. Expression of E-cadherin-GFP in L Cells significantly decreased the number of single cells. However, expression of W2A-E-cadherin-GFP in L cells does not affect single cells number significantly compared to L cells. N=3. Error bars show SEM.

3.5. Disruption of cis interaction by V81D/V175D mutation

In order to examine the effects of cis-interaction on E-cadherin mobility I used V81D/V175D mutant E-cadherin-GFP. This mutation destroys the hydrophobic core of the cis interface and inhibits cis interaction between E-cadherin molecules (Harrison 2011).

Here, FRAP was used to analyse E-cadherin in PDAC^{fl} cells expressing high and low levels of cis mutant E-cadherin-GFP (figure 3.14). The data for wild-type E-cadherin-GFP and ΔEC1Δcyt mutant are duplicated from figure 3.4. The data showed that, in both high and low, cells cis mutants had significantly lower immobile fraction and T1/2 compared to cells expressing wild-type E-cadherin-GFP. (T test p values in high expressing cells for Fi% and T1/2 are P=<0.001 and P=<0.001).The immobile fraction of the cis mutant was similar to the ΔEC1Δcyt mutants, which indicates that cis interactions are necessary to immobilize E-cadherin-GFP molecules in adhesive complexes in cell-cell junctions.

However, the ΔEC1Δcyt mutant recovered significantly faster than V81D/V175D-E-cadherin-GFP molecules (p values in high expressing cells for Fi% and T1/2 are P=0.075 and P=<0.001), this indicates that interaction with actin is responsible for slowing down the recovery of cis mutant compared to non-binding freely diffusing ΔEC1Δcyt mutant cadherins.

A)
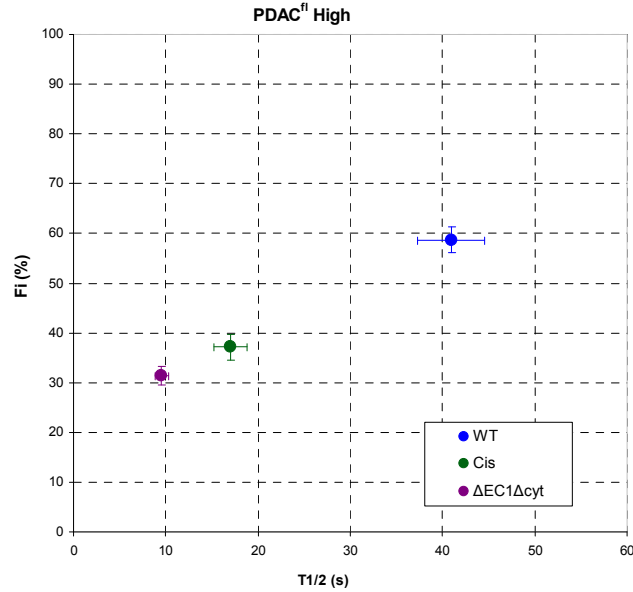
B)
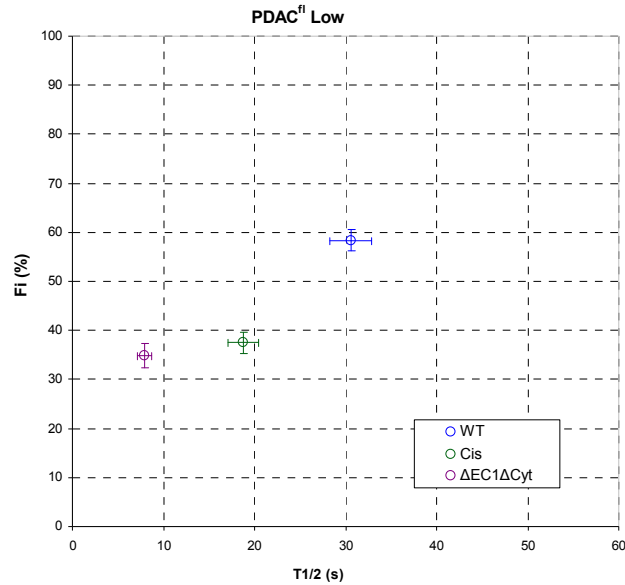
Figure 3.14. FRAP data for V81D/V175D-E-cadherin-GFP (cis interaction mutant) compared to WT E-cadherin-GFP and ΔEC1Δcyt-E-cadherin-GFP in PDAC^{fl} cells. The data for wild-type E-cadherin-GFP and ΔEC1Δcyt mutant are duplicated from figure 3.4. A) FRAP results for high expressing cells. $N_{cis\,Hi}$=26. B) Data for low expressing cell. $N_{cis\,Low}$=31. Error bars show SEM.

Next to analyse how the presence of endogenous wild-type E-cadherin affect the cis mutant E-cadherins, I expressed V81D/V175D mutant in L cells. The FRAP data showed that for the V81D/V175D mutant Fi is 37% and T1/2 is around 17 seconds in L cells with high GFP expression. L cells with low expression also showed similar FRAP data (figure 3.15.A and B). In high expressing cells, the V81D/V175D mutant showed a significant decrease in both Fi% and T1/2 compared to wild-type E-cadherin-GFP in high expressing L cells (p values for Fi% and T1/2 are P=<0.001 and P=<0.001). Moreover, the V81D/V175D mutant had significantly higher T1/2 than the non-binding mutant ΔEC1Δcyt-E-cadherin-GFP but there is no significant difference between their immobile fractions (p values in high expressing cells for Fi% and T1/2 are P=0.671 and P=<0.001). These data indicates that similar to PDAC^{fl} cell results V81D/V175D-E-cadherin-GFP molecules are not able to form stationary E-cadherin clusters in cell-cell junctions.

A)
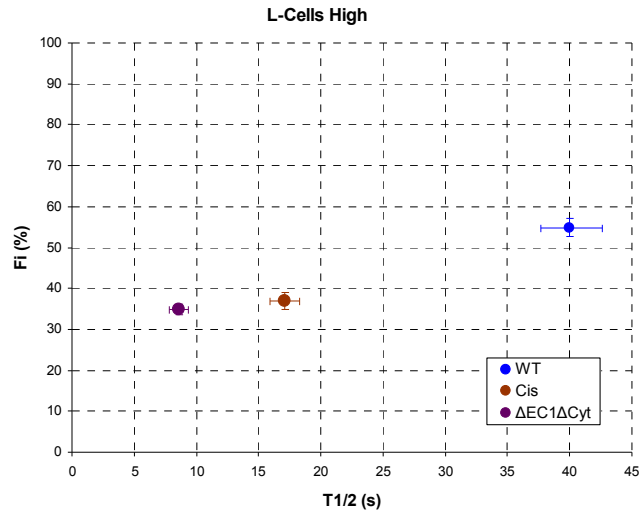
B)
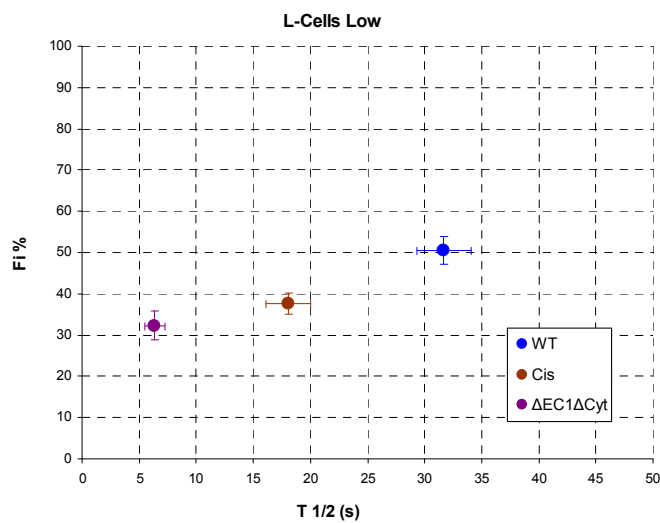
Figure 3.15. FRAP data for V81D/V175D-E-cadherin-GFP (cis interaction mutant) compared to WT E-cadherin-GFP and ΔEC1Δcyt-E-cadherin-GFP in L cells. The data for wild-type E-cadherin-GFP and ΔEC1Δcyt mutant are duplicated from figure 3.5. A) FRAP results for high expressing cells. $N_{cis\ Hi}$=28. B) Data for low expressing cell. $N_{cis\ Low}$=25. Error bars show SEM.

Next, I analysed junctional integrity in L cells expressing V81D/V175D mutant E-cadherin-GFP by measuring TEER. L cells expressing high or low level of V81D/V175D-E-cadherin-GFP have same level of TEER (figure 3.21). This indicates that cis mutant E-cadherin was unable to engage in adhesive E-cadherin complexes and expressing this mutant in L cells did not affect junctional integrity in L cells.

3.6. Deletion of EC1 domain interrupts both cis and trans interactions.

In order to study the combined effect of cis and trans interaction disruption, I made a E-cadherin-GFP mutant with deletion of EC1 domain. In this mutant, residues 2-109 were deleted. Therefore, the ΔEC1 mutant is unable to form both cis and trans interactions. I analyzed the mobility of this mutant using FRAP in PDAC^{fl} cells expressing high and low level of ΔEC1-E-cadherin-GFP (figure 3.16). The data for wild-type E-cadherin-GFP and ΔEC1Δcyt mutant are duplicated from figure 3.4. Interestingly, the FRAP data showed that ΔEC1 mutant had the same Fi% and T1/2 as trans or cis mutants (in both high and low expressing cells) (p values for t test comparing trans mutant (W2A-E-cadherin-GFP) and ΔEC1 mutant in high expressing cells for Fi% and T1/2 are P=0.593 and P=625). Moreover, cis, trans and ΔEC1 mutants, which all retained cytoplasmic tail, had significantly higher T1/2 than ΔEC1Δcyt-E-cadherin-GFP in PDAC^{fl} (p values for t test comparing ΔEC1 and ΔEC1Δcyt mutants in high expressing PDAC^{fl} cells are P=0.178 and P=<0.001for Fi% and T1/2). Therefore, cytoplasmic interaction and binding to actin significantly decreased the mobility of E-cadherin molecules.

A)
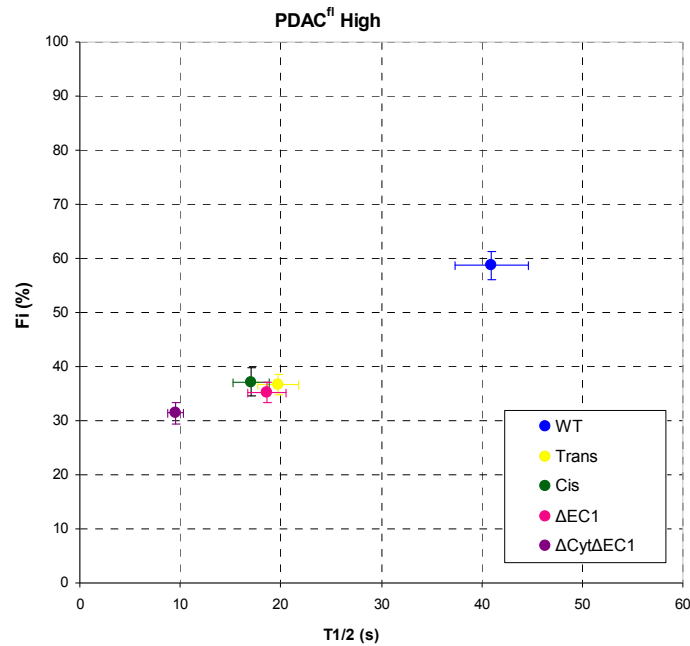
B)
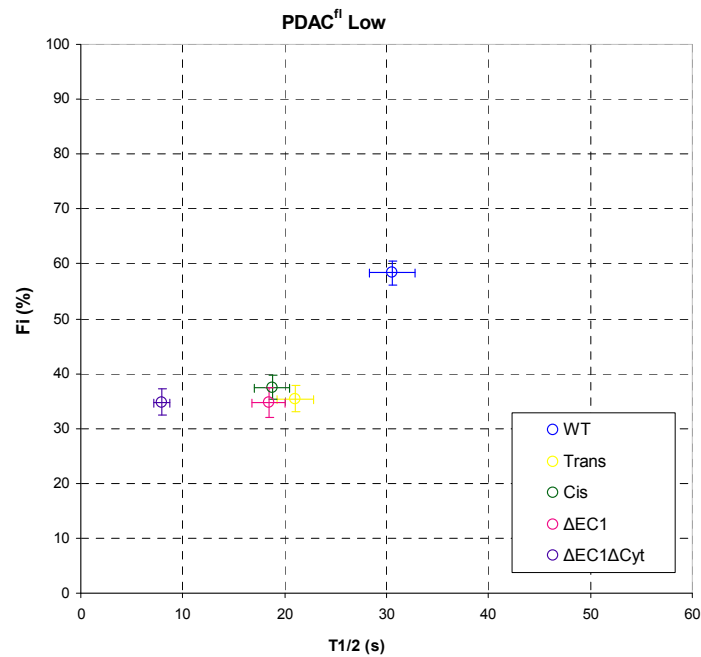
Figure 3.16. Mobility of ΔEC1-E-cadherin-GFP (cis and trans interaction mutant) compared to WT E-cadherin-GFP and ΔEC1Δcyt-E-cadherin-GFP in PDAC^{fl}. ΔEC1 mutant (pink circle) has same Fi% and T1/2 as trans mutant (yellow circle) and cis mutant (green circle). ΔEC1 expressing cells have significantly higher T1/2 than ΔEC1Δcyt. The data for wild-type E-cadherin-GFP and cis, trans and ΔEC1Δcyt mutants are duplicated from figure 3.4, 3.10 and 3.14. A) FRAP results for high expressing cells. N$_{ΔEC1\ Hi}$=32. B)Data for low expressing cell. N$_{ΔEC1\ Hi}$=24. Error bars show SEM.

Next, I expressed ΔEC1-E-cadherin-GFP in L cells. The FRAP data in L cells was similar to PDAC^{fl} cells (figure 3.17). The ΔEC1 mutant has the same Fi% and T1/2 as trans mutant and cis mutant in both high and low expressing cells (p values for t

test comparing cis and ΔEC1 mutant in high expressing cells for Fi% and T1/2 are P=0.297 and P=1.0). ΔEC1 expressing cells have significantly slower rate of mobility than the ΔEC1Δcyt mutant (p values for t test comparing ΔEC1 and ΔEC1Δcyt mutants in high expressing L cells are P=0.824 and P=<0.001for Fi% and T1/2).

A)
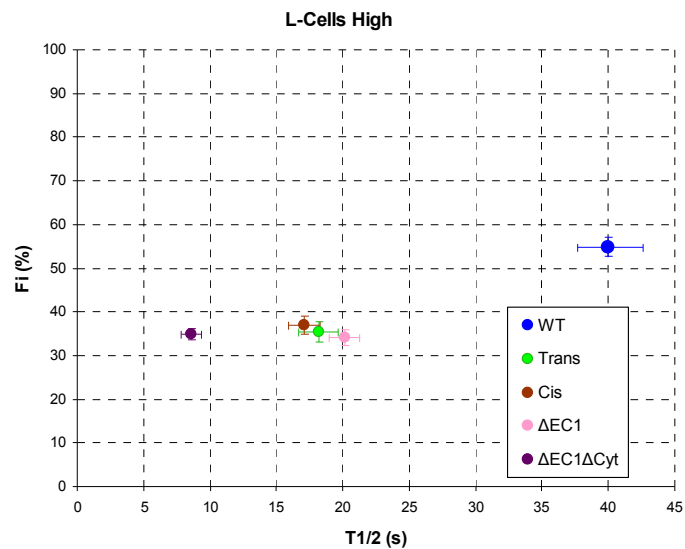
B)
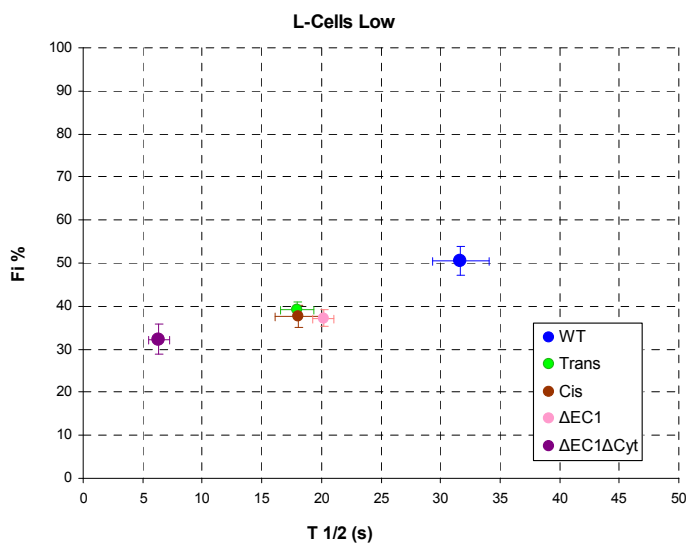
Figure 3.17. Mobility of for ΔEC1-E-cadherin-GFP (cis and trans interaction mutant) compared to Wild-type E-cadherin-GFP and ΔEC1Δcyt-E-cadherin-GFP in L cells. ΔEC1 mutant (pink circle) has same Fi% and T1/2 as trans mutant (yellow circle) and cis mutant (green circle). The data for wild-type E-cadherin-GFP and cis, trans and ΔEC1Δcyt mutants are duplicated from figure 3.5, 3.11 and 3.15. ΔEC1 expressing cells have significantly higher T1/2 than ΔEC1Δcyt. A) FRAP results for high expressing cells. N$_{\Delta EC1\ Hi}$=31. B) Data for low expressing cell. N$_{\Delta EC1\ Hi}$=22. Error bars show SEM.

Moreover, in order to see whether ΔEC1 mutants form functional adhesive complexes or not, I analysed junctional integrity in L cells expressing high and low level of ΔEC1 mutant using TEER. The results showed that TEER in L cells expressing ΔEC1 mutant was similar to L cells with no E-cadherin expression (figure 3.21) (p values for t test comparing L cell with high or low expressing EC1 mutant with are P = 0.996 and P = 0.996 respectively), indicating that GFP-ΔEC1-E-cadherin did not form adhesive complexes and can not affect cell-cell junction strength.

In summary, these data showed that disruption of trans or cis interactions, or both reduces the immobile fraction to similar level of ΔEC1Δcyt mutant. However, all three of these mutants recovered more slowly than the non-binding ΔEC1Δcyt mutant, which recovers at the rate of free diffusion. These three mutants all retain the cytoplasmic tail. Therefore, the cytoplasmic tail is responsible for the reduced rate of mobility in W2A, V81D/V175D and ΔEC1-E-cadherin-GFP mutants (which retained the cytoplasmic tail) compared to the ΔEC1Δcyt mutant. The cytoplasmic tail binds to actin, which suggests that actin binding could slow recovery. In next section, I analysed the effect of disrupting actin binding in E-cadherin dynamics.

3.7. Deletion of cytoplasmic domain disrupts interaction with actin cytoskeleton:

The cytoplasmic tail of E-cadherin has two domains: JMD (Juxta-membrane domain), which binds to p120, and the β-catenin binding domain. Interaction with catenins connects the cytoplasmic domain of E-cadherin to the actin cytoskeleton. To understand how disrupting interaction with actin affects E-cadherin mobility, I expressed an E-cadherin-GFP mutant with deletion of residues 580 to 726 in PDAC[fl] cells. In this deletion, the cytoplasmic domain of E-cadherin, which consists of both the juxta-membrane domain and the β-catenin binding domain, is deleted. Therefore, this mutant is unable to form any interaction with the actin cytoskeleton.

FRAP analysis of Δcyt mutants in PDAC[fl] cells with high and low expression level showed that in high expressing cells, the Δcyt mutant has the same immobile fraction and recovery rate as the ΔEC1Δcyt mutant (figure 3.18) (p values for Fi% and T1/2 are P=0.465 and P=0.718). This means that retention of both cis and trans interactions did not slow down the diffusion of the Δcyt mutant compared to rate of free diffusion of the ΔEC1Δcyt mutant. Moreover, cis and trans interactions in

ΔEC1-E-cadherin molecule were not able to immobilize E-cadherin molecules stably within E-cadherin adhesive clusters in the membrane.

Comparing FRAP data for all E-cadherin-GFP mutants in high expressing cells reveals that all mutants have similar immobile fraction. Which indicates all three interactions of E-cadherin molecules: cis, trans and actin are necessary for immobilizing E-cadherin in adhesive clusters and disrupting any one of these interaction is enough to bring down the immobilized E-cadherin fraction to the same level as the non-binding mutant. However, the recovery rate was significantly faster for E-cadherin mutants in which actin interaction is disrupted.

Next, I analysed FRAP of the Δcyt mutant in low expressing PDAC[fl] cells (figure 3.18.B). In low expressing cells Δcyt mutant have smaller Fi% and T1/2 than wild-type E-cadherin (P values for Fi and T1/2 are P = 0.033 and P = 0.003). However, low expressing Δcyt mutant have significantly higher Fi% and T1/2 compared to ΔEC1Δcyt mutant (P = <0.001 and P = 0.001). The t test showed there is significant difference between Fi% and T1/2 in Δcyt mutants between high and low expressing cells (P = <0.001 and P = <0.001).

A)
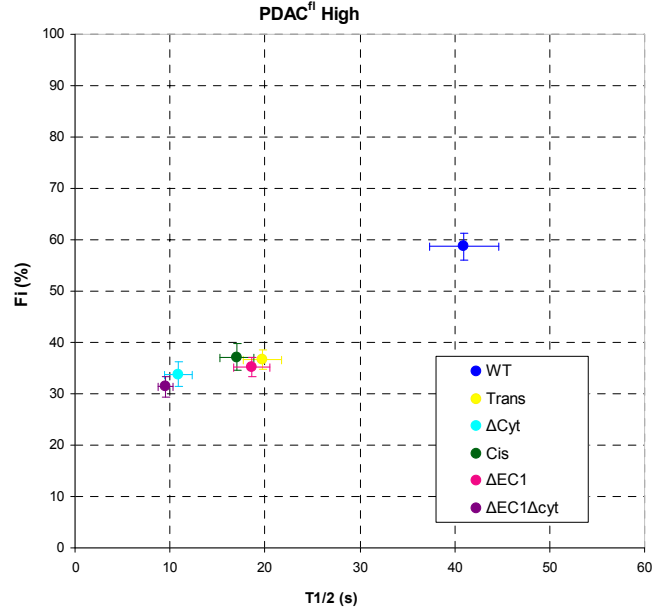
B)
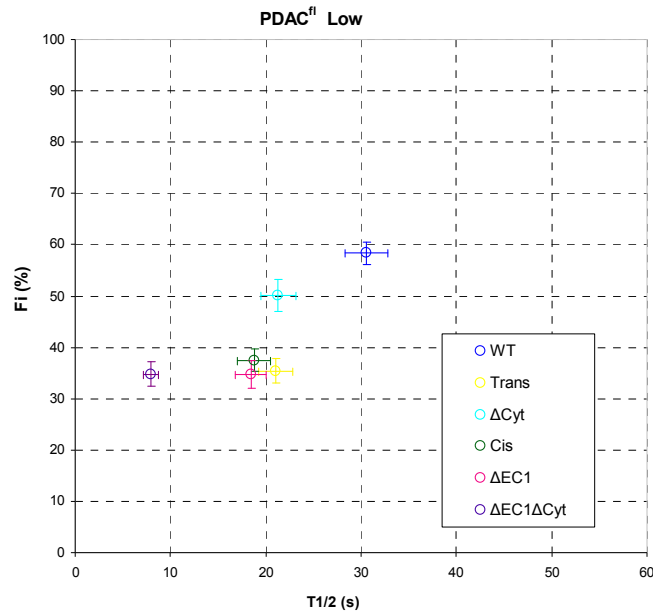
Figure 3.18. FRAP data for GFP-Δcyt-E-cadherin compared to other mutant and WT-E-cadherin-GFP and ΔEC1Δcyt-E-cadherin-GFP in PDAC^{fl} cells. . The data for wild-type E-cadherin-GFP and cis, trans, ΔEC1 and ΔEC1Δcyt mutants are duplicated from figure 3.4, 3.10, 3.14 and 3.16. A) FRAP results for high expressing cells. Δcyt mutant have same Fi% and T1/2 as ΔEC1Δcyt mutant. $N_{Δcyt\ High}$=18. B) Data for low expressing cell. $N_{Δcyt\ Low}$=26. Error bars show SEM.

To further investigate the different mobility of GFP-Δcyt-E-cadherin in high and low expressing cells, I looked at junctional integrity of high and low expressing PDAC^{fl} cells using TEER (figure 3.19). High expression of the Δcyt mutant in PDAC^{fl} cells significantly lowered cell layer electrical resistance compared to PDAC^{fl} cells (P = 0.006); in contrasts, low expressing cells have similar barrier function as PDAC^{fl}

cells (P = 0.100). Moreover, high expression of the ΔEC1Δcyt mutant in PDAC cells reduces TEER in PDAC^fl cells as well (data duplicated from figure 3.7.). These data suggest that a small amount of mutant Δcyt molecules in PDAC^fl cells, which already express wild-type endogenous E-cadherin, was tolerated by adhesion complexes. Under these circumstances, the Δcyt mutant can interact via cis and trans interactions with other E-cadherin molecules. Therefore, low expressing Δcyt mutant cells are more immobile and recover slower than the ΔEC1Δcyt mutant that do not foms clusters. However, at higher expression levels, TEER measurements indicated that cell-cell adhesion decreased compared to PDAC^fl cells, and the immobile fraction of GFP-Δcyt-E-cadherin was reduced to the same level as other E-cadherin mutants.
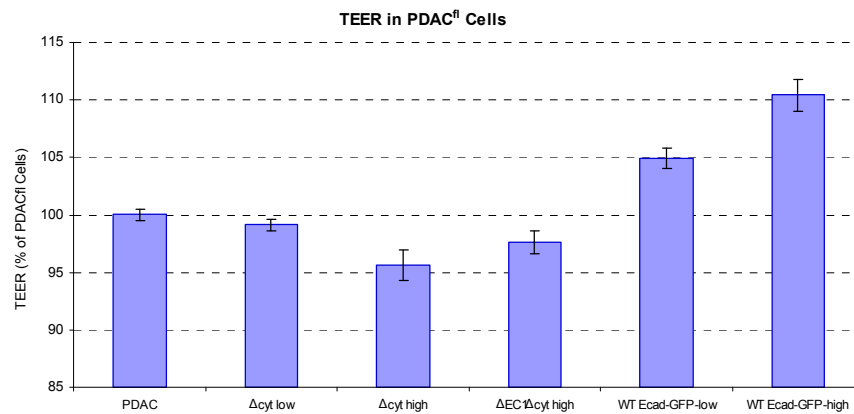
3.19. Junctional integrity in PDAC^fl cells expressing high and low level of GFP-Δcyt-E-cadherin. The trans-epithelial electrical resistance is normalized to PDAC^fl cells. Low expressing GFP-Δcyt-E-cadherin cells have TEER similar to PDAC^fl cells, but high expression of GFP-Δcyt-E-cadherin mutant significantly decreased cell-cell adhesion in these cells. TEER for high expression of ΔEC1Δcyt-E-cadherin-GFP and high and low expression of wild-type E-cadherin-GFP are duplicated from figure 3.7. N=3. Error bars show SEM.

Subsequently, I expressed the tailless Δcyt mutant in L cells. FRAP analysis revealed that, this mutant had a significantly lower immobile fraction and increased rate of mobility than wild-type E-cadherin-GFP in both high and low expressing cells (figure 3.20) (p values for t test comparing WT and Δcyt mutant in high expressing cells for Fi% and T1/2 are P=<0.001 and P=<0.001. P values are P=0.004 and P=<0.001 for low expressing cells). L cells (which do not express wild type endogenous E-cadherin) had similar Fi% and T1/2 for high and low expressing cells

(P values for Fi% and T1/2 are P=0.702 and P=0.947). These data confirm that, the difference between high and low expression of Δcyt mutant in PDAC^{fl} cells is due to interactions between mutant E-cadherin molecules with wild-type endogenous E-cadherin molecules.

A)
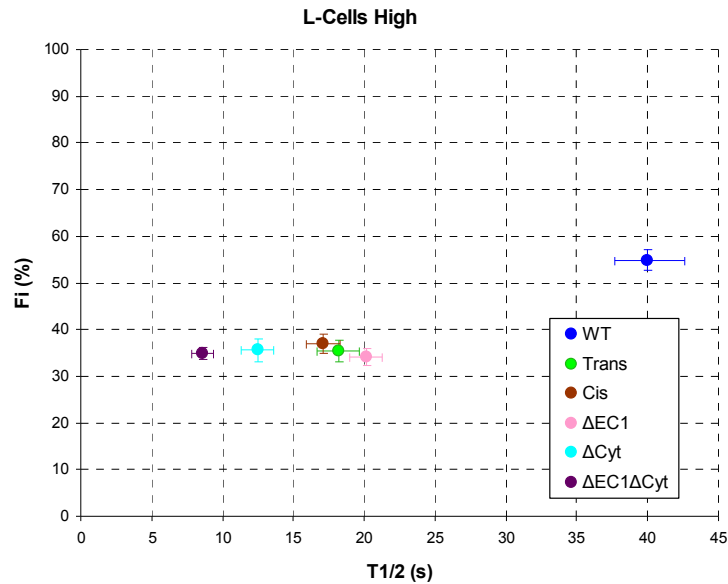
B)
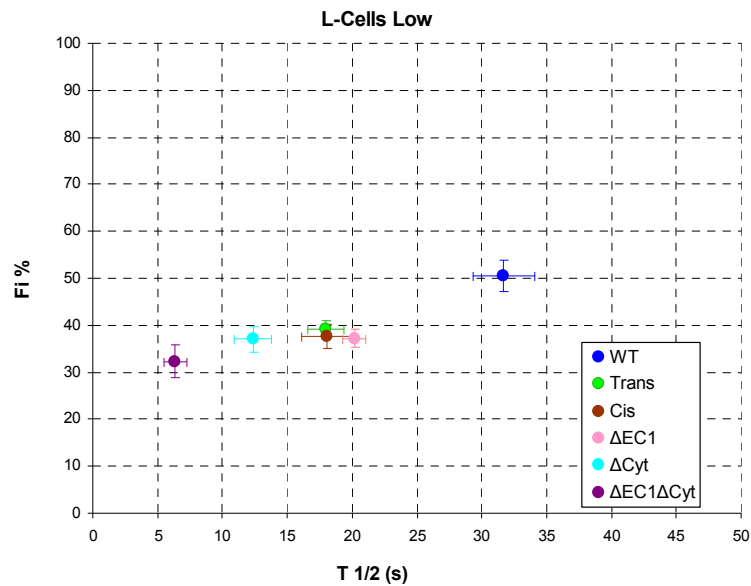
Figure 3.20. Mobility of Δcyt-E-cadherin-GFP compared to other mutant and wild-type E-cadherin-GFP and ΔEC1Δcyt-E-cadherin-GFP in L cells. The Δcyt mutant recovers significantly faster than ΔEC1 and cis or trans mutants in both high and low expressing cells. The data for wild-type E-cadherin-GFP and cis, trans, ΔEC1 and ΔEC1Δcyt mutants are duplicated from figure 3.5, 3.11, 3.15 and 3.17. A) FRAP results for high expressing cells. N$_{Δcyt\ Hi}$=23. B) Data for low expressing cell. N$_{Δcyt\ Low}$=21. Error bars show SEM.

The FRAP results demonstrate that all E-cadherin mutants have Fi% similar to ΔEC1Δcyt mutant in L cells. Mutation of any single interaction reduces the immobile fraction to the level of the non-functional mutant. This indicates that, all mutants are incapable of forming adhesive E-cadherin complexes. To confirm this, I measure TEER in L cells expressing high and low expression level of wild-type E-cadherin-GFP and cis, trans, ΔEC1 and Δcyt mutants (figure 3.21). The results revealed that only wild-type E-cadherin-GFP expression increased junctional integrity in L cells. Moreover, this increase in TEER is dependent on the amount of E-cadherin-GFP expressed in the cells. However, high or low expression level of cis, trans, ΔEC1 or Δcyt mutant molecules do not increases TEER in L cells. This indicates that none of these mutants are able to form adhesive E-cadherin complexes.
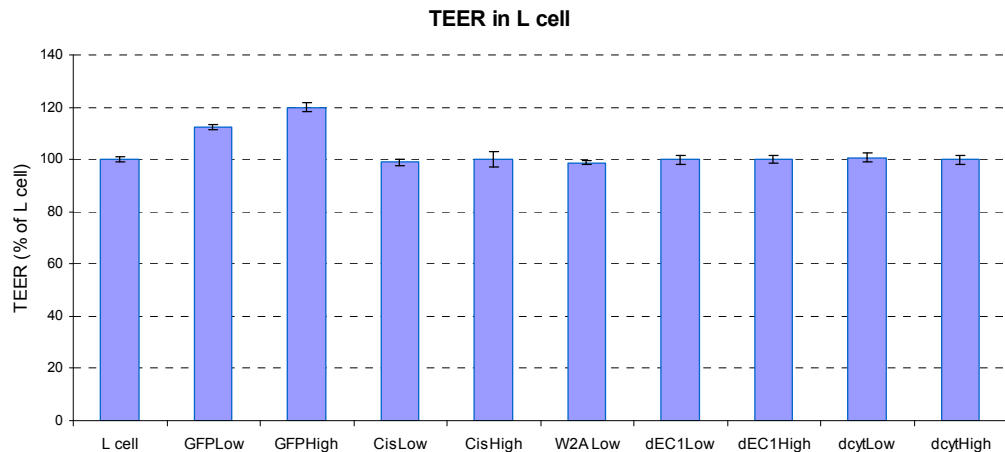
3.21. Junctional integrity of L cells expressing high and low levels of wild-type E-cadherin-GFP, cis, trans, ΔEC1 and Δcyt mutants. Wild-type E-cadherin-GFP expression increased cell-cell adhesion in L cells. However, high or low expression level of cis, trans, ΔEC1 or Δcyt mutant molecules do not increases TEER in L cells. This indicates that none of these mutants are able to form adhesive E-cadherin complexes. The data for L cell expressing high and low wt-E-cadherin_GFP are duplicated from figure 3.8. N=3. Error bars show SEM.

In summary, these data showed that disruption of any single interaction of the E-cadherin molecule was sufficient to reduce Fi to 30%. This 30% immobile fraction is the same level as the non-functional mutant ΔEC1ΔCyt-E-cadherin-GFP and is most likely due to non-specific trapping in the plasma membrane (Kusumi 2005). This indicates that, all three interactions (cis-, trans-, and actin) are required for inclusion of E-cadherin-GFP into adhesive immobile E-cadherin clusters in junctions.

Moreover, all the mutants recovered faster than E-cadherin-GFP. In PDAC^{fl} cells, the cytoplasmic deletion mutant ΔCyt-E-cadherin-GFP recovered at the rate of ΔEC1ΔCyt mutant, demonstrating that cis- and trans- interactions mediated by the EC1 domain did not restrain the diffusion of this mutant. In contrast, mutants retaining the cytoplasmic tail recovered significantly more slowly, irrespective of the cis and trans interactions which retained by the EC1 domain. However, none of the mutants recovered as slowly as wild-type E-cadherin retaining all three interactions. This suggests that the slow mobility of wild-type E-cadherin-GFP depends on the ability to form all three interactions: cis, trans, and actin.

3.8. Wild-type E-cadherin-GFP but not mutants have diffusion uncoupled FRAP recovery.

The results in section 3.2 showed that the recovery rate of ΔEC1ΔCyt-E-cadherin-GFP was much faster than wild-type E-cadherin-GFP, suggesting that wild-type E-cadherin binds to stationery complexes in the membrane by the cis, trans and actin interactions. These associations immobilize 30% of E-cadherin molecules, and that is the source for reduction of Fi from 60% in wild-type E-cadherin-GFP to 30% in GFP-ΔEC1ΔCyt-E-cadherin. In addition, ΔEC1ΔCyt-E-cadherin-GFPmutants (or other mutants) recovered much faster than wild-type E-cadherin-GFP, which indicates that cis, trans and actin interactions also bind E-cadherin to stationary adhesive clusters transiently. The recovery of the non-binding ΔEC1ΔCyt-E-cadherin-GFP mutant does not depend on any binding so it recovers as fast as the diffusion rate. However, binding\unbinding from these adhesive clusters delayed the diffusion rate of wild-type E-cadherin-GFP molecules. One way to confirm that FRAP recovery is determined by association\dissociation rates and not by the rate of diffusion is to vary the size of the bleached region (Sprague 2005, Nanes 2012). If recovery occurs by diffusion only, T1/2 will depend on the diffusion of monomers from the centre to the edge of the ROI. Therefore, T1/2 should increase with growing ROI diameter. On the other hand, if recovery is driven by binding\unbinding of stationary complexes rather than diffusion, the ROI size does not affect T1/2 and the recovery rate reflects the molecular association and dissociation rates.

Analyzing FRAP recovery time for GFP-f, GFP-ΔEC1ΔCyt-E-cadherin, ΔEC1-E-cadherin-GFP and wild-type E-cadherin-GFP molecules in PDAC^{fl} cells using ROIs

of 2, 3, and 4 μm in diameter in PDAC^fl cells showed that the recovery time of GFP-f and ΔEC1ΔCyt-E-cadherin-GFP significantly increased with increasing ROI diameter (Figure 3.22.A). GFP-f and ΔEC1ΔCyt-E-cadherin-GFP cannot bind to anything in the plasma membrane. Therefore, their FRAP recovery are only driven by diffusion rates.

In addition, FRAP analysis of the ΔEC1-E-cadherin-GFP mutant in PDAC^fl cells using different ROI sizes showed there is a significant difference between T1/2 of 2 μm and 4 μm ROI diameter (P = 0.013). This mutant is able to bind to the actin cytoskeleton and this interaction slows down the recovery compared to ΔEC1ΔCyt-E-cadherin-GFP mutants. However, the recovery still depends on ROI size. This indicates that the recovery of ΔEC1-E-cadherin-GFP mutants diffusion coupled (see section 1.4.5.2). This indicates that the time for diffusion of molecules across the ROI is longer than the time needed to form new binding and E-cadherin molecules may bind and unbind several times as they move across the bleached region.

In contrast, there is no significant difference between recovery time of wild-type E-cadherin-GFP molecules in 2, 3, and 4 μm ROIs and the recovery time remained constant with increasing ROI diameter (p value for t test between 2 and 4 μm ROIs is P = 0.801). This indicates that recovery of wild-type E-cadherin-GFP molecules is diffusion-uncoupled recovery. In other words, diffusion of wild-type E-cadherin-GFP molecules is much faster than the rate of association\dissociation of cadherin molecules with stationary complexes. This means that the recovery due to diffusion happens first, and is followed by dissociation of bleached molecules and binding of unbleached molecules.

FRAP analysis of GFP-f and wild-type E-cadherin-GFP in L cells showed similar results to PDAC^fl cells. The recovery of GFP-f molecules, which diffuse freely, significantly increased as the ROI size increased from 2 to 3 and from 3 to 4 μm in diameter (figure 3.22.B) (p value for t test between 2 and 4 μm ROIs is P = 0.005). In addition, similar to PDAC^fl cells, there is no significant difference between T1/2 of wild-type E-cadherin-GFP in different ROI sizes, which indicates that the recovery of wild-type E-cadherin-GFP molecules is diffusion uncoupled in L cells (p value for t test between 2 and 4 μm ROIs is P = 0.804).

A)
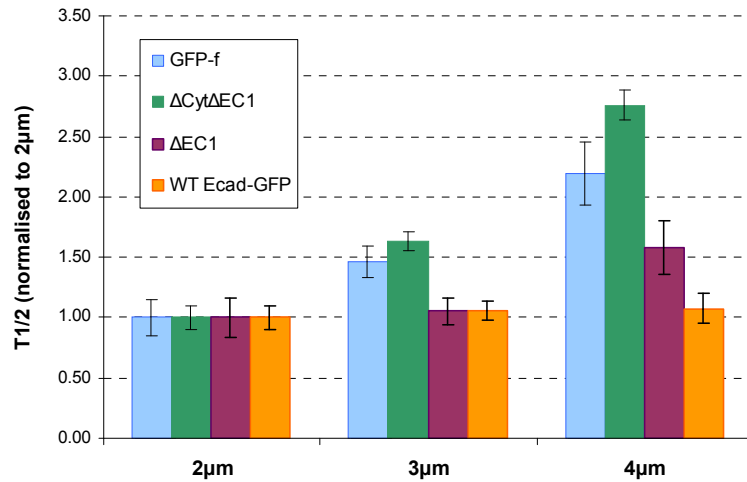
B)
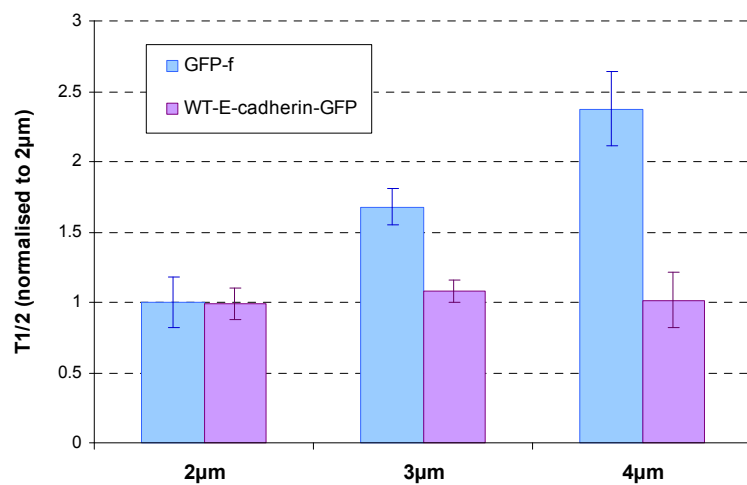
Figure 3.22. FRAP data for different bleach sizes. A) T1/2 for GFP-f and ΔEC1Δcyt-E-cadherin-GFP, GFP-ΔEC1-E-cadherin compared to WT E-cadherin-GFP in high expressing PDAC[fl] cells. B) T1/2 for GFP-f and WT-E-cadherin-GFP in high expressing L cells. Data for 3 and 4 μm ROI are normalized to 2 μm ROI. Error bars show SEM.

3.9. Cross-linking showed that the mobile fraction of E-cadherin-GFP molecules consists of two components.

The FRAP results using different ROI sizes showed that wild-type E-cadherin-GFP molecules had diffusion uncoupled recovery but recovery of E-cadherin mutants are limited by the rate of diffusion only. This indicates that the recovery of wild-type E-cadherin molecules depends on the rate of association\dissociation from E-cadherin clusters in membrane. To confirm that the recovery of E-cadherin was driven by binding\unbinding from stationary complexes, a cross-linker was used to covalently

bind E-cadherin molecules in clusters and then the recovery rate was analysed by FRAP.

For cross-linking experiment the cell-impermeable homo-bifunctional cross-linker Bis[sulfosuccinimidyl] substrate (BS3) was used. Based on the short linking radius of this compound (11.4 Å), it is expected only to cross-link molecules in direct proximity. For comparison with wild-type E-cadherin-GFP, I used ΔEC1ΔCyt-E-cadherin-GFP mutants as these molecules are unable to form extracellular interactions (cis or trans dimerization) and should not be cross-linked.

Initially, I established conditions in which BS3 cross-linked E-cadherin effectively by western blot analysis (Figure 3.23). 20 minutes of treatment with 35 mM BS3 resulted in a weak band of cross-linked E-cadherin. However, 10 minutes of 100 mM BS3 treatment increases the cross linked E-cadherin-GFP band and 20 minutes of 100 mM BS3 treatment resulted in the majority of both E-cadherin and E-cadherin-GFP monomers being cross-linked.

Endogenous E-cadherin has 120 KD molecular weight and GFP fusion with E-cadherin increases the molecular weight of E-cadherin-GFP molecule to around 147 KD. Therefore, the molecular weight of the dimer between two endogenous E-cadherin molecules is around 240 KD and the molecular weight of dimers between two E-cadherin-GFP molecules is 294 KD. The molecular weight of a dimer between an endogenous E-cadherin molecule and an E-cadherin-GFP fusion is 267 KD. Therefore, in the PDAC[fl] cells expressing wt-E-cadherin-GFP, the E-cadherin cross-linked dimers could have three different molecular weight ranges between 240 to 294 KD. Analysing cell lysate from these cells in western blot probed with E-cadherin antibody showed three bands between 240 and 300 molecular weight. However, by probing the blot with anti-GFP antibody only two bands was recognized between 240 and 300 Molecular weigh markers. This indicates that cross-linker is able to cross-link dimers from endogenous E-cadherins and E-cadherin-GFP. Moreover, cross-linking was able to cross-link endogenous and E-cadherin-GFP molecules, which confirms that E-cadherin-GFP is able to form dimers with endogenous E-cadherin in PDAC[fl] cells.

Cell lysates from PDAC[fl] cells expressing ΔEC1ΔCyt-E-cadherin-GFP probed with an anti-E-cadherin antibody demonstrated that BS3 cross-linking only shows one band between 250 and 300 molecular weights. Moreover probing with GFP antibody does not show any cross-linked band on western-blot. Therefore, the dimers in E-

cadherin antibody probed blot are Endogenous E-cadherin molecules and cross-linker is not able to cross-link ΔEC1ΔCyt-E-cadherin-GFP molecules. This indicates that ΔEC1ΔCyt mutant are binding together and they are only presents as monomers in the plasma membrane. This suggests that BS3 treatment is only able to cross-link cis or trans dimerized molecules in the plasma membrane.
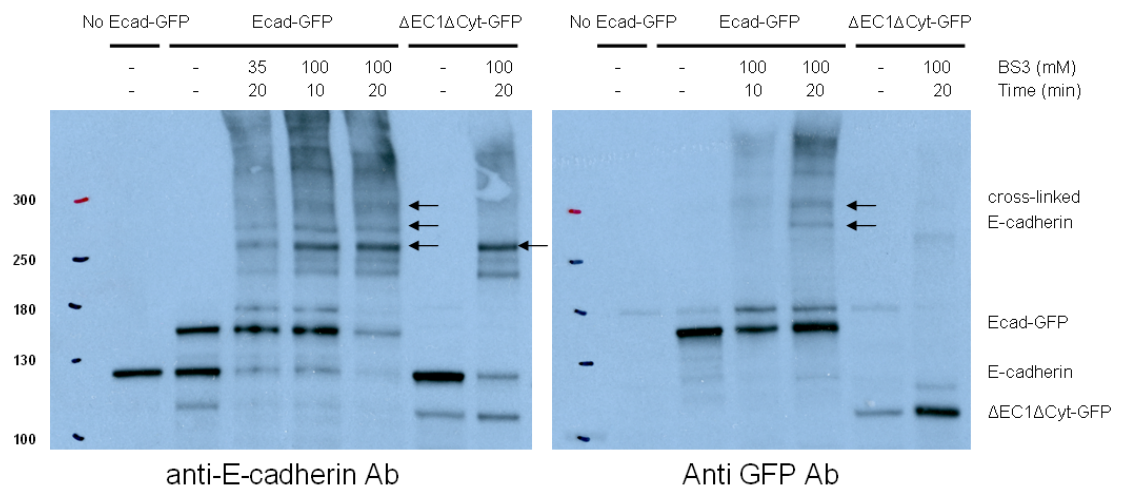
Figure 3.23. The western blots for demonstrating cross-linking of E-cadherin. The blot on the right is probed with GFP antibody and the plot o the right is probed with anti-E-cadherin antibody. First lane from left on both blots is PDAC[fl] cells with no E-cadherin-GFP expression. cell lysates from PDAC[fl] cells with high expression of E-cadherin-GFP are treated with 0, 35, 100 mM concentrations of BS3 cross-linker for 10 or 20 min. Two lanes on the right on both blots show cell lysate form PDAC[fl] cells expressing high level of ΔEC1ΔCyt-E-cadherin-GFP analysed before and after treatment with 100 mM cross-linker for 20 min. BS3 is not able to cross-linking ΔEC1ΔCyt-E-cadherin-GFP molecules.

FRAP analysis on BS3-treated PDAC[fl] cells expressing a high level of wild-type E-cadherin-GFP showed that the treatment with cross-linker in all the conditions (20min 35mM, 20min 100mM or 10min 100mM) significantly increased the amount of E-cadherin immobilized and decreases T1/2 compared to non-treated cells (Figure 3.24).

In agreement with western blot analysis, BS3 cross-linker was unable to affect the mobility of ΔEC1ΔCyt-E-cadherin-GFP mutants (p values for t test comparing before and after cross-linker treatments are P = 0.138 and P = 0.060 for Fi% and T1/2).

FRAP data showed that 20 minutes of 100mM BS3 treatment significantly increased the Fi% of E-cadherin-GFP from 60% to 85% (p values are P = <0.001 and P =

<0.001 for Fi% and T1/2). Furthermore, T1/2 was dramatically reduced from 50 seconds to 7 seconds, which is not statistically different from the recovery rate of freely diffusing ΔEC1ΔCyt-E-cadherin-GFP molecules (P = 0.353).

Moreover, following 20 min of treatment with BS3, increasing the ROI size from 3 μm to 6μm in diameter caused an increase in the recovery rate of E-cadherin-GFP (P=<0.001). This indicates that the recovery of E-cadherin-GFP became diffusion coupled following treatment with BS3.

When the time of cross-linking was reduced from 20 minutes to 10 minutes, the resulting partial decrease in T1/2 between 3 μm to 6 μm diameter ROI was not statistically significant (P = 0.270).

These data suggest that the 40% mobile fraction of E-cadherin-GFP is comprised of two components. The first component is not cross-linkable. It represents the mobile fraction, which remains after cross-linking E-cadherin-GFP. This component is approximately 15% of total E-cadherin-GFP and consisting of free monomers which are not affected by BS3 treatment. The second component is the difference between the immobile fractions of cross-linked and non-cross-linked E-cadherin-GFP and consists of monomers, which transiently bind\unbind from stationary E-cadherin clusters. Cross-linking with BS3 covalently bound the transiently associated cadherins molecules and prevented dissociation of these molecules from stationary complexes. Therefore, cross-linking significantly increased immobile fraction of E-cadherin molecules from 60% to 85%. This 25% represents the component of mobile E-cadherin molecules that are able to bind\unbind from stationary complexes.
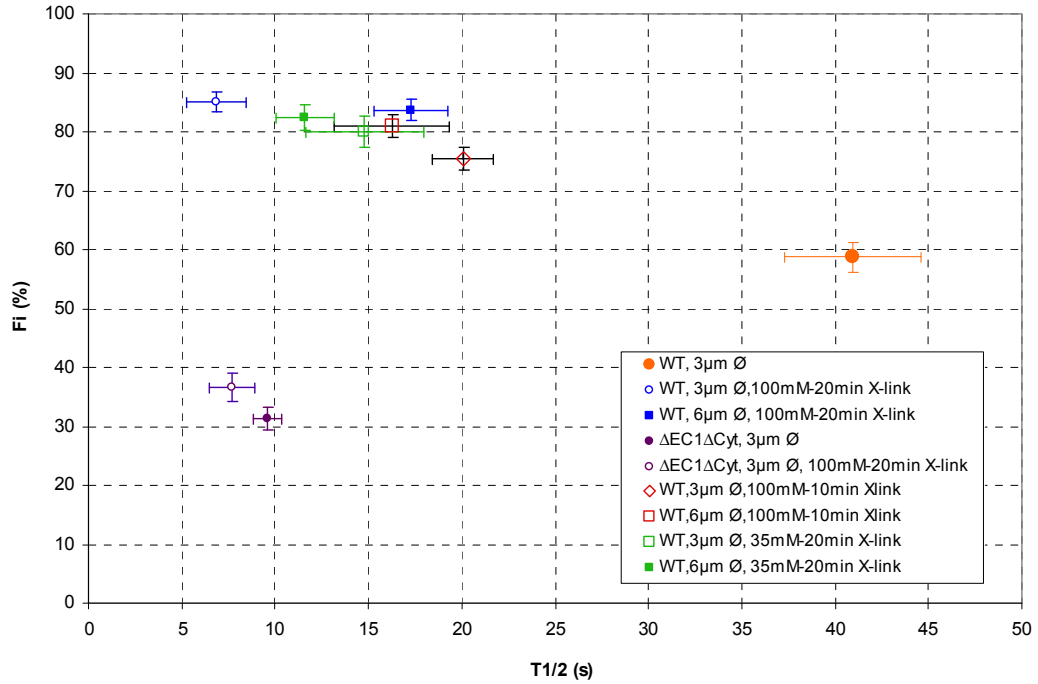
Figure 3.24. FRAP results in PDAC^fl cells expressing either WT E-cadherin-GFP or ΔEC1ΔCyt-E-cadherin-GFP, after treatment with BS3 cross-linker. Treatment with BS3 cross-linker significantly increased Fi% and decreases T1/2 compared to no cross-linking (orange circle)**.** Green squares show FRAP results after 20 min treatment with 35 mM of BS3 for 3 μm ROI size (3μm Ø) and 6μm Ø. Orange diamond and red square show FRAP result after 10 min treatment 100 mM BS3 for 3μm Ø and 6μm Ø respectively. The FRAP data show there is no significant difference between 3μm Ø and 6μm Ø in both cases. However, after 20 min treatment with 100 mM BS3 there is a significant difference between T1/2 of 3μm Ø and 6μm Ø (blue circle and blue square). BS3 treatment on ΔEC1ΔCyt-E-cadherin-GFP expressing cells doesn't has any significant difference in FRAP data (purple circles). Data for WT-E-cadherin-GFP and ΔEC1ΔCyt-E-cadherin-GFP is duplicated from figure 3.4. Error bars show SEM.

$N_{WT,3μmø,100mM,20minXlink}$=15, $N_{WT,6μmø,100mM,20minXlink}$=16, $N_{ΔEC1ΔCyt,3μmø100mM,20minXlink}$=16,

$N_{WT,3μmø,100mM,10minXlink}$=27, $N_{WT,6μmø,100mM,10minXlink}$=10, $N_{WT,3μmø,35mM,20minXlink}$=14,

$N_{WT,3μmø,35mM,20min\ Xlink}$=14.

PDAC^fl cells: T test values:

	N	Fi%	±SEM	T1/2	±SEM		N	Fi%	±SEM	T1/2	±SEM	FI%	t1/2
wtEcad Hi	24	40.9	2.57	40.9	3.64	w2a Hi	24	36.7	1.89	19.76	1.99	P=<0.001	P=<0.001
wtEcad Hi	24	40.9	2.57	40.9	3.64	Δcyt Hi	18	33.8	2.47	10.85	1.48	P=<0.001	P=<0.001
wtEcad Hi	24	40.9	2.57	40.9	3.64	cis Hi	26	37.1	2.58	17.01	1.80	P=<0.001	P=<0.001
wtEcad lo	24	40.9	2.57	40.9	3.64	Δcyt lo	26	50.2	3.13	21.29	1.86	**P = 0.033**	**P = 0.003**
wtEcad Hi	24	40.9	2.57	40.9	3.64	ΔEC1 Hi	32	35.2	1.94	18.58	1.92	P=<0.001	P=<0.001
wtEcad Hi	24	40.9	2.57	40.9	3.64	ΔΔ Hi	39	31.4	1.96	9.57	0.78	P=<0.001	P=<0.001
wtEcad lo	32	58.3	2.17	30.6	2.25	wtEcad Hi	24	40.9	2.57	40.94	3.64	P = 0.916	P = 0.014
w2a Hi	24	36.7	1.89	19.8	1.99	w2a lo	20	35.4	2.36	21.01	1.78	P = 0.679	P = 0.650
Δcyt lo	26	50.2	3.13	21.3	1.86	Δcyt Hi	18	33.8	2.47	10.85	1.48	**P=<0.001**	**P=<0.001**
cis lo	31	37.5	2.18	18.8	1.71	cis Hi	26	37.1	2.58	17.01	1.80	P = 0.755	P = 0.543
ΔEC1 lo	24	34.7	2.70	18.4	1.60	ΔEC1 Hi	32	35.2	1.94	18.58	1.92	P = 0.875	P = 0.637
ΔΔ lo	23	34.8	2.45	7.91	0.78	ΔΔ Hi	39	31.4	1.96	9.57	0.78	P = 0.284	P = 0.153
Δcyt Hi	18	33.8	2.47	10.9	1.48	cis Hi	26	37.1	2.58	17.01	1.80	P = 0.382	P = 0.009
Δcyt Hi	18	33.8	2.47	10.9	1.48	ΔEC1 Hi	32	35.2	1.94	18.58	1.92	P = 0.676	P = 0.002
Δcyt Hi	18	33.8	2.47	10.9	1.48	ΔΔ Hi	39	31.4	1.96	9.57	0.78	P = 0.465	P = 0.718
Δcyt Hi	18	33.8	2.47	10.9	1.48	GFP-f	9	26.3	1.82	5.54	0.48	P = 0.047	P = 0.010
cis Hi	26	37.1	2.58	17.0	1.80	ΔEC1 Hi	32	35.2	1.94	18.58	1.92	P = 0.540	P = 0.521
cis Hi	26	37.1	2.58	17.0	1.80	ΔΔ Hi	39	31.4	1.96	9.57	0.78	P = 0.076	P=<0.001
ΔEC1 Hi	32	35.2	1.94	18.58	1.92	ΔΔ Hi	39	31.4	1.96	9.57	0.78	P = 0.178	P=<0.001
ΔΔ Hi	39	31.4	1.96	9.57	0.78	GFP-f	9	26.3	1.82	5.54	0.48	P = 0.210	P = 0.005
w2a Hi	24	36.7	1.89	19.8	1.99	Δcyt Hi	18	33.8	2.47	10.85	1.48	P = 0.360	P=<0.001
w2a Hi	24	36.7	1.89	19.8	1.99	cis Hi	26	37.1	2.58	17.01	1.80	P = 0.869	P = 0.303
w2a Hi	24	36.7	1.89	19.8	1.99	Δec1 Hi	32	35.2	1.94	18.58	1.92	P = 0.593	P = 0.625
w2a Hi	24	36.7	1.89	19.8	1.99	ΔΔ Hi	39	31.4	1.96	9.57	0.78	P = 0.074	P=<0.001
Δcyt lo	26	50.2	3.13	21.3	1.86	cis lo	31	37.5	2.18	18.75	1.71	P=0.001	P = 0.697
Δcyt lo	26	50.2	3.13	21.3	1.86	ΔEC1 lo	24	34.7	2.70	18.43	1.60	P=<0.001	P = 0.854
Δcyt lo	26	50.2	3.13	21.3	1.86	ΔΔ lo	23	34.8	2.45	7.91	0.78	P=<0.001	P=0.001
Δcyt lo	26	50.2	3.13	21.3	1.86	GFP-f	9	26.3	1.82	5.54	0.48	P <0.001	P=0.001
w2a lo	20	35.4	2.36	21.0	1.78	Δcyt lo	26	50.2	3.13	21.29	1.86	P = 0.007	P = 0.724
w2a lo	20	35.4	2.36	21.0	1.78	cis lo	31	37.5	2.18	18.75	1.71	P = 0.786	P = 0.875
w2a lo	20	35.4	2.36	21.0	1.78	ΔEC1 lo	24	34.7	2.70	18.43	1.60	P = 0.720	P = 0.943
w2a lo	20	35.4	2.36	21.0	1.78	ΔΔ lo	23	34.8	2.45	7.91	0.78	P = 0.740	P=<0.001
w2a lo	20	35.4	2.36	21.0	1.78	GFP-f	9	26.3	1.82	5.54	0.48	P = 0.113	P=<0.001
cis lo	31	37.5	2.18	18.8	1.71	ΔEC1 lo	24	34.7	2.70	18.43	1.60	P = 0.411	P = 0.893
cis lo	31	37.5	2.18	18.8	1.71	ΔΔ lo	23	34.8	2.45	7.91	0.78	P = 0.372	P=<0.001
cis lo	31	37.5	2.18	18.8	1.71	GFP-f	9	26.3	1.82	5.54	0.48	P = 0.007	P=<0.001
ΔEC1 lo	24	34.7	2.70	18.4	1.60	ΔΔ lo	23	34.8	2.45	7.91	0.78	P = 0.969	P=<0.001
ΔEC1 lo	24	34.7	2.70	18.4	1.60	GFP-f	9	26.3	1.82	5.54	0.48	P = 0.056	P=<0.001
ΔΔ lo	23	34.8	2.45	7.91	0.78	GFP-f	9	26.3	1.82	5.54	0.48	P = 0.036	P = 0.063
wtEcad lo	32	58.3	2.17	30.6	2.25	w2a lo	20	35.4	2.36	21.01	1.78	P <0.001	P = 0.009
wtEcad lo	32	58.3	2.17	30.6	2.25	cis lo	31	37.5	2.18	18.75	1.71	P=<0.001	P=<0.001
wtEcad lo	32	58.3	2.17	30.6	2.25	ΔEC1 lo	24	34.7	2.70	18.43	1.60	P=<0.001	P=<0.001
wtEcad lo	32	58.3	2.17	30.6	2.25	ΔΔ lo	23	34.8	2.45	7.91	0.78	P=<0.001	P=<0.001

Table 3.1. Summary of FRAP data and T test values for PDAC^fl cells.

L cell

T test values

	N	Fi%	±SEM	T1/2	±SEM		N	Fi%	±SEM	T1/2	±SEM	imob	t1/2
wtEcad lo	19	50.5	3.33	31.7	2.39	wtEcad Hi	30	54.9	2.25	40.0	2.66	P = 0.281	P=<0.001
wtEcad lo	19	50.5	3.33	31.7	2.39	w2a lo	33	39.1	1.89	18.0	1.37	P = 0.003	P=<0.001
wtEcad lo	19	50.5	3.33	31.7	2.39	Δcyt lo	21	37.0	2.76	12.3	1.46	P = 0.004	P=<0.001
wtEcad lo	19	50.5	3.33	31.7	2.39	cis lo	25	37.7	2.54	18.1	1.97	P=0.001	P=<0.001
wtEcad lo	19	50.5	3.33	31.7	2.39	ΔEC1 lo	22	37.1	1.95	20.2	0.92	P = 0.003	P=<0.001
wtEcad lo	19	50.5	3.33	31.7	2.39	ΔΔ lo	11	32.3	3.48	6.4	0.86	P=0.001	P=<0.001
wtEcad lo	19	50.5	3.33	31.7	2.39	GFP-f	26	28.8	2.16	4.5	0.36	P=<0.001	P=<0.001
wtEcad Hi	30	54.9	2.25	40.0	2.66	w2a Hi	41	35.5	2.28	18.2	1.48	P=<0.001	P=<0.001
wtEcad Hi	30	54.9	2.25	40.0	2.66	Δcyt Hi	23	35.6	2.48	12.4	1.16	P=<0.001	P=<0.001
wtEcad Hi	30	54.9	2.25	40.0	2.66	cis Hi	28	36.9	1.99	17.1	1.18	P=<0.001	P=<0.001
wtEcad Hi	30	54.9	2.25	40.0	2.66	ΔEC1 Hi	31	34.1	1.78	20.1	1.15	P=<0.001	P=<0.001
wtEcad Hi	30	54.9	2.25	40.0	2.66	ΔΔ Hi	15	34.9	1.32	8.6	0.78	P=<0.001	P=<0.001
wtEcad Hi	30	54.9	2.25	40.0	2.66	GFP-f	26	28.8	2.16	4.5	0.36	P=<0.001	P=<0.001
w2a lo	33	39.1	1.89	18.0	1.37	w2a Hi	41	35.5	2.28	18.2	1.48	P = 0.258	P = 0.798
Δcyt lo	21	37.0	2.76	12.3	1.46	Δcyt Hi	23	35.6	2.48	12.47	1.16	P = 0.702	P = 0.947
cis lo	25	37.7	2.54	18.1	1.97	cis Hi	28	36.9	1.99	17.1	1.18	P = 0.699	P = 0.670
ΔEC1 lo	22	37.1	1.95	20.2	0.92	ΔEC1 Hi	31	34.1	1.78	20.1	1.15	P = 0.103	P = 0.814
ΔΔ lo	11	32.3	3.48	6.4	0.86	ΔΔ Hi	15	34.9	1.32	8.6	0.78	P = 0.449	P = 0.133
w2a lo	33	39.1	1.89	18.0	1.37	Δcyt lo	21	37.0	2.76	12.3	1.46	P = 0.529	P = 0.010
w2a lo	33	39.1	1.89	18.0	1.37	cis lo	25	37.7	2.54	18.1	1.97	P = 0.657	P = 0.808
w2a lo	33	39.1	1.89	18.0	1.37	ΔEC1 lo	22	37.1	1.95	20.2	0.92	P = 0.500	P = 0.091
w2a lo	33	39.1	1.89	18.0	1.37	ΔΔ lo	11	32.3	3.48	6.4	0.86	P = 0.091	P=<0.001
w2a lo	33	39.1	1.89	18.0	1.37	GFP-f	26	28.8	2.16	4.5	0.36	P = 0.018	P=<0.001
Δcyt lo	21	37.0	2.76	12.3	1.46	cis lo	25	37.7	2.54	18.1	1.97	P = 0.887	P = 0.042
Δcyt lo	21	37.0	2.76	12.3	1.46	ΔEC1 lo	22	37.1	1.95	20.2	0.92	P = 0.757	P=<0.001
Δcyt lo	21	37.0	2.76	12.3	1.46	ΔΔ lo	11	32.3	3.48	6.4	0.86	P = 0.316	P = 0.008
Δcyt lo	21	37.0	2.76	12.3	1.46	GFP-f	26	28.8	2.16	4.5	0.36	P = 0.124	P = 0.002
cis lo	25	37.7	2.54	18.1	1.97	ΔEC1 lo	22	37.1	1.95	20.2	0.92	P = 0.871	P = 0.127
cis lo	25	37.7	2.54	18.1	1.97	ΔΔ lo	11	32.3	3.48	6.4	0.86	P = 0.204	P=<0.001
cis lo	25	37.7	2.54	18.1	1.97	GFP-f	26	28.8	2.16	4.5	0.36	P = 0.019	P=<0.001
ΔEC1 lo	22	37.1	1.95	20.2	0.92	ΔΔ lo	11	32.3	3.48	6.4	0.86	P = 0.204	P=<0.001
ΔEC1 lo	22	37.1	1.95	20.2	0.92	GFP-f	26	28.8	2.16	4.5	0.36	P = 0.045	P=<0.001
ΔΔ lo	11	32.3	3.48	6.4	0.86	GFP-f	26	28.8	2.16	4.5	0.36	P = 0.685	P = 0.591
w2a Hi	41	35.5	2.28	18.2	1.48	Δcyt Hi	23	35.6	2.48	12.4	1.16	P = 0.972	P = 0.004
w2a Hi	41	35.5	2.28	18.2	1.48	cis Hi	28	36.9	1.99	17.1	1.18	P = 0.656	P = 0.691
w2a Hi	41	35.5	2.28	18.2	1.48	ΔEC1 Hi	31	34.1	1.78	20.1	1.15	P = 0.541	P = 0.064
w2a Hi	41	35.5	2.28	18.2	1.48	ΔΔ Hi	15	34.9	1.32	8.6	0.78	P = 0.890	P=<0.001
w2a Hi	41	35.5	2.28	18.2	1.48	GFP-f	26	28.8	2.16	4.5	0.36	P = 0.342	P=<0.001
Δcyt Hi	23	35.6	2.48	12.47	1.16	cis Hi	28	36.9	1.99	17.1	1.18	P = 0.666	P = 0.008
Δcyt Hi	23	35.6	2.48	12.47	1.16	ΔEC1 Hi	31	34.1	1.78	20.1	1.15	P = 0.631	P=<0.001
Δcyt Hi	23	35.6	2.48	12.47	1.16	ΔΔ Hi	15	34.9	1.32	8.6	0.78	P = 0.585	P = 0.018
Δcyt Hi	23	35.6	2.48	12.47	1.16	GFP-f	26	28.8	2.16	4.5	0.36	P = 0.208	P=<0.001
cis Hi	28	36.9	1.99	17.1	1.18	ΔEC1 Hi	31	34.1	1.78	20.1	1.15	P = 0.297	P = 1.000
cis Hi	28	36.9	1.99	17.1	1.18	ΔΔ Hi	15	34.9	1.32	8.6	0.78	P = 0.671	P=<0.001
cis Hi	28	36.9	1.99	17.1	1.18	GFP-f	26	28.8	2.16	4.5	0.36	P = 0.070	P=<0.001
ΔEC1 Hi	31	34.1	1.78	20.1	1.15	ΔΔ Hi	15	34.9	1.32	8.6	0.78	P = 0.824	P=<0.001
ΔEC1 Hi	31	34.1	1.78	20.1	1.15	GFP-f	26	28.8	2.16	4.5	0.36	P = 0.296	P=<0.001
ΔΔ Hi	15	34.9	1.32	8.6	0.78	GFP-f	26	28.8	2.16	4.5	0.36	P = 0.374	P = 0.037

Table 3.1. Summary of FRAP data and T test values for L cells.

4. FRAP Analysis of E-Cadherin Dynamics as a Read-Out for Cell Motility

4. FRAP Analysis of E-Cadherin Dynamics as a Read-Out for Cell Motility

In the previous chapter, I showed how FRAP was used on to analyse the molecular dynamics of E-cadherin molecules in cell-cell junctions in pancreatic cancer cells. In this chapter, I will analyze how E-cadherin dynamics are related to cell motility and invasion. In many cancer cells, mis-regulation of adherens junctions causes increased progression and invasion of cancer (Birchmeier 1994). Alteration in E-cadherin dynamics could therefore serve as an early molecular biomarker of metastasis. In this chapter, I employed FRAP to compare E-cadherin dynamics in two PDAC cell lines derived from primary pancreatic tumours of the KPC mouse model. In this model tumour formation is driven by mutant KRAS; however, tumour metastasis is driven by mutant p53 (Morton 2010). In particular, I will focus on the effect of the local micro environments on the mobility of E-cadherin in cell lines derived from mouse primary tumours.

4.1. P53 mutation drives cell invasion in PDAC cells.

In the KPC mouse model $KRAS^{G12D}$ mutation drives formation of PanINs, then loss of p53 promotes formation of pancreatic tumours. Mice with Pdx1-Cre, LSL-$KRAS^{G12D/+}$, $Trp53^{LoxP/+}$ genetic background form tumours which are not invasive. In this study, I used a cell line derived from pancreatic tumours of these mice. These PDAC cells with loss of p53 expression will be referred to as $PDAC^{fl}$ cells. On the other hand, mice with Pdx1-Cre, LSL-$KRAS^{G12D/+}$, LSL-$Trp53^{R172H/+}$ genetic background form invasive tumours. In this chapter, cell line derived from these tumours is called $PDAC^{R172H}$. $PDAC^{fl}$ cell which derived from pancreatic tumours with Pdx1-Cre, LSL-$KRAS^{G12D/+}$, $Trp53^{LoxP/+}$ genetic background were stably transfected with plasmid with $p53^{R175H}$ or empty vector. Here, these cell lines are called $PDAC^{fl}R175H$ and $PDAC^{fl}vector$ respectively. In FRAP experiments reported in this thesis all this cell lines are stably transfected with E-cadherin-GFP plasmid.
PDAC cell with loss of p53 expression ($PDAC^{fl}$) are not invasive in organotypic assay and xenograft tumours. On the other hand, PDAC cells from tumours with $p53^{R172H}$ mutation ($PDAC^{R172H}$) are more progressive and invasive than $PDAC^{fl}$

cells. Moreover, expression of human mutant p53 protein (p53^{R175H}) in PDAC^{fl} cells is sufficient to activate cell invasion in PDAC^{fl} cells (Morton 2010). Here, I studied PDAC cell line stably transfected with E-cadherin-GFP plasmid.

Initially, an organotypic assay was used to study the invasion of PDAC^{fl} and PDAC^{R172H} cells lines. To perform organotypic assay, 4×10^4 PDAC cells were seeded on top of the matrix in complete media and allowed to grow to confluence for 5 days. The matrix was then mounted on a metal grid and raised to the air/liquid interface resulting in the matrix being fed from below with complete media. The cells media was changed every 2 days and the cells were grown for 8–12 days. Then the cultures were fixed and stained by H&E method. Representative images in figure 4.1 (A, B and C) showed that PDAC^{fl} cells continue to grow on the surface but did not invade in to the organotypic gel. In contrast, PDAC^{R172H} cells were highly invasive. Additionally, as previously reported by Morton et al, transfecting PDAC^{fl} cells with human p53 mutant protein (p53^{fl}R175H) was adequate to make these cells invasive. The PDAC^{R172H} cells invade to the gel as single cells and have a more mesenchymal phenotype; in contrast PDAC^{fl}R175H cells have stronger cell-cell adhesions and invade collectively into the gel (figure 4.1 B and C).

In order to study the effects of mutant p53 on E-cadherin dynamics using FRAP, I transfected these cells with a plasmid for E-cadherin-GFP. As shown previously in section 3.3.1, increasing the expression level of E-cadherin could affect cell-cell adhesion. Therefore, I analysed how expression of E-cadherin-GFP on top of endogenous E-cadherin would affects PDAC cell invasion. I repeated the organotypic assay using the same cell lines which now expressed E-cadherin-GFP (Figure 4.1. D, E and F). Representive figures show that PDAC^{R172H} and PDAC^{fl}R175H cells with expression of E-cadherin-GFP are still highly invasive. To quantify the invasion, I measured the depth of each cell in the gel (Figure 4.2). On the Y axis the average of depth of invasion of single cells are shown. The data showed that PDAC^{R172H} and PDAC^{fl}R175H cells with E-cadherin-GFP expression are still highly invasive, and there was no significant difference in depth of invasion between original cells and E-cadherin-GFP expressing cells (t test p values were P = 0.305 and P = 0.330 respectively).

A) PDAC^{fl}

D) PDAC^{fl} +E-cadherin-GFP

B) PDAC^{R172H}

E) PDAC^{R172H} +E-cadherin-GFP

C) PDAC^{fl}R175H

F) PDAC^{fl}R175H+E-cadherin-GFP
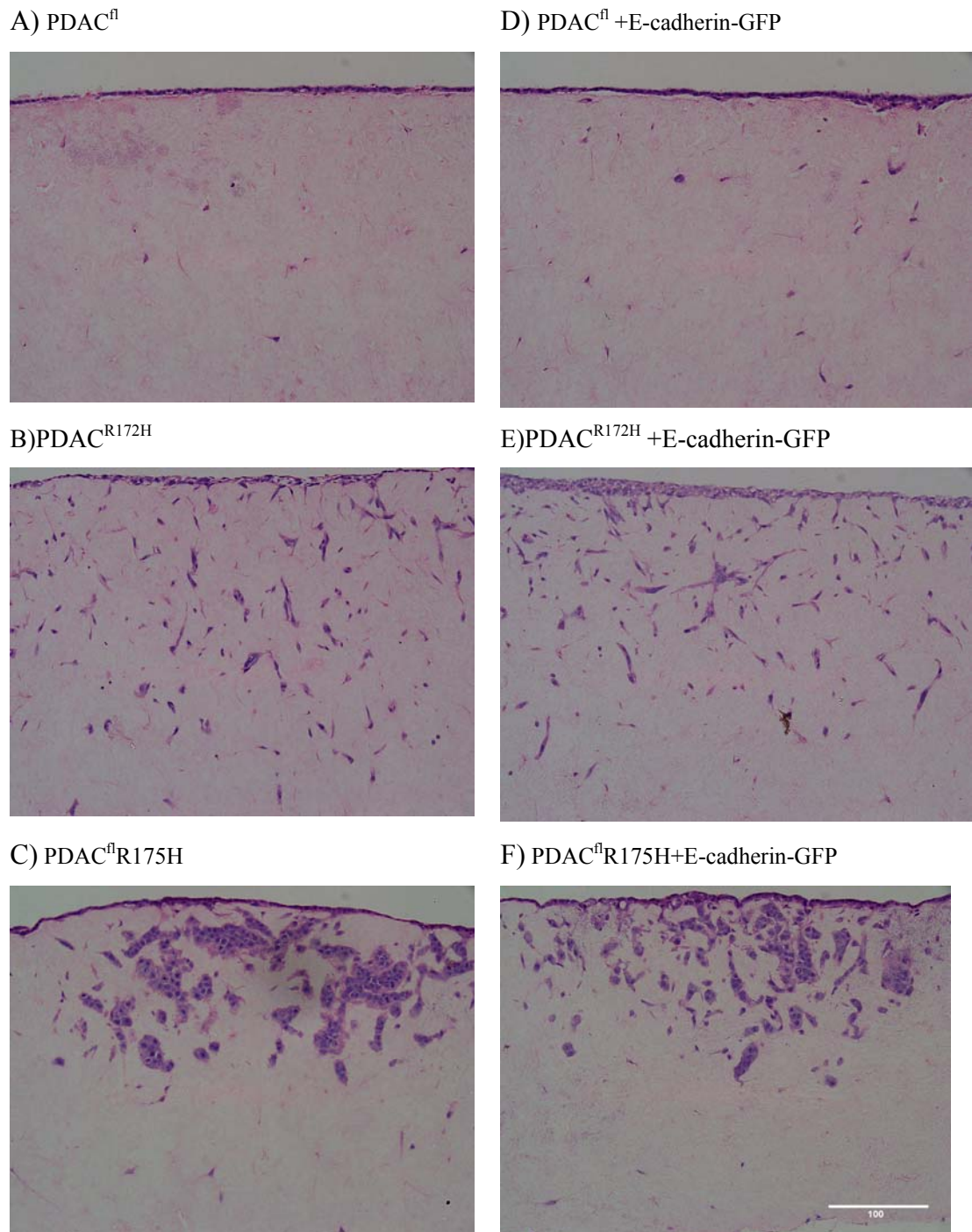
Figure 4.1. PDAC cells expressing mutant p53 are invasive in Organotypic assays. A-F show representative images of organotypic gels. PDAC^{fl} cells (A) do not invade in the organotypic gel. However, PDAC^{R172H} (B) and PDAC^{fl}R175H (C) cells are highly invasive. D-F show PDAC cells with E-cadherin-GFP expression. Expression of E-cadherin-GFP in these cells does not inhibit cell invasion. (Bar is 100 μm.)

Comparing organotypic invasion of PDAC^{R172H} cells which are directly driven from p53 mutant mouse tumours with PDAC^{fl}R175H cells which are driven from p53 null mice tumours and then the human mutant p53 protein is expressed in them shows

that although both cells are invasive; the invasion mode is different in two cell lines. PDAC^{R172H} cells migrated as individual cells and invaded far more in the gel. But PDAC^{fl}R175H cells invaded more in groups of cells and the depth of invasion is slightly less than PDAC^{R172H} cells. The PDAC^{R172H} cells are from mice tumours and these cells might acquire additional genetic alteration during progression tumorigenesis. Moreover, these cells are exposed to the immune response in vivo which could affect these cells invasive phenotype.
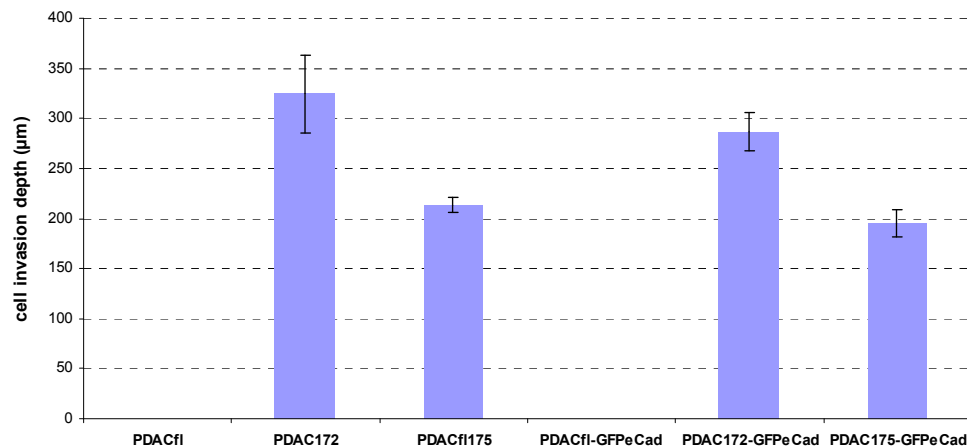
Figure 4.2. Quantification of depth of invasion of PDAC cells. Depth of each cell in the gel is averaged. PDAC^{fl} cells do not invade in the gel and cell invasion for these cells is zero. PDAC^{R172H} and PDAC^{fl}R175H cells with E-cadherin-GFP expression are still highly invasive, and there is no significant difference in depth of invasion between original cells and E-cadherin-GFP expressing cells. Error bars are SEM. (each organotypic assay repeated three times).

Moreover, I studied the effect of E-cadherin-GFP expression in PDAC cells on xenograft tumours in nude mice. PDAC^{fl}vector and PDAC^{fl}R175H cells were trypsinized and 10^6 cells were injected subcutaneously into the flank of CD1 nude mice. The Home Office guidelines dictate that the mice were culled before the tumours reached 15 mm size or alternatively if the tumours became ulcerated. The data showed that the tumours from PDAC^{fl}R175H cells with E-cadherin-GFP expression grow faster than PDAC^{fl}vector cell tumours (Figure 4.3.A).

This showed that xenograft tumours from PDAC cells with mutant p53 are more progressive than tumours with loss of p53 and stable expression of E-cadherin-GFP does not have any affect on it.

A)
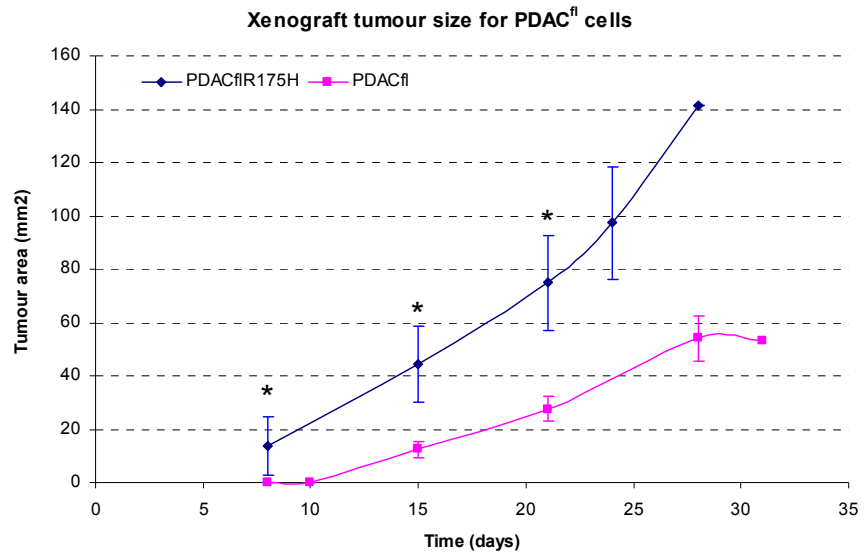
B)
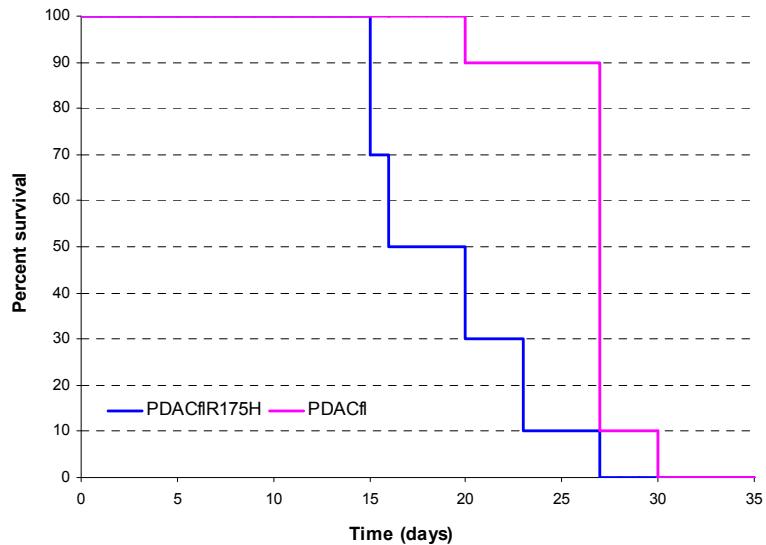
Figure 4.3. Xenograft tumours expressing mutant p53 are more progressive. (A) Analysis of the rate of tumour growth, as assessed by the increase in tumour area over time in PDAC^{fl}R175H cells with E-cadherin-GFP expression compared to PDAC^{fl}vector cells expressing E-cadherin-GFP. The tumour shape is assumed an oval shape and length and width of tumour is measured to estimate the tumour area. Statistically significant difference (*) as assessed by Mann-Whitney Rank Sum Test at days 8, 15, 21; $P = 0.002$, $P = <0.001$ and $P = 0.003$ respectively. (B) Analysis of the survival time in PDAC^{fl}R175H xenografts compared to PDAC^{fl}vector tumours. Error bars shows STDV (n=10)

4.2. Mutant p53 weakens cell-cell adhesion in PDAC cells.

The organotypic data showed that p53 mutation dramatically promotes PDAC cell invasion. Subsequently, I used a dispase assay to study how this mutation affects cell-cell adhesion in these cells (Figure 4.4.A). For performing the Dispase assays, a confluent cell monolayer in a 6 well dish was treated with dispase II, the detached monolayer then was broken up by pipetting up and down, and after passing through a cell strainer, the single cells were counted using a hemocytometer. The single cell number was reported as percentage of the PDAC^{fl}vector cells. The data showed that, PDAC^{fl}R175H cells have significantly higher number of single cells than PDAC^{fl}vector cells (P = <0.001). Moreover, TEER was used to measure cell-cell junctional integrity. For measuring TEER cells were seeded on 12 well transwells, and then electrical resistance was measured using an EVOM2 epithelial voltohmmeter. The results were reported as percentage of PDAC^{fl}vector cell resistance. Measurement of TEER across a confluent monolayer showed that cells expressing mutant p53 have significantly lower junctional integrity than cells expressing no p53 (figure 4.4.B) (P = 0.047).

A)   B)
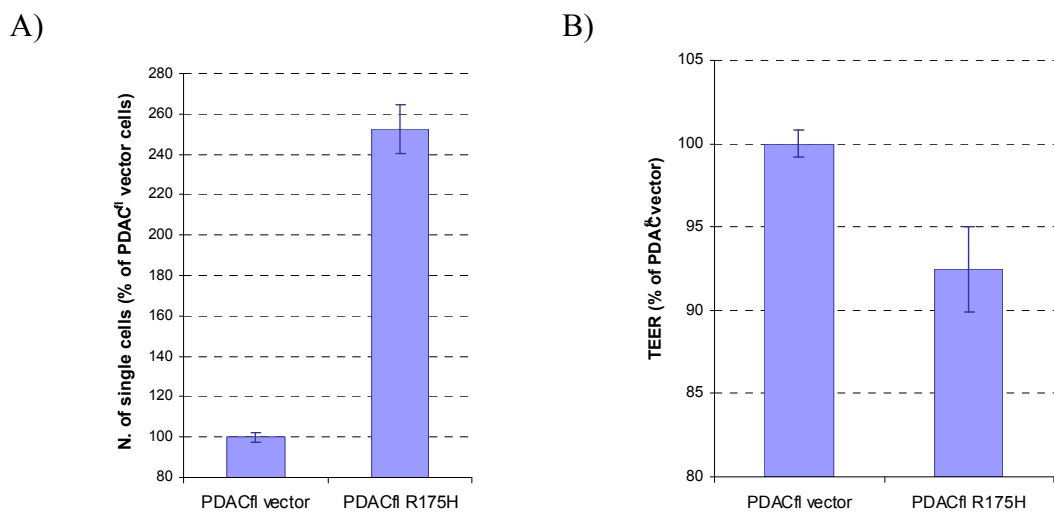
Figure 4.4. Mutant p53 reduces cell-cell adhesion and junctional integrity in PDAC cells. A) Dispase assay results comparing PDAC^{fl}R175H with PDAC^{fl}vector cells. The data shows that p53^{R175H} mutation significantly increased the number of single cells, which indicates that cell-cell adhesion is disrupted in PDAC^{fl}R175H cells. B) TEER measurements in PDAC^{fl}R175H and PDAC^{fl}vector cells. Electrical resistance is significantly lower in p53 mutant cells indicating reduced barrier function. Error bars shows SEM. (n=3)

4.3. Mutant p53 increases the mobility of E-cadherin on cells grown on CDM but not glass.

The data showed that mutant p53 has a significant effect on invasion and cell-cell adhesion in PDAC cells. Serrels et al have previously shown that E-cadherin in cell-cell junctions is mobilized in migrating A431 cells (Serrel 2009). Therefore, I hypothesized that mutant p53 might promote invasion by mobilizing E-cadherin in PDAC cells. To test this idea, PDAC[fl]vector and PDAC[fl]R175H cells were grown on glass bottom dishes and FRAP was used to look at E-cadherin dynamics. As shown in blue and green colours in figure 4.5, PDAC[fl]R175H and PDAC[fl]vector cells grown on glass have similar recovery curves.
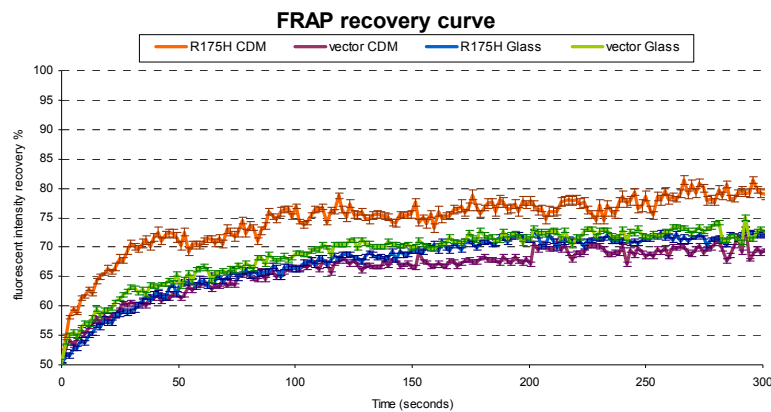
Figure 4.5. Mutant p53 affects dynamics of E-cadherin-GFP in PDAC cells grown on CDM not glass. FRAP curves for PDAC[fl]vector and PDAC[fl]R175H cells growing on glass or CDM. PDAC[fl]R175H cell line when grown on CDM show more dynamic E-cadherin-GFP compared to PDAC[fl]vector cells. Error bars show SEM. (n=at least 10 for each curve)

However, many aspects of cell migration depend on features of the local environment including elasticity, protein composition, or pore size, which are not represented by glass substrates. So, I studied the effect of mutant p53 on E-cadherin dynamics on CDM, which is a widely used 3D model to study cell motility (Hakkinen 2011). Cell Derived Matrix (CDM) is a collagen and fibronectin-rich matrix formed by the deposition of ECM and growth factors by fibroblasts in vitro. The formed matrix is ~30 μm thick and highly fibrous and with high stiffness. Cells have been shown to migrate faster along ECM fibers. The FRAP data showed that when these cells were grown on cell derived matrix (CDM), PDAC[fl]R175H cells

showed different recovery curve (orange colour in figure 4.5) compared to PDAC^{fl}vector cells (red).

Quantification of the Fi% and T1/2 of FRAP results in figure 4.6 shows there was no significant difference in immobile fraction and T1/2 values between PDAC^{fl}vector and PDAC^{fl}R175H cells grown on glass (p values for Fi% and T1/2 are P = 0.890 and P = 0.921). However, when PDAC^{fl}R175H cells were grown on CDM, the immobile fraction and T1/2 were significantly reduced compared to PDAC^{fl}vector cells (p values are respectively P = <0.001 and P = <0.001)
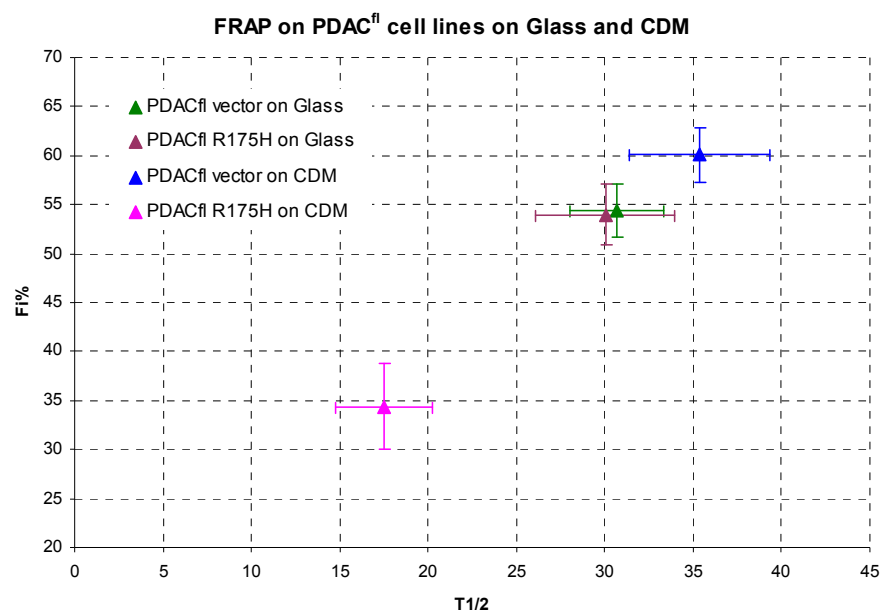
Figure 4.6. Mutant p53 decreased the Fi and T1/2 of E-cadherin when cells are cultured on CDM. FRAP results for PDAC^{fl}R175H cells growing on glass showed no significant difference in Immobile fraction and T1/2 compared to PDAC^{fl}vector cells (purple and green triangles). However, for the cells grown on CDM there is a significant decrease in Fi% and T1/2 in p53 mutants (pink and blue triangles). Error bars show SEM. (n=at least 10 junctions for each data point)

Analysis of FRAP in PDAC^{fl} and PDAC^{R172H} shows similar results (figure 4.7). There is no statistically significant difference in E-cadherin dynamics between PDAC^{fl} and PDAC^{R172H} cells grown on glass (p values for Fi% and T1/2 are P=0.663 and P=0.683). However, when cells were grown on CDM, there is significant increase in mobility of E-cadherin in PDAC^{R172H} cells (p values for Fi% and T1/2 are P = <0.001 and P = <0.001).
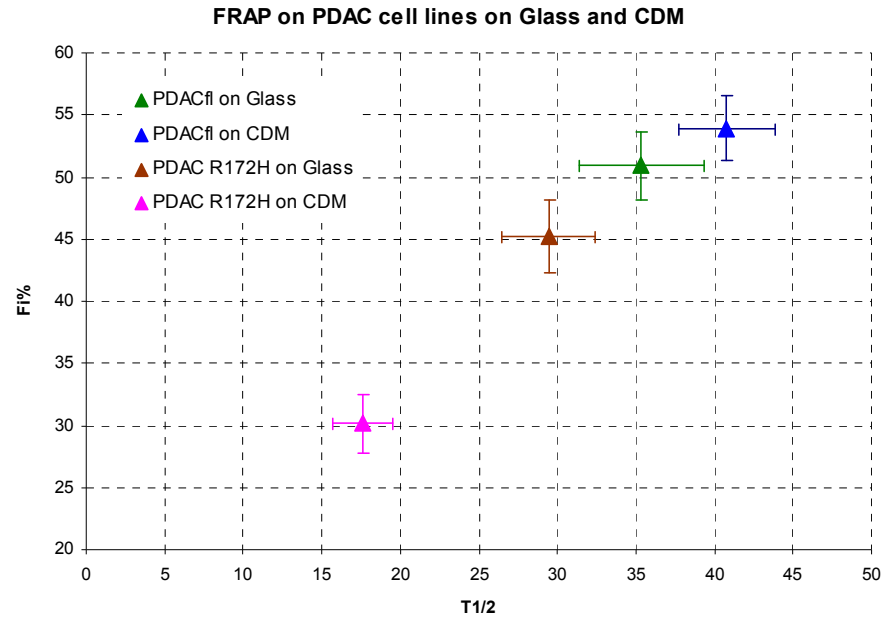
Figure 4.7. The effect of mutant p53 on E-cadherin dynamics depends on the cell environment. Mutant p53 does not affect the dynamics of E-cadherin in PDAC[fl] and PDAC[R172H] cells grown on glass (green and brown triangles). However, for the cells grown on CDM there is a significant decrease in immobile fraction and recovery rate in cells with mutant p53. There is a significant difference between T1/2 and Immobile fraction of PDAC[fl] and PDAC[R172H] cells (blue and pink triangles). Error bars show SEM. (n=at least 10 junctions for each data point)

These data suggests that the effect of mutant p53 on E-cadherin dynamics depends on the local cell environment. Figure 4.6 showed E-cadherin mobility was significantly increased in PDAC[fl]R175H cells in comparison to PDAC[fl]vector cells when grown on CDM. Similar results were obtained with PDAC[fl] and PDAC[R172H] cells (Figure 4.7). As discussed in chapter 3, when cells express comparable levels of E-cadherin Fi is related to the amount of E-cadherin stabilized at junctions. Consequently, higher Fi indicates more stabilized junctions and stronger cell-cell adhesion. Next, the dispase assay was used to study cell-cell adhesion in PDAC[fl]vector and PDAC[fl]R175H cells in CDM (Figure 4.8). There was a significant reduction in single cell number of PDAC[fl]R175H cells when grown in CDM compared to PDAC[fl]vector cells (P = 0.041). The FRAP data are consistent with the dispase assay results, which also indicates that mutant p53 loosens cell-cell junctions by mobilizing E-cadherin.
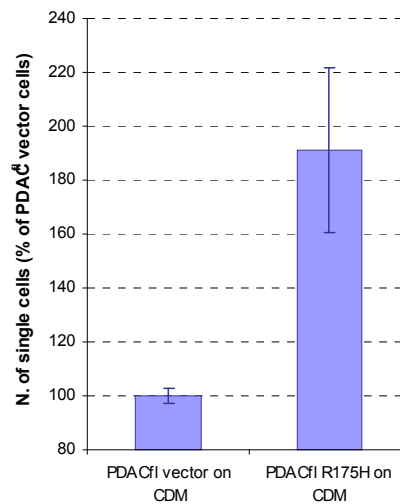
Figure 4.8. Mutant p53 reduces cell-cell adhesion in PDAC cells grown on CDM. Dispase assay results comparing cell-cell adhesion of PDAC^{fl}R175H with PDAC^{fl}vector cells growing on CDM. The data shows that p53^{R175H} mutation significantly increased the number of single cells, which indicates that cell-cell adhesion is disrupted in PDAC^{fl}R175H cells. Error bars shows SEM. (n=3)

4.4. Mutant p53 increases mobility of E-cadherin in PDAC cells in xenograft tumours.

The data suggested that micro environment plays an important role in determining the effects of mutant p53 on E-cadherin dynamics and cell migration. Extracellular matrix strongly affects cell migration. However, CDM is a very artificial environment compared to tumours. The composition of ECM and its rigidity is different compared to in vivo. Moreover, presence of immune cells and inflammation could affect cell invasion. FRAP experiments on cells in xenograft tumours show different E-cadherin dynamics compared to cells in culture (Serrels 2009). Therefore, for better understanding of the effects of mutant p53 on E-cadherin dynamics in the functional and physiological context of real tumors, I have measured FRAP in xenograft tumors. To do this, the PDAC cells were injected subcutaneously into the flank of nude mice and then allowed to grow until the tumour reached a length of between 1-1.4 cm. Then while the mouse was under anesthesia the tumour was dissected and the exposed tumor placed on a glass bottom dish while the blood flow was kept through a skin flap attached to the body. After FRAP the mouse was culled

and the tumour was fixed and stained with H&E to investigate how PDAC cell invade. Many cell lines derived from metastatic tumours are non-invasive when cultured subcutaneously in nude mice. However, xenograft tumours derived from PDAC^{fl}R175H cell line were highly invasive compared to PDAC^{fl}vector tumours and the cells invaded through muscle and peritoneal cavity (Figure 4.9. A and B).

The E-cadherin FRAP results showed that immobile fraction was significantly smaller in mutant p53 xenograft tumours compared to PDAC^{fl}vector cells in xenografts (Figure 4.9.C). This reduction in immobile fraction was similar to the effect of p53 mutation on mobilizing E-cadherin, and consequently weakening cell-cell adhesions, in mutant p53 cells cultured on CDM.

In contrast, p53 mutation had a different effect on T1/2 in xenograft tumours compared to CDM. On CDM mutant p53 reduced T1/2 but in xenograft tumours PDAC^{fl}R175H cells have larger T1/2 compared to PDAC^{fl}vector cells.

Moreover, FRAP results showed higher immobile fraction and much smaller T1/2 for xenogfrats compared for cells growing on glass or CDM. The higher Fi could be due to increased non-adhesive immobile fraction (which is because of non-specific trapping of molecules in membrane structures (see section 5.1.5)) or increased adhesive clustering. This question will be addressed later in section 4.5. Moreover, the reduction in mobile fraction in conjunction with decrease in the recovery rate of E-cadherin in tumours indicates that the adhesive mobile fraction of E-cadherin is smaller in cells in xenograft than CDM. In other word although fewer E-cadherin molecules are mobile in xenograft compared to cells in CDM, the interaction of the mobile molecules to adhesive complexes are weaker or less frequent.

The dramatic change in FRAP data in xenograft tumours compared to cells in culture suggested that the local cell environment could significantly alter the regulation of E-cadherin within cell-cell junctions. Alternatively, this difference in E-cadherin dynamics could be due to altered cell membrane structure in vivo which affect E-cadherin dynamics non-specifically. My data on chapter 3 showed that non-specific trapping of free transmembrane proteins in membrane structure or cell cytoskeleton underneath could dramatically affects their mobility. To address this question, a mutant form of E-cadherin-GFP was expressed in PDAC^{fl}vector xenograft tumours and FRAP used to study diffusion rate of E-cadherin in the plasma membrane.

A) PDAC^{fl}vector+E-cadherin-GFP   B) PDAC^{fl}R175H+E-cadherin-GFP
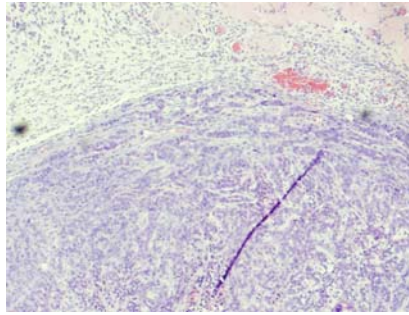
C)
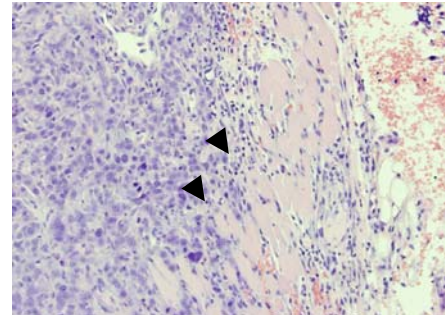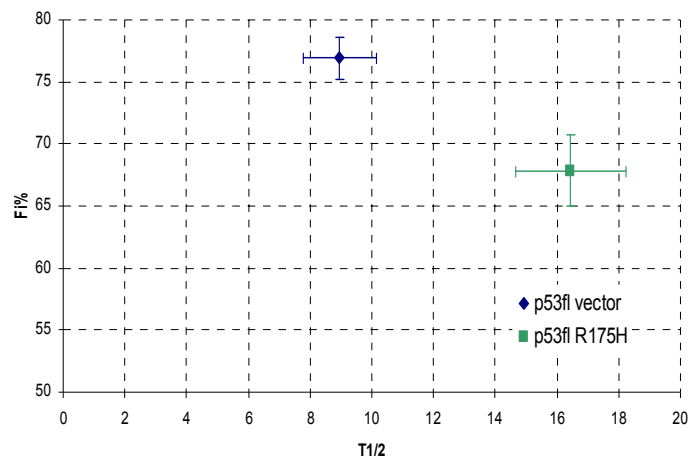
Figure.4.9. PDAC^{fl}R175H cells are more invasive in xenografts and have more mobile E-cadherin. (A and B) H&E staining of tumours shows p53 mutant cells are more invasive than PDAC^{fl}vector cells. (A) The PDAC^{fl}vector cells are not invasive and have a smooth boundary tumour. (B) PDAC^{fl}R175H xenografts are highly invasive and the black arrows show where cells invaded through muscle. (C) FRAP on xenografts showed that E-cadherin in PDAC^{fl}R175H xenograft tumours is significantly more mobile than in PDAC^{fl}vector tumours (p=0.002). T1/2 is significantly higher in p53 mutant xenografts compared to PDAC^{fl}vector xenografts (p=0.001). Error bars show SEM. (n=at least 14 junctions for each data point)

4.5. The mobile fraction of wild-type E-cadherin recovers at the rate of free diffusion in vivo.

In order to explore the possibility that differences in membrane properties could explain the differences between E-cadherin dynamics of cells grown on CDM or in vivo, the ΔEC1ΔCyt mutant (see section 3.2) of E-cadherin-GFP was stably expressed in PDAC^{fl}vector cells. These cells were injected into mice as described in section 4.4 and allowed to form tumours which were analysed by FRAP.

As I showed in chapter 3, the mutant ΔEC1ΔCyt E-cadherin can not form cis or trans dimers or interact with actin cytoskeleton. So it can be used to estimate the level of immobile fraction due to non-specific trapping. ΔCytΔEC-E-cadherin-GFP in PDAC^{fl} xenograft had approximately 60% immobile fraction which is significantly higher than 30% Fi in these cells grown in culture (figure 4.10). This establishes the baseline for non-adhesive immobile fraction in PDAC^{fl} cells in xenograft tumours.

Next, the ΔCyt-E-cadherin-GFP mutant was expressed in PDAC^{fl}vector cells. This mutant can form cis and trans dimers but can not bind to actin, and does not form any adhesive immobile fraction (see section 3.7). As expected the dynamics of ΔCyt mutant are not significantly different than the dynamics of the ΔEC1ΔCyt-E-cadherin-GFP mutant. Next, the ΔCyt mutant was expressed in PDAC^{fl}R175H cells. In PDAC^{fl}R175H xenografts, the ΔCyt mutant had the same immobile fraction as ΔEC1ΔCyt-E-cadherin-GFP mutant in PDAC^{fl}vector xenografts. This data confirms that the non-adhesive immobile fraction due to non-specific trapping in membrane structure is similar in PDAC^{fl}R175H and PDAC^{fl}vector xenografts. So the significant difference observed in Fi in wild-type E-cadherin in xenografts is due to a difference in the adhesive immobile fraction and indicates that cell-cell adhesion is stronger in PDAC^{fl}vector tumours compared to PDAC^{fl}R175H xenografts.

Moreover, the FRAP data for the ΔCyt-E-cadherin-GFP mutant showed that there was no significant difference in Fi% compared to wild-type E-cadherin-GFP in PDAC^{fl}R175H xenografts (figure 4.10 red triangle and square). In contrast, the ΔCyt mutant in PDAC^{fl}vector xenograft tumour had a significantly higher immobile fraction than wild-type E-cadherin. This indicates that mutant p53 significantly reduced the adhesive immobile fraction in E-cadherin-GFP molecules in xenograft tumours.

Moreover, the ΔEC1ΔCyt mutant does not form any interaction to adhesive cadherin complexes so it can be used as a control for rate of recovery of a free diffusing molecule with the approximate size of E-cadherin. The results showed that although there is a significant difference in Fi% between wild-type E-cadherin-GFP and the ΔEC1ΔCyt mutant in PDAC^{fl}vector xenograft, there is no significant difference between T1/2 (blue square and green circle in figure 4.10). Thus, in xenograft tumours wild-type E-cadherin recovers very fast, similar to the recovery rate of the non-binding mutant. This similarity in T1/2 shows that the mobile fraction of wild-type E-cadherin-GFP molecules does not interact with any cadherin complexes in

membrane. In other word, there are no transient interactions in wild-type E-cadherin-GFP in cells in tissue. The cadherin molecules are either immobile (in junctions or trapped non-specifically) or completely freely diffusing in the membrane. In contrast, in cell culture wild-type E-cadherin-GFP had a significantly higher T1/2 than $\Delta EC1\Delta Cyt$ mutant. These data indicate that in cell culture the mobile E-cadherin molecules in the membrane could bind to adhesive complexes and this interaction slows down their recovery rate. In cell culture, E-cadherin interactions can be stable during FRAP time (as in immobile fraction) or transient during FRAP time (mobile fraction with slow recovery time). But in tumours, the E-cadherin molecules are either stably bound to adhesive complexes or do not have any interactions. So the recovery time of wild-type E-cadherin-GFP is as fast as the non binding mutant. However, when p53 was expressed in PDAC tumour the adhesive immobile fraction significantly reduced while the recovery rate increases. This indicates that p53 mutation inhibits immobilization of wild-type E-cadherin molecules in adhesive cadherin complexes. But, the mobilized wild-type E-cadherin-GFP molecules now form transient interactions which slow its diffusion and increase the recovery time of E-cadherin.
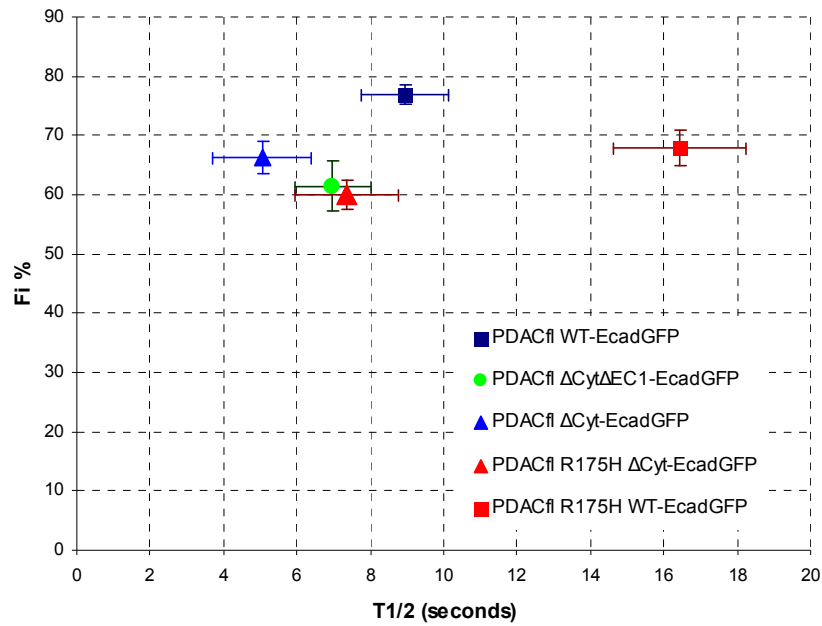
Figure.4.10. Wild-type E-cadherin-GFP and the ΔCyt mutant have similar Fi in PDAC^{fl}R175H cells in xenograft tumours. PDAC^{fl}vector and PDAC^{fl}R175H cell lines were transfected with wild-type E-cadherin-GFP, or mutant E-cadherin with the cytoplasmic domain deleted (ΔCyt-Ecadherin-GFP). FRAP on PDAC^{fl}vector cells with wild-type E-cadherin-GFP compared to ΔCyt-Ecadherin-GFP or ΔEC1ΔCyt mutant showed a significant decrease in Fi%. However, in PDAC^{fl}R175H cells expressing wild-type E-cadherin-GFP showed no increase in Fi% compared to ΔCyt-Ecadherin-GFP. Error bars shows SEM. (n=at least 12 junctions for each data point)

4.6. E-cadherin dynamics in a mouse model of pancreatic cancer.

Although xenografts are good models for studying cells in vivo, cell migration in vivo is a complex process strongly affected by the tissue environment on or through which the cell migrates. Interaction with other cell types, including stromal fibroblasts and immune cells, has been shown to play a critical role in promoting the invasion of cancer cells and subcutaneous growth of pancreatic tumour cells does not recapitulate the native environment. Moreover, pancreatic cells growing under skin have different local micro environment compared to pancreas. Ideally, it would be best to study cell migration in its naturally occurring context in living organisms.

In order to investigate E-cadherin dynamics in the context of pancreatic tumours, I used a mouse engineered to express E-cadherin-GFP from the Rosa26 locus under the control of cre-recombinase which was generated by D. Strathdee and colleagues in the Beatson Transgenic Production facility. Crossing this mouse with mice

expressing cre recombinase under control of the PDX1 promoter, lead to expression of E-cadherin-GFP in the pancreas (figure 4.11. A and B). This mouse was crossed with KPC mice to express E-cadherin-GFP in pancreatic tumours. This enabled us to use FRAP to asses E-cadherin dynamics for the first time in pancreatic normal tissue and tumours (Fig. 4.11. C and D).
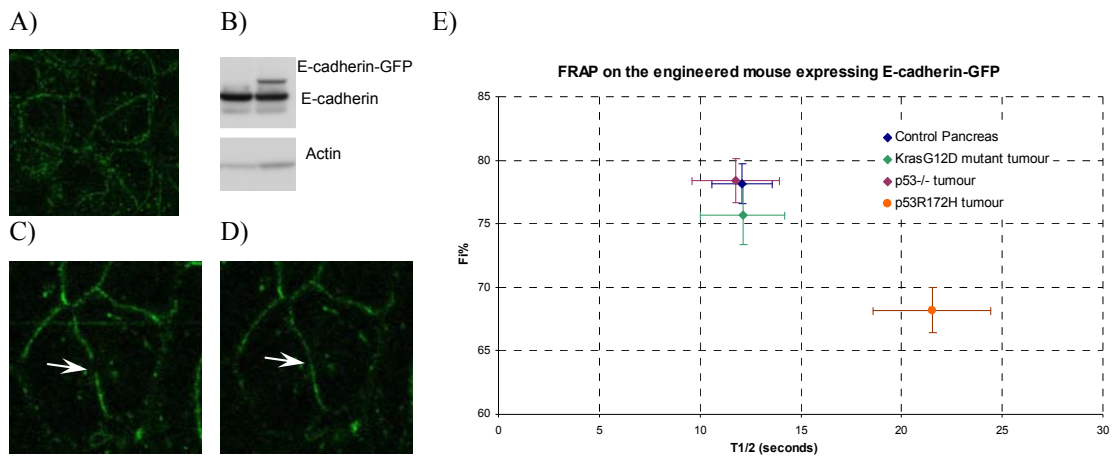
Figure.4.11. FRAP on healthy and diseased pancreas. (A) E-cadherin-GFP was expressed in the mouse pancreas under the control of PDX1 cre-recombinase. (B) Expression of E-cadherin-GFP in the pancreas in addition to endogenous E-cadherin is shown by western blot. (C and D) E-cadherin-GFP mice crossed with KPC mice to express E-cadherin-GFP in pancreatic tumours and FRAP used to study E-cadherin dynamics in normal pancreatic tissue or tumours. (E) FRAP on ex vivo pancreas tissue compared to KRAS driven tumours and p53 mutant tumours reveals, that p53 mutation decreases the Immobile fraction significantly in these tumours. T1/2 is measured in normal tissue, KRAS tumours and p53 mutant tumours. Error bars show SEM. (For each data point 3 mice is studied and n=at least 12 recovery curves)

Due to the location of the pancreas deep within the peritoneal cavity, it was not possible to image this organ in situ. Instead pancreata were excited and examined ex vivo. To confirm that performing the FRAP ex vivo is comparable with in vivo I designed an experiment to FRAP on xenograft tumours ex vivo and compare it with in vivo results. The formation of tumour and preparation for imaging was similar to in vivo situation but just before starting the imaging the skin flap that attached the tumour to body and kept the blood flow was cut. For imaging the tumours in vivo the mouse was kept under anesthesia for 3 hours. The same time period of 3 hours was used for ex vivo imaging. The FRAP results showed no significant difference in Fi and T1/2 between ex vivo and in vivo tumours either in for PDAC[fl]R175H or

PDAC^{fl}vector cells (figure 4.12). The results showed that E-cadherin FRAP can be performed ex vivo up to 3 hours. (P values for PDAC^{fl}R175H cells for Fi% and T1/2 are P = 0.512 and P = 0.992. For PDAC^{fl}vector cells p values are P = 0.238 and P = 0.360).
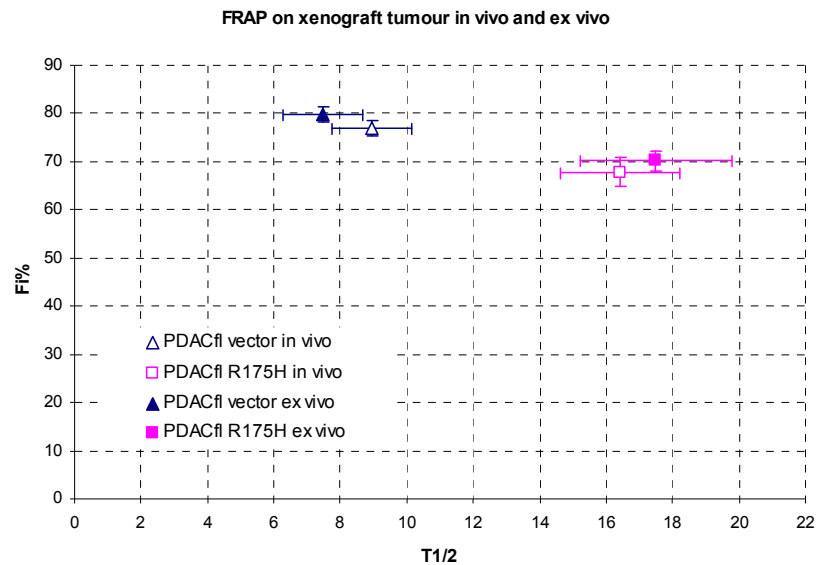
Figure 4.12. FRAP in xenograft tumours showed the same results ex vivo and in vivo. FRAP is performed in xenograft tumours from PDAC^{fl}R175H and PDAC^{fl}vector cells either at tumours with blood flow through a skin flap attached to the mouse (in vivo) or at tumours excited from skin flap just before imaging (ex vivo). The results showed no significant difference of Fi and T1/2 between ex vivo and in vivo tumours. Error bars show SEM. (n=at least 12 junctions for each data point)

Ex vivo analysis of p53 mutant tumours revealed significant differences in E-cadherin mobility compared to normal pancreatic tissue tumours or tumours with loss of p53 expression (figure 4.11.E). However, normal pancreatic tissue and tumours with loss of p53 expression showed no significant difference in E-cadherin dynamics. Also, pancreatic tumours in mouse with just the KRAS mutation had similar FRAP results to normal pancreatic tissue. This indicates loss of p53 does not alter E-cadherin dynamics. However, the FRAP data on ex vivo normal pancreas tissue compared to tumours from Pdx1-Cre, LSL-KRAS$^{G12D/+}$, Trp53$^{LoxP/+}$ mice revealed that p53 mutation decreases the immobile fraction significantly in these tumours and increased the T1/2 (t test p values are P = <0.001 and P = 0.011 respectively) (figure 4.11.E).

The effect of mutant p53 on E-cadherin mobility in pancreas tissue is similar to xenograft tumours. My data suggest that mutation in p53 is a gain of function mutation which weakened E-cadherin molecules interaction, therefore reduced the adhesive immobile fraction and increased the T1/2. This increased mobility of E-cadherin in junctions disrupts cell-cell adhesion between p53 mutant tumour cells which enables these cells to metastasize from the primary tumour.

Previous experiments in the KPC mouse model showed that treatment of mice with the Src inhibitor dasatinib hinders the tumour cells metastasis by approximately 50%. In addition, dasatinib was able to inhibit PDAC^{R172H} cell migration and invasion in vitro (Morton 2010-2). Performing FRAP on PDAC^{fl}R175H and PDAC^{fl}vector cells grown on CDM showed that dasatinib significantly increased the Fi and T1/2 of mutant p53 cells (figure 4.13.A). Mutant p53 cells treated with dasatinib Fi and T1/2 significantly increased (T1/2: P=0.023 Fi%: P=0.017). Fi and T1/2 of PDAC^{fl}R175H and PDAC^{fl}vector cells treated with dasatinib is not significantly different (T1/2: P=0.191 Fi%: P = 0.484).

Moreover, FRAP showed that treating PDAC^{fl}R175H xenograft tumours with dasatinib increased the immobile fraction and decreased T1/2 (T1/2: P=<0.001 Fi%: P=0.001). The Fi and T1/2 of E-cadherin on PDAC^{fl}R175H xenograft tumours treated with dasatinib is not significantly different than PDAC^{fl}vector tumours (T1/2: P =0.441 Fi%: P = 0.223) (figure 4.13.B).

A)

B)
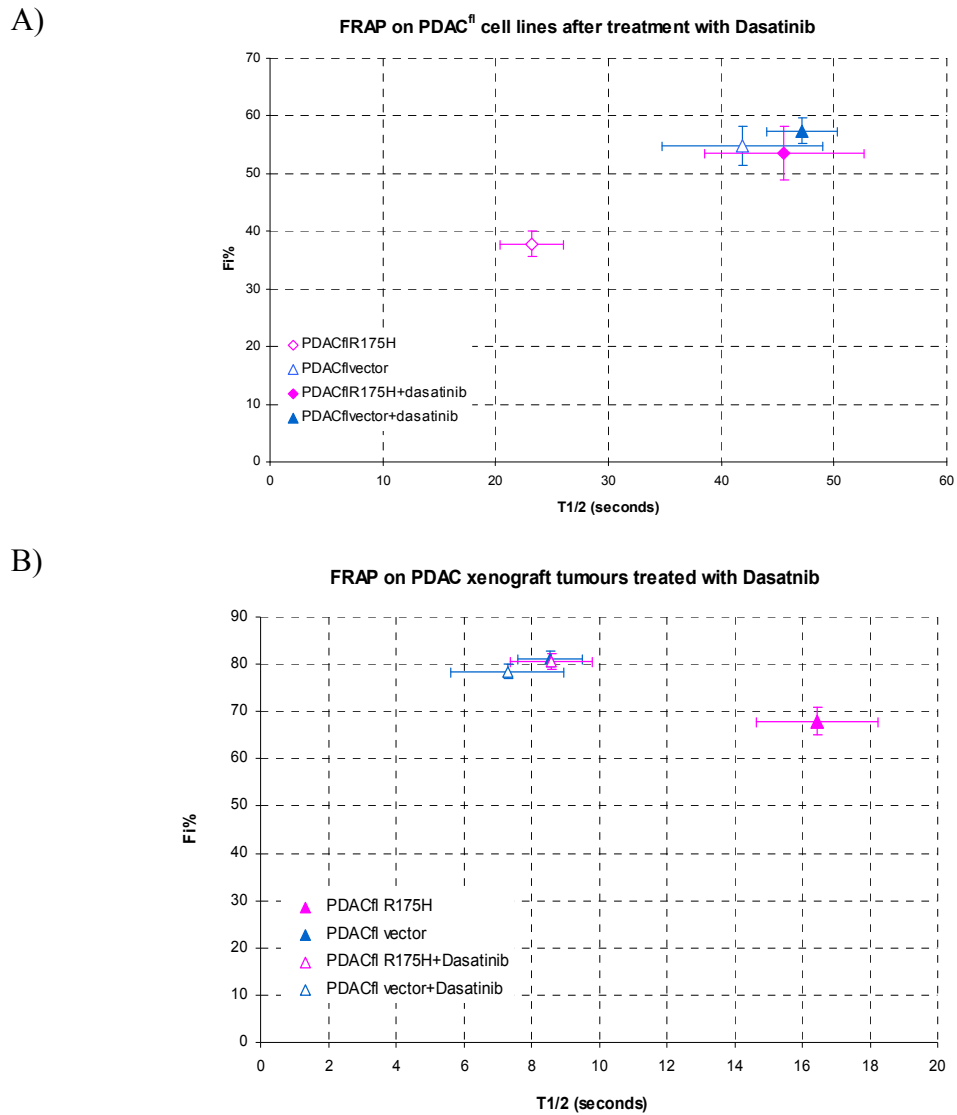
Figure 4.13. Dasatinib overturns the effect of mutant p53 on the reduction in mobility of E-cadherin. A) FRAP results for PDAC^{fl}R175H and PDAC^{fl}vector cells grown on CDM treated with anti invasive drug. Dasatinib is a Src inhibitor. PDAC^{fl}R175H cells grown on CDM had significantly lower Fi and T1/2 than PDAC^{fl}vector cells. But when the Mutant p53 cells treated with dasatinib Fi and T1/2 significantly increased. Fi and T1/2 of PDAC^{fl}R175H and PDAC^{fl}vector cells treated with dasatinib is not significantly different. B) FRAP results for PDAC^{fl}R175H and PDAC^{fl}vector cells in xenograft tumours in nude mice treated with anti invasive drug dasatinib. PDAC^{fl}R175H tumours have significantly lower Fi and higher T 1/2 compared to PDAC^{fl}vector tumours. However, after treatment with dasatinib FRAP data showed no significant difference in FI and T1/2 in PDAC^{fl}R175H and PDAC^{fl}vector tumours. Error bars show SEM. (n=at least 10 junctions for each data point)

This suggests that the mutant p53 weakens cell-cell adhesion by mobilizing E-cadherin in junctions and dasatinib inhibits metastasis through stabilizing E-cadherin

at adhesions. Then, I used FRAP to assess how dasatinib treatment affects E-cadherin dynamics in mutant p53 pancreatic tumours. Mutant p53 significantly lowered Fi in pancreatic tumours compared to tumours with loss of p53 or normal pancreas tissue. The FRAP results showed that dasatinib treatment significantly decreased mobility of E-cadherin in mutant p53 tumours (blue triangle in figure 4.14) (T1/2: P = 0.008 Fi%: P = <0.001). This indicates that FRAP can be used to asses real time dynamics of cadherin junctions in tumours. Regulation of cell-cell adhesion strongly affects cancer cell metastasis. Consequently, FRAP can be used as biosensor marker to asses metastasis in vivo.
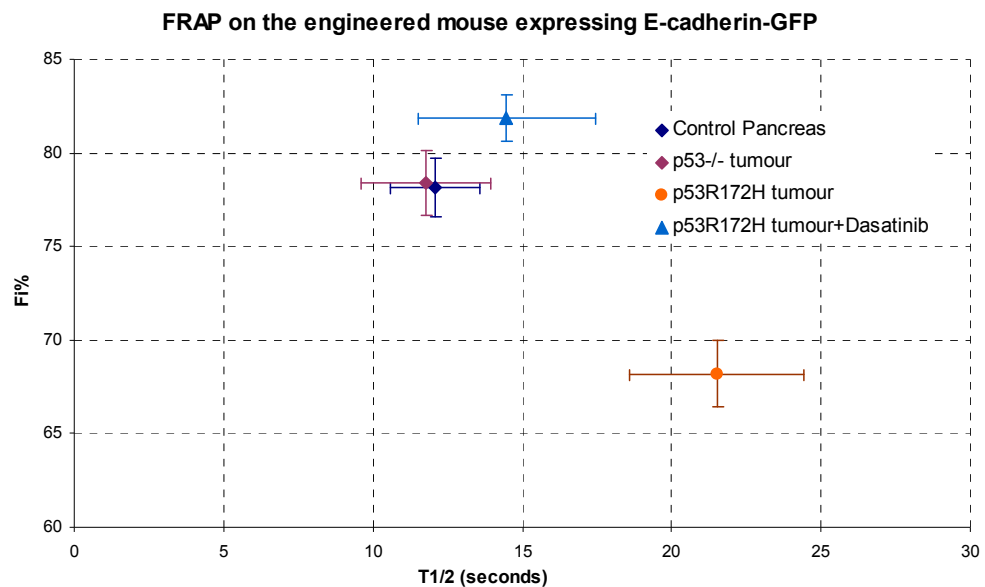
Figure 4.14. Dasatinib overturns the effect of mutant p53 on the reduction in mobility of E-cadherin in pancreatic tumours. FRAP on ex vivo p53 mutant pancreatic tumours after treatment with dasatinib. dasatinib treatment increased the Fi% and decreased the T1/2. E-cadherin-GFP dynamics in p53 mutant tumours treated with dasatinib is similar to normal pancreatic tissue or tumours with loss of 53. The data for normal pancreas, p53172 and p53-/- tumours are duplicated from figure 4.11.E. Error bars show SEM. (For each data point 3 mice is studied and n=at least 12 recovery curves).

5. Discussion

5.1. E-cadherin molecules need cis, trans and actin interactions to form adhesions:

E-cadherin is a cell adhesion protein required for epithelial tissue integrity. Down-regulation of E-cadherin expression is often associated with a phenotypic switch from a benign epithelial state to a metastatic mesenchymal state (Birchmeier 1994). However disruption of cell-cell adhesion occurs not just through down-regulation of E-cadherin levels, but also through mis-regulation of its dynamics and interaction with other proteins (Gumbiner 2000). Many forms of metastatic cancer retain E-cadherin expression (Gaida 2012), and recent evidence supports the hypothesis that mis-regulation of E-cadherin dynamics can also drive metastasis (Serrels 2009).

E-cadherin can form extra-cellular interactions with monomers from the same cell (cis) and interactions with monomers from adjacent cells (trans) via association of the EC1 domain (Thiery 2002, Harrison 2011, Hong 2011), and interact with the cortical actin cytoskeleton via association of its cytoplasmic domain with beta-catenin and alpha-catenin (Desai 2013). However the interactions governing E-cadherin dynamics remain poorly understood. To address this issue I have systematically investigated the mobility of mutant E-cadherins which can not form cis, trans dimers or bind to actin.

FRAP (Fluorescence Recovery After Photobleaching) has been widely used to study E-cadherin dynamics (Harrison 2011, Serrels 2009, Yamada 2005, de Beco 2009, Hong 2010). The technique involves rapid bleaching of a small region of interest (ROI) at the mid point of a cell-cell junction, and observation of fluorescence recovery into the bleached region using time-lapse microscopy. Simple quantification of FRAP is achieved by fitting an exponential curve to a time series of fluorescence intensity measurements from the ROI, which results in 2 primary read-outs: the half-time of recovery (T1/2) and the immobile fractions (Fi) (Lippincott 2001, Sprague 2005). T1/2 is a measure of the rate at which mobile molecules moves in and out of the bleached ROI, whereas Fi represents fluorescent molecules trapped in the ROI.

It is unclear how E-cadherins different interactions regulate its partitioning into mobile and immobile fractions, and determine the recovery rate of the mobile fraction. In the present study, I have used a pancreatic cancer model (Morton 2010-1,

Morton 2010-2) to systematically investigate the molecular determinants of E-cadherin FRAP, using mutant analysis, chemical cross-linking and co-culturing of expression level variants. FRAP experiments are commonly designed to compare a single mutant, or a group of related mutants, with wild-type E-cadherin. By interfering with all three E-cadherin interactions, individually and in selected pairs, I have revealed general behavior about E-cadherin binding which could not be deduced from any single comparison with wild-type protein.

5.1.1. Immobilization of E-cadherin-GFP in cell-cell junctions is due to both non-specific trapping and binding to adhesive clusters.

I analysed FRAP in PDAC^{fl} cells derived from tumors from KRAS$^{G12D/+}$ p53$^{+/-}$ which were stably transfected with wild-type E-cadherin-GFP (and mutants). The results showed that around 60% of wild-type E-cadherin-GFP molecules are immobilized in cell-cell junction in cells in a complete confluent monolayer grown on glass.

It has been previously shown that photo-activatable GFP (PA-GFP) linked to the plasma membrane via the H-Ras membrane targeting sequence (farn-farn-palm) had an Fi of approximately 25% in vivo (Serrels 2009). PA-GFP is not expected to bind to any component of the actin cytoskeleton; however it has been proposed that membrane components could be non-specifically trapped through a membrane fence mechanism (Kusumi 2005). I hypothesized that non-specific trapping might also contribute to the immobile fraction of E-cadherin.

To test this idea I generated a GFP-labelled mutant of E-cadherin lacking both the EC1 and cytoplasmic domains (ΔEC1ΔCyt-GFP) and compared its FRAP with wild-type E-cadherin-GFP. This mutant is unable to form cis-, trans-, or actin interactions and its fluorescence intensity should therefore recover completely by a diffusion only mechanism. Although this mutant recovered quickly, it had an unexpectedly high immobile fraction (30%), which was half the level of wild-type E-cadherin-GFP (60%).

To provide a reference for unrestrained diffusion, FRAP analysis was performed on PDAC^{fl} cells stably transfected with GFP alone targeted to the inner leaflet of the plasma membrane via the farn-farn-palm sequence (GFP-F). Again I found a surprisingly high Fi supporting the idea that ΔEC1ΔCyt-GFP was trapped in the

plasma membrane through non-specific interactions. Taken together, these data suggested that the 60% Fi of wild-type E-cadherin-GFP was comprised of two components: 30% non-specifically trapped in the manner of ΔEC1ΔCyt-GFP, and 30% trapped via specific interactions involving the EC1 and/or cytoplasmic domains. Analysis of the same mutant in L cells which do not express endogenous E-cadherin showed that the high non-adhesive immobile fraction of E-cadherin is presents in L cells as well.

5.1.2. The recovery rate of wild-type E-cadherin-GFP is limited by monomer turnover within adhesive clusters.

Next I analysed whether the recovery of mobile E-cadherin molecules is determined by diffusion or by dissociation from adhesive complexes in membrane. One approach for distinguishing between diffusion-coupled and uncoupled recoveries is to vary the size of the ROI used for bleaching and analysis. For a diffusion-coupled process, the recovery half-time should increase with increasing ROI diameter, because T1/2 depends on the diffusion of monomers from the centre to the edge of the ROI. Conversely, the ROI size should not affect T1/2 for diffusion uncoupled recovery because the rate of monomer turnover is related to dissociation\association rate from clusters and it is independent of ROI size (see section 1.4.5.3). I analyzed GFP-F, ΔEC1ΔCyt-GFP, ΔEC1-E-cadherin-GFP and wild-type E-cadherin-GFP using ROIs of 20, 30, and 40 pixels in diameter. GFP-F and ΔEC1ΔCyt-GFP are not able to bind to any immobile complex in the plasma membrane. Consequently the recovery is just due to diffusion. As expected, the recovery time of both GFP-F and ΔEC1ΔCyt-GFP increased with increasing ROI diameter, confirming that these processes are driven by diffusion alone. In contrast, wild-type E-cadherin-GFP can bind through cis and trans dimmerization and by interaction with actin with stationary complexes in the membrane. The recovery time of E-cadherin-GFP remained constant with increasing ROI diameter, indicating that this recovery is diffusion uncoupled and it is limited by the interaction of E-cadherin with stationary binding partners. This diffusion uncoupled behaviour of FRAP recovery was also reported for VE-cadherin molecules (Nanes 2012).

Moreover, the mutant ΔEC1-E-cadherin-recovery time increased by increasing ROI size. So by disrupting the cis and trans interactions the dissociation rate of cadherin molecules increased and the recovery of E-cadherin became diffusion coupled.

To confirm that recovery rate of E-cadherin FRAP depends on the rate association\dissociation rather than diffusion rate, I performed cross-linking experiments using the cell-impermeable zero-order cross-linker BS3. Based on the small size of the linker (11.4 Å), it is expected to only cross-link molecules in direct proximity. For comparison with wild-type E-cadherin-GFP I used ΔEC1ΔCyt-GFP. Cell lysates probed with an anti-E-cadherin antibody demonstrated that BS3 was able to cross-link E-cadherin-GFP but not ΔEC1ΔCyt-GFP. This indicates that a component of E-cadherin-GFP is self-associated in the plasma membrane, whereas ΔEC1ΔCyt-GFP is entirely present as monomers. I next performed FRAP analysis on PDAC^{fl} cells treated with BS3. Interestingly, I found that cross-linking significantly increased the Fi of E-cadherin-GFP from 60% to 85% and dramatically reduced T1/2 from 50 seconds to 7 seconds, similar to the recovery rate of freely diffusing E-cadherin-ΔEC1ΔCyt-GFP. Moreover, in PDAC^{fl} cells treated with the cross-linker, increasing ROI size increased the recovery time which indicates that the recovery of E-cadherin-GFP became diffusion coupled. Interestingly, when the incubation time of cross-linking was reduced by half, the resulting partial increase in Fi and decrease in T1/2 suggested a partial shift from diffusion coupled to diffusion uncoupled recovery. In contrast to E-cadherin-GFP, and in agreement with western blot analysis, ΔEC1ΔCyt-GFP was unaffected by BS3 cross-linking. These data confirm the diffusion uncoupled nature of wild-type E-cadherin recovery. The recovery of the non binding mutant E-cadherin (ΔEC1ΔCyt-E-cadherin-GFP) is due to diffusion of moleculese in and out of the bleached ROI. But the recovery of wild-type E-cadherin-GFP is not limited by diffusion rate and it is determined by the rate of association and dissociation of E-cadherin molecules from stationary complexes in the membrane. When these transient interactions (association and dissociation from stationary complexes) are stabilized by cross-linking then the recovery is just determind by diffusion of non cross-linkable E-cadherin molecules which recovered at the rate of freely diffusing mutant E-cadherin.

Consequently, the cross-linking experiment results suggest that the 40% mobile fraction (Fm) of E-cadherin-GFP is comprised of two components. The first component is the Fm of cross-linked E-cadherin-GFP, consisting of free monomers

which could not be cross-linked by BS3 treatment and representing approximately 15% of total E-cadherin-GFP. The other component is the difference between cross-linked and non-cross-linked E-cadherin-GFP, consisting of monomers prevented from leaving stationary complexes after cross-linked with BS3 and representing approximately 25% of the total E-cadherin-GFP. These data suggest that some mobile E-cadherin molecules in the membrane are unable to form any interaction with other cadherin molecules or bind to actin. Moreover, the remaining cross-linkable cadherin molecules form transient interactions with adhesive clusters which associate\disassociate from adhesive complexes during FRAP recovery time. Further investigation is required to uncover the basis for this differential behaviour.

5.1.3. Trans-dimer equilibrium regulates the size of Fi

Subsequently I wanted to explore the relationship between Fi and cell adhesion strength. In order to analyse how the expression level of E-cadherin influences cell adhesion strength, first I sorted PDAC[fl] cells into high and low groups according to the level of E-cadherin-GFP expression. The integrity and strength of cell-cell adhesions of confluent cell monolayers was assessed using trans-epithelial electrical resistance (TEER) and resistance to dispase treatment, which confirmed that the integrity and strength of cell-cell junctions depends on the E-cadherin-GFP expression level, and was greater for high expressing cells. I next performed FRAP on E-cadherin-GFP-high and E-cadherin-GFP-low cells and found that the immobile fraction was equal for both cell types, indicating that Fi was not directly linked to cell adhesion strength when E-cadherin expression levels are not similar.

In contrast, the recovery half-time of E-cadherin-GFP-low cells was substantially reduced compared to E-cadherin-GFP-high cells. In other words, the E-cadherin-GFP molecules recovered more quickly in cell-cell junction in cells with lower E-cadherin expression level. Then I studied whether the immobile fraction of E-cadherin in one cell depends on the availability of E-cadherin on the neighbouring cell. PDAC[fl] cells expressing E-cadherin-GFP-high were co-cultured with the parental PDAC[fl] line. The total level of E-cadherin expression is lower in the parental line because it does not express E-cadherin-GFP on top of endogenous levels, and FRAP experiments therefore report on behaviour only within the E-cadherin-GFP-high cells. I found that both Fi and T1/2 were significantly reduced compared to FRAP performed between

two E-cadherin-GFP-high cells. This demonstrates that the availability of E-cadherin in the partner cell of a junction significantly influences the amount of cadherin stabilized in the junctions. Moreover, analysis of E-cadherin mobility at a free cell edge, in the absence of any trans-dimer associations, revealed that Fi and T1/2 were reduced nearly to the level of ΔEC1ΔCyt-GFP, demonstrating that trans-interactions are necessary for formation of stationary clusters.

The data showed that the major difference between E-cadherin-GFP-high and low cells was in T1/2 not immobile fraction. E-cadherin FRAP recovery is diffusion uncoupled, so the diffusion of bleached molecules happens very fast and the recovery rate is limited by rate of association\dissociation of E-cadherin molecules

Imaging E-cadherin-GFP-high junctions and E-cadherin-GFP-low junctions using NSTORM super-resolution microscopy revealed that E-cadherin-GFP formed clusters of similar sizes in both junction types, but that the average distance between cluster centres was 65% greater for the E-cadherin-GFP-low cells (Figure 5.1).

These data indicate that PDAC^{fl} cells respond to different expression levels of E-cadherin by varying the density of similarly sized clusters, rather than maintaining the same density of differentially sized clusters. This indicates that a higher density of stationary clusters in E-cadherin-GFP-high cells slows down the movement of E-cadherin molecules probably by decreasing the distance that released monomers diffuse before binding to a new stationary cadherin cluster. This result suggests that individual E-cadherin monomers undergo multiple rounds of unbinding, diffusion, and rebinding before moving out of bleached ROI. In other word, recovery of E-cadherin is related to association rate of monomers to stationary binding sites (K_{on}) rather that just dissociation rates (K_{off}). This implies that the recovery of E-cadherin molecules should be diffusion coupled. This is in contrast to FRAP results in different ROI size which suggested a diffusion uncoupled FRAP behaviour. One simple explanation would be that when binding interactions are present the effect of ROI size on recovery is small and the FRAP analysis is not sensitive enough to detect the difference.

However, E-cadherin recovery is not due to just one binding\unbinding reaction. E-cadherin molecules attach to other molecules through cis, trans and actin binding. There are two mobile components that determine the recovery rate of E-cadherin: Adhesive mobile fraction and non-adhesive mobile fraction (see section 5.1.5). The difference in recovery rate of E-cadherin could be due to change in proportion of

these two populations rather than change in association\dissection rate of E-cadherin monomers.
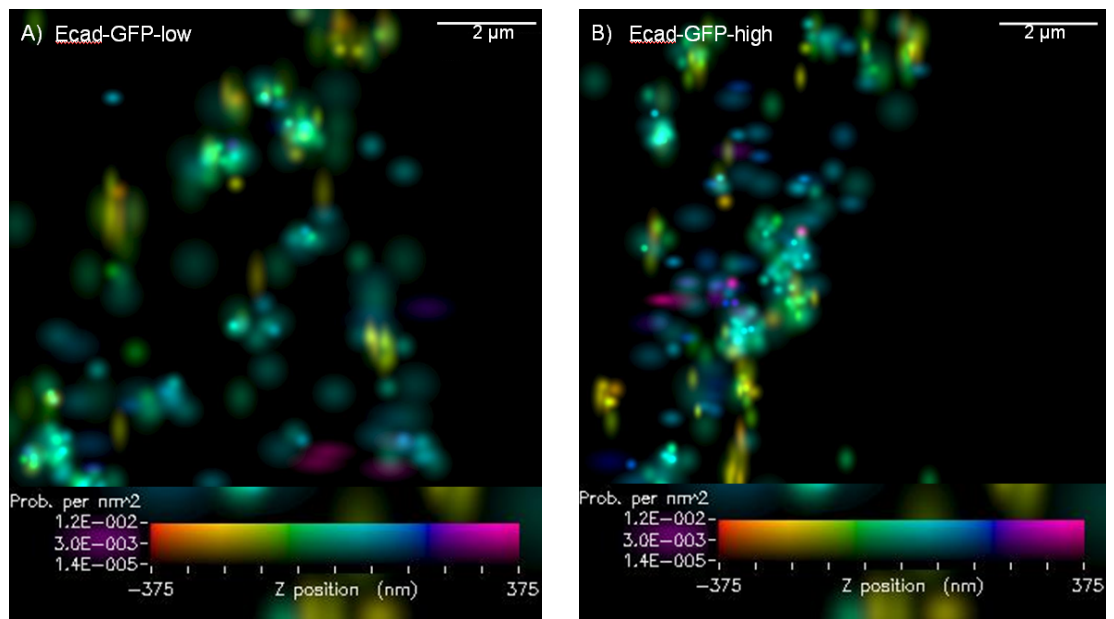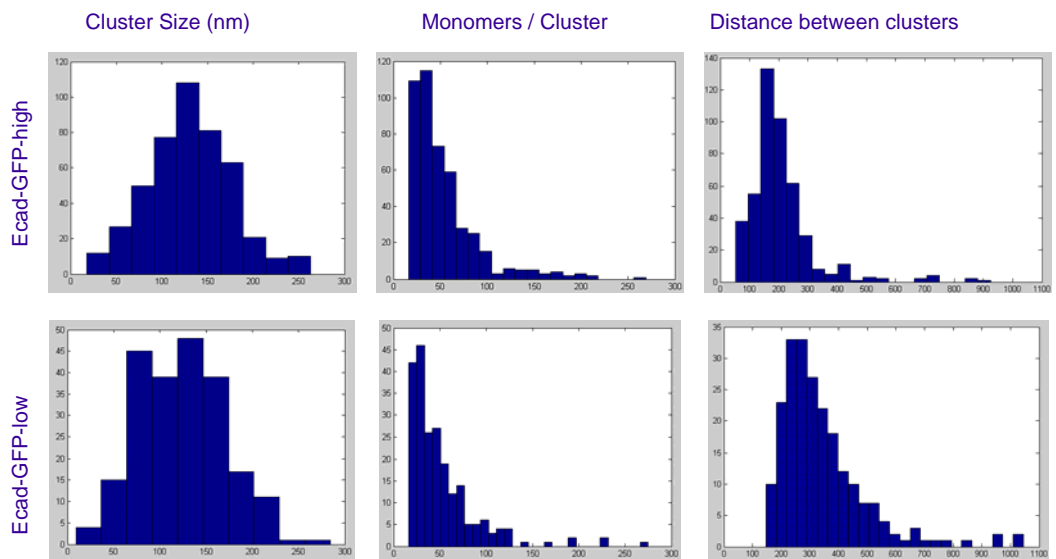
Figure 5.1. Cells expressing high level of E-cadherin have similar size clusters which spaced more densely. E-cadherin-GFP-high (A) and -low (B) cells were imaged using N-STORM super resolution microscopy. C) The quantification of the data showed that the average cluster size was the same for both high and low cells (131.0 ± 45.6 nm vs. 123.8 ± 46.5 nm, respectively), but the spacing between clusters was smaller for E-cadherin-GFP-high cells (205.9 ± 113.5 nm vs. 341.6 ± 151.6 nm). (The bars is 0.2 microns) (unpublished data in collaboration with Wu Yao and Ronen Zaidel-Bar)

5.1.4. Inclusion of E-cadherin into the adhesive Fi requires cis-, trans-, and cytoplasmic interactions

FRAP analysis of E-cadherin at a free cell edge suggested that trans- interactions contribute to Fi and T1/2. To further determine the relative contribution of these interactions to E-cadherin FRAP, I made mutants defective for each interaction. Disruption of any single interaction was sufficient to reduce Fi to the non-specific level of the free diffusing mutant ΔEC1ΔCyt-E-cadherin-GFP. This suggests that all three interactions (cis-, trans-, and actin) are required for inclusion of E-cadherin-GFP into the adhesive immobile fraction.

It has been previously suggested that formation of cis and trans interactions in tailless E-cadherin is enough for clustering E-cadherins at junctions (Hong 2010). However, my TEER and dispase assay results showed that although ΔCyt-E-cadherin mutant may form clusters at the cell-cell junctions in absence of actin interaction, they are unable to increase cell-cell adhesion strength.

My data showed that all three E-cadherin interactions cis, trans and actin binding are necessary to form adhesive clusters. By disrupting any interaction the E-cadherin mutants are unable to increase cell-cell adhesion. Hong et al also reported similar effect, that cis and trans dimerization cooperate with actin binding to decrease mobility of E-cadherin molecules (Hong 2013).

With respect to T1/2, the mutants clustered into two groups: mutants retaining the cytoplasmic tail recovered more slowly, whereas the cytoplasmic deletion mutants recovered more quickly. It is interesting to note that the recovery of E-cadherin-GFP at the free cell edge was similar to the recovery of E-cadherin mutants that retained the cytoplasmic interaction with the actin cytoskeleton. These data show that cytoplasmic interactions significantly slow the free diffusion of E-cadherin-GFP, whereas cis- or trans-interactions (alone or in conjunction) do not.

5.1.5. There are four distinct components of E-cadherin in cell-cell junctions.

I have systematically investigated the determinants of E-cadherin FRAP in pancreatic cancer cells. By interfering with all three E-cadherin interactions, individually and in selected pairs, the data revealed a general behaviour about E-cadherin binding which could not be deduced from any single comparison with wild-

type protein. The data clearly showed that E-cadherin FRAP is diffusion uncoupled, and that the mobile and immobile fractions have adhesive and non-adhesive components, which can be defined according to specific molecular interactions. On this basis I can define four distinct components that contribute to E-cadherin FRAP:

	Non-Adhesive	**Adhesive**
Immobile	**Non-adhesive immobile fraction** 30% • Fi% (ΔEC1ΔCyt) • Non- specifically trapped in membrane structures	**Adhesive immobile fraction** 30% = 60% - 30% • Fi (wt Ecad) – Fi(ΔEC1ΔCyt) • Stabilized in adhesive clusters • Requires cis, trans, and actin
Mobile	**Non-adhesive mobile fraction** 15% = 100% - 85% • Fm (X-linked wt Ecad) • Diffusion Coupled • presents in monomeric form	**Adhesive mobile fraction** 25% = 85% - 60% • Fi (X-linked) – Fi (wt Ecad) • Diffusion Uncoupled • Transiently bind\unbinds from adhesive clusters

Table .5.1. Four fractions of E-cadherin in plasma membrane in cells grown on glass.

5.1.5.1. The non-adhesive immobile fraction

This sub-population (~30% in PDAC cells) consists of E-cadherin non-specifically trapped in the plasma membrane in the same way as GFP-F and ΔEC1ΔCyt-E-cadherin-GFP, neither of which can form cis-, trans-, or actin interactions. My results are consistent with single molecule imaging of E-cadherin in the plasma membrane, which previously suggested that a significant fraction of E-cadherin is restrained in its diffusion (Iino 2001). Such non-adhesive trapping has been previously demonstrated in the plasma membrane for trans-membrane proteins and phospholipids and appears to be a consequence of membrane compartmentalization induced by the cortical actin meshwork (Kusumi 2005, Kusumi 1993). However, Kusumi et al. used FRAP and SPT (single particle tracking) to study the E-cadherin mobility in dorsal surface of cell, which is not similar to mobility of E-cadherin at cell-cell junctions. Dynamics of actin cytoskeleton is different in cell-cell contacts which could affect trapping of trans-membrane molecules in membrane. However, in this study, the non-specific immobile fraction of ΔEC1ΔCyt mutant E-cadherin was measured at cell-cell contacts, and the mobility of wild-type E-cadherin-GFP was

measured in similar way. This provides a control for non-specific trapping of E-cadherin molecules to distinguish between specific immobilization in adhesive E-cadherin clusters and non-specific trapping at cell-cell junctions.

5.1.5.2. The adhesive immobile fraction

Deletion of cis-, trans-, or actin interactions reduced the Fi of E-cadherin-GFP from 60% to the level of ΔEC1ΔCyt-GFP (~30% in PDAC cells), suggesting that all three interactions are required for adhesive immobilization of E-cadherin in cell-cell junctions. These data are consistent with a model in which individual interactions are weak, and multiple interactions are required in order to stabilize E-cadherin within the adhesive immobile fraction. Moreover, the regulation of any single interaction (cis-, trans-, or actin) is sufficient to drive E-cadherin out of the adhesive Fi. This suggests a mechanism in which regulation of actin association alone could be sufficient to regulate adhesive complex formation.

Furthermore, the mechanism by which association\dissociation of E-cadherins from adhesive clusters are regulated remains unclear. One possible mechanism could be regulation of catenins by phosphorylation. Tension also could play a role in further stabilizing E-cadherin within the adhesive immobile fraction (de Rooij 2005, Huveneers 2013).

5.1.5.3. The adhesive mobile fraction

This fraction (~25% in PDAC cells) has a slow recovery time, and the recovery depends on dissociation\association of molecules from adhesive complexes rather than just free diffusion. Changing the size of the analysis ROI had no effect on T1/2, further suggesting that recovery was limited by dynamic equilibrium of monomers with stationary binding partners rather than diffusion. Cross-linking experiments, which reduced the mobile fraction of E-cadherin-GFP from 40% to 15%, established the size of this fraction.

Recent work has shown that cytoplasmic domain deletion mutants of E-cadherin (ΔCyt-E-cadherin-GFP) can form patches at sites of cell-cell contact, which approximate the localization of wild-type E-cadherin seen in the light microscope (Harrison 2011, Hong 2010, Ozaki 2010). The ability of these mutants to cluster has

suggested a mechanism for junction assembly in which extracellular interactions precede intracellular interactions (Brasch 2012). However, the ability of cytoplasmic deletion mutants to cluster does not necessarily imply that extracellular interactions are the preferred first step of assembly if cytoplasmic interactions are possible. My data showed that cytoplasmic interactions significantly slowed the diffusion of E-cadherin mutants, whereas cis- and trans- interactions did not. This suggests that cytoplasmic interactions may precede extracellular interactions during junction assembly. The reduction in diffusion due to cytoplasmic interactions could be due to the strength of cytoplasmic interactions, the abundance of binding sites within the cortical actin meshwork, or both.

5.1.5.4. The non-adhesive mobile fraction

This sub-population (~15% in PDAC cells) is represented by the 15% of E-cadherin-GFP which could be not cross-linked by BS3 treatment. The recovery of this fraction at the rate of free diffusion suggests it is unable to form transient interactions with stationary adhesive complexes, which would otherwise limit its recovery rate. A possible explanation for this is that this 15% is unable to bind β-catenin due to phosphorylation of β-catenin at Y489 by Abl kinase and at Y654 by Src or EGF receptor (Lilien 2002, Rhee 2002, Roura 1999, Hoschuetzky 1994). In wild-type cells, the rapid recovery of this non-adhesive mobile fraction (15% of total) is masked by the slower recovery of the adhesive mobile fraction (25% of total).

A further conclusion of my work is the importance of certain control experiments for the interpretation of E-cadherin FRAP data. The most important is the use of ΔEC1ΔCyt-GFP to establish the baseline rate of diffusion coupled recovery and the non-adhesive Fi. The analysis of different ROI sizes is also useful in order to determine whether recovery of a mutant is diffusion coupled or uncoupled. As my results demonstrate, full comparison of a mutant series can reveal general behaviour patterns not obvious on the basis of a single mutant data point.
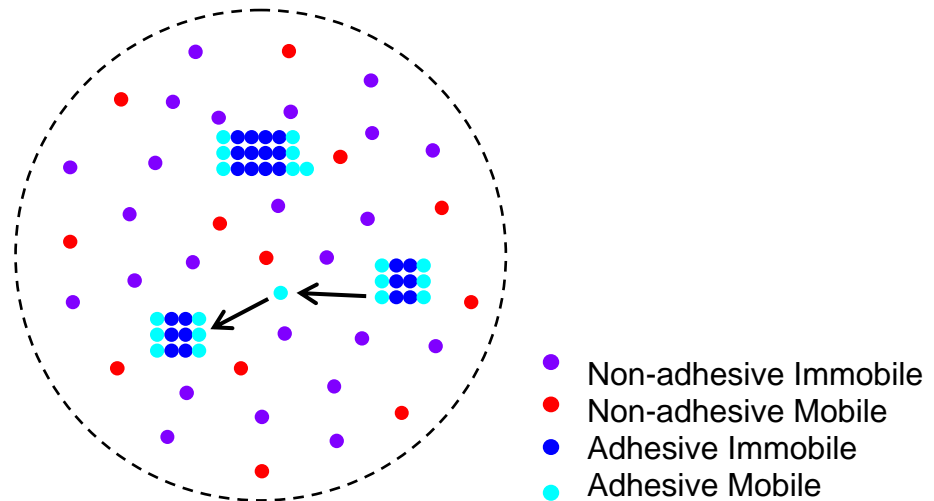
Figure 5.2. There are four E-cadherin populations within the ROI of a FRAP experiment. Non-adhesive immobile monomers (purple) are trapped through non-specific interaction with the cortical cytoskeleton. Non-adhesive mobile monomers freely move and do not bind to complexes. Adhesive immobile monomers are bound to clusters and remain stationary. Adhesive mobile monomers alternate between transient binding and diffusion.

5.2. FRAP Analysis of E-Cadherin Dynamics as a Read-Out for Cell Motility.

In many cancer cells mis-regulation of adherens junctions causes increased progression and invasion of cancer (Birchmeier 1994). Alteration in E-cadherin dynamics could therefore serve as an early molecular biomarker of metastasis. Here, I had analyzed how E-cadherin dynamics are related to cell motility and invasion in two PDAC cell lines derived from primary pancreatic tumours of the KPC mouse model. In this model tumour formation is driven by mutant KRAS; however, tumour metastasis is driven by mutant p53 (Morton 2010). Here, I studied the effect of local environments on the mobility of E-cadherin in cell lines derived from mouse primary tumours. Moreover, I have used FRAP both in vitro and in vivo to analyse the dynamics of E-cadherin in invasive and non-invasive cells, and in response to therapeutic intervention with the Src inhibitor Dasatinib.

5.2.1. P53 mutation drives cell invasion in PDAC cells and weakens cell-cell adhesions.

In the KPC mouse model KRAS^{G12D} mutation drives formation of PanINs, then loss of p53 promotes formation of pancreatic tumours. Mice with Pdx1-Cre, LSL-KRAS$^{G12D/+}$, Trp53$^{LoxP/+}$ genetic background form tumours which are not invasive. On the other hand, mice with Pdx1-Cre, LSL-KRAS$^{G12D/+}$, LSL-Trp53$^{R172H/+}$ genetic background form invasive tumours. PDAC cell derived from the tumours with loss of p53 expression (PDAC^{fl}) are not invasive in organotypic assay and xenograft tumours. On the other hand, PDAC cells from tumours with p53^{R172H} mutation (PDAC^{R172H}) are more progressive and invasive than PDAC^{fl} cells. Moreover, expression of human mutant p53 protein (p53^{R175H}) in PDAC^{fl} cells is sufficient to activate cell invasion in PDAC^{fl} cells (Morton 2010). Here, I studied PDAC cell line stably transfected with E-cadherin-GFP plasmid. The PDAC^{R172H} and PDAC^{fl}R175H cells with E-cadherin-GFP expression are still highly invasive, and there was no significant difference in depth of invasion between original cells and E-cadherin-GFP expressing cells.

Moreover, analysing cell-cell adhesion and integrity of junctions through dispase assay and TEER measurements showed that mutant p53 dramatically weakens cell-cell adhesion compared to cells with loss of p53 expression.

5.2.2. Mutant p53 mobilizes E-cadherin on cells grown on CDM but not glass.

My data showed that the effect of mutant p53 on E-cadherin dynamics depends on the local cell environment. E-cadherin mobility increased in PDAC^{fl}R175H cells in comparison to PDAC^{fl}vector cells when grown on CDM but not glass. P53 mutant cells have significantly lower Fi and T1/2 in cells grown on CDM. When cells express comparable levels of E-cadherin, Fi is related to the amount of E-cadherin stabilized at junctions. Consequently, higher Fi indicates more stabilized junctions and stronger cell-cell adhesion. Moreover, the dispase assay was used to study cell-cell adhesion in PDAC^{fl}vector and PDAC^{fl}R175H cells grown on CDM, which confirmed that mutant p53 loosens cell-cell junctions by mobilizing E-cadherin.

It has been previously shown that ECM components such as integrins could affect the regulation of E-cadherin cell-cell adhesions (deRooji 2005). My data also showed

that interaction of cell derived matrix (CDM) components with cells is necessary for mutant p53 de-regulation of E-cadherin cell-cell adhesion.

Moreover, in colon cancer cells integrin signalling is necessary for disruption of E-cadherin cell-cell adhesion by Src. Src phosphorylation of focal adhesion kinase (FAK) which is regulated by integrin signalling disrupts E-cadherin cell-cell adhesions (Avizienyte 2002). My results also showed that treatment of PDAC^{fl}R175H cells growing on CDM with Src inhibitor dasatinib decreased mobility of E-cadherin in mutant p53 cells. This suggests that mutant p53 could regulate E-cadherin dynamics through Src activation. Moreover, interaction of ECM and integrin signalling is required for weakening of cell-cell adhesions by p53 mutants.

5.2.3. Mutant p53 drives invasion by increasing the mobility of E-cadherin in PDAC cells in xenograft tumours:

The data suggested that micro environment plays an important role in determining the effects of mutant p53 on E-cadherin dynamics and cell migration. Extracellular matrix strongly affects cell migration. However, CDM is a very artificial environment compared to tumours. The composition of ECM and its rigidity is different in CDM compared to tissue. Moreover, the presence of immune cells and inflammation affects cells invasion (Smith 2013). Therefore, for a better understanding of dynamics of E-cadherin in functional and physiological context of real tumors, I measured FRAP in xenograft tumors.

Xenograft tumours derived from the PDAC^{fl}R175H cell line were highly invasive compared to PDAC^{fl}vector tumours. The histological analysis of xenograft tumours showed that mutant p53 cells invade through muscle and the peritoneal cavity. The FRAP results showed that the immobile fraction of E-cadherin was significantly reduced in PDAC^{fl}R175H xenografts compared to PDAC^{fl}vector tumours. This reduction in E-cadherins stabilized at cell-cell junctions is similar to the effect of mutant p53 on mobilizing E-cadherin and consequently weakening cell-cell adhesions in cells cultured on CDM. In contrast, p53 mutation had a different effect on the rate of E-cadherin recovery in xenograft tumours compared to CDM. On CDM mutant p53 reduced T1/2 but in xenograft tumours PDAC^{fl}R175H cells have larger T1/2 compared to PDAC^{fl}vector cells. This indicates that the recovery time of

E-cadherin which determined by rate of dissociation\association of E-cadherin molecules from stationary complexes is dramatically different in vivo compared to in vitro.

5.2.4. PDAC cells showed different E-cadherin dynamics in tissue compared to CDM.

My FRAP results showed that xenografts, have higher immobile fraction and much smaller T1/2 compared to cells growing on glass or CDM. The higher Fi could be due to increased non-adhesive or adhesive immobile fraction. To answer this question, the mutant $\Delta EC1\Delta Cyt$ E-cadherin-GFP was stably expressed in PDAC^{fl}vector cells in xenografts to estimate the level of non-adhesive immobile fraction. The Fi% of the $\Delta Cyt\Delta EC$ mutant in PDAC^{fl} xenograft was approximately 60% which is significantly higher than 30% the Fi for these cells grown in culture. This 60% immobile fraction establishes the baseline for non-adhesive immobile fraction in PDAC^{fl} cells in xenograft tumours.

Moreover, the FRAP on $\Delta EC1\Delta Cyt$ mutant that recovers as fast as free molecule of approximate size of E-cadherin showed that although there is a significant difference between Fi% in wild-type E-cadherin-GFP and $\Delta EC1\Delta Cyt$ mutant in PDAC^{fl}vector xenograft, there is no significant difference between T1/2. Thus, in xenograft tumours wild-type E-cadherin recovered very fast, approximately similar to recovery rate of non-binding mutant. This similarity in T1/2 suggests that the mobile fraction of wild-type E-cadherin-GFP molecules does not form any transient interaction with adhesive cadherin complexes in membrane to slow down its recovery. This suggests that the rate of dissociation of E-cadherins from stationary complexes are so slow that they are appeared stable and immobilized during the FRAP time period.

Thus, the adhesive mobile fraction in PDAC^{fl}vector tumours is vey small. In other words, cadherin molecules are either immobile (in junctions or trapped non-specifically) or completely freely diffusing in the membrane. In contrast, in cell culture, 25% adhesive mobile fraction of wild-type E-cadherin-GFP forms transient interactions which significantly slowed its recovery.

Next I analysed the non-interacting E-cadherin mutant in p53 mutant tumours. The FRAP data for the ΔCyt mutant showed that there is no significant difference in Fi%

compared to wild-type E-cadherin-GFP in PDAC$^{\text{fl}}$R175H xenografts, which indicates that mutant p53 significantly reduced the adhesive immobile fraction in E-cadherin-GFP molecules. However, T1/2 is significantly increased in wild-type E-cadherin-GFP compared to ΔCyt mutant. In other word, p53 mutation reduces the adhesive mobile fraction of E-cadherin while increased the adhesive immobile fraction. This indicates cadherin molecules which are stable in adhesive clusters became unstable and this dissociation\association from the clusters slows down their recovery.

Moreover, comparison of the ΔCyt mutant dynamics in PDAC$^{\text{fl}}$vector and PDAC$^{\text{fl}}$R175H cells showed similar Fi and T1/2 values. This data indicates that the difference in Fi between PDAC$^{\text{fl}}$vector and PDAC$^{\text{fl}}$R175H xenografts is not due to different non-adhesive immobile fraction. Therefore, the mutant p53 specifically changed cell-cell adhesion by decreasing the E-cadherin immobilized at junctions.

5.2.5. p53 mutation, not loss, removes the E-cadherins from junctions in pancreatic tissue.

Although xenografts are a convenient model for studying cells in vivo, the subcutaneous growth of pancreatic tumour cells does not recapitulate the native environment of the pancreas. Ideally, it would be best to study cell migration in its naturally occurring context in living organisms. So, I used a genetically engineered mouse expressing GFP-E-cadherin crossed with the KPC mouse model to be able to study FRAP in the pancreas and pancreatic tumours. Due to the location of the pancreas deep within the peritoneal cavity, it was not possible to image this organ in situ. So imaging was performed on excised pancreatic tissue ex vivo.

Comparison of FRAP results in xenograft tumours in vivo and ex vivo showed no significant difference, which implies that dynamics of E-cadherin measured in ex vivo tissue is comparable to in the vivo situation.

I studied E-cadherin dynamics in healthy pancreas, tumours with loss of p53 expression (from mice with Pdx1-Cre, LSL-KRAS$^{\text{G12D/+}}$, Trp53$^{\text{LoxP/+}}$ genetics) and tumours with mutant 53 expression (Pdx1-Cre, LSL-KRAS$^{\text{G12D/+}}$, Trp53$^{\text{R172H/+}}$). The FRAP data showed that mutant p53 decreased the immobile fraction of E-cadherin and increased the recovery time similar to PDAC cells in xenograft tumours.

Moreover, normal pancreatic tissue and tumours with loss of p53 expression showed no significant difference in FRAP data. This indicates loss of p53 does not alter E-cadherin dynamics. Mutation in p53 is a gain of function mutation which weakened the interaction between E-cadherin molecules, reduced the adhesive immobile fraction and increased the T1/2. This increased mobility of E-cadherin in junction disrupts cell-cell adhesion in p53 mutant tumour cells which promotes the metastasis of these cells from the primary tumour.

Previously it has been shown that treatment of mice with the Src inhibitor dasatinib hinders the tumour cells metastasis. Treating PDAC^{fl}R175H xenograft tumours with dasatinib increased the immobile fraction and decreased T1/2. Thus mutant p53 weakens the cell-cell adhesion by mobilizing E-cadherin in junctions and dasatinib inhibits metastasis through stabilizing E-cadherin at adhesions. Then, I used FRAP to assess how dasatinib treatment affects E-cadherin dynamics in mutant p53 pancreatic tumours. Dasatinib treatment significantly decreased the mobility of E-cadherin in mutant p53 tumours. Moreover, this indicates that I can use FRAP as a pharmacodynamic marker to assess the effect of dasatinib in pancreatic tumours.

In conclusion, I showed that E-cadherin FRAP can be used to asses real time dynamics of cadherin junctions in vivo. The cadherin junctions dynamics can be used as marker for prediction of tumour cells potential to metastasize. Moreover, this project provided a comprehensive framework for understanding E-cadherin dynamics at cell-cell junctions based on specific and non-specific molecular interactions. This framework will support the design and interpretation of future pharmacological and genetic experiments to probe the function of E-cadherin in development, disease progression, and response to therapy.

6. References:

Aberle, H., Bauer, A., Stappert, J., Kispert, A., and Kemler, R. 1997. Beta-catenin is a target for the ubiquitin–proteasome pathway. EMBO J. 16, pp. 3797–3804.

Aberle, H., Butz, S., Stappert, J., Weissig, H., Kemler, and R., Hoschuetzky, H. 1994. Assembly of the cadherin–catenin complex in vitro with recombinant proteins. J. Cell Sci., 107, pp. 3655–3663.

Aberle, H., Butz, S., Stappert, J., Weissig, H., Kemler, R., and Hoschuetzky, H. 1994. Assembly of the cadherin-catenin complex in vitro with recombinant proteins. J. Cell Sci., 107, pp. 3655–3663.

Adams, C.L., Chen, Y.T., Smith, S.J., and Nelson, W.J.. 1998 Mechanisms of epithelial cell–cell adhesion and cell compaction revealed by highresolution tracking of E-cadherin-green fluorescent protein. J. Cell Biol., 142, pp. 1105–1119.

Adams, C.L., and Nelson, W.J.. 1998-2. Cytomechanics of cadherin-mediated cell-cell adhesion. Curr Opin Cell Biol, 10, pp. 572–577.

Adorno M., Cordenonsi M., Montagner M., Dupont S., Wong C., Hann B., 2009. A mutant-p53/Smad complex opposes p63 to empower TGFβ-induced metastasis. Cell. 137: 87 – 98.

Alexander M,. Bendas, G.. 2011. The Role of Adhesion Receptors in Melanoma Metastasis and Therapeutic Intervention Thereof, Research on Melanoma - A Glimpse into Current Directions and Future Trends, Murph, M. (Ed.)

Almoguera, C., Shibata, D., Forrester, K., Martin, J., Arnheim, N., Perucho, M. 1988. Most human carcinomas of the exocrine pancreas contain mutant c-K-ras genes. Cell, 53, pp. 549–554.

Anastasiadis, P.Z., Reynolds, A.B. 2000. The p120 catenin family: complex roles in adhesion, signaling and cancer. J. Cell Sci., 113, pp. 1319–1334.

Anderson, K.E., Mack, T., Silverman, D. 2006. Cancer of pancreas. In Schottenfeld D, Fraumeni JF Jr. Cancer Epidemiology and Prevention. 3rd Ed. New York: Oxford University Press; 2006.

Attardi LD, Jacks T. 1999. The role of p53 in tumour suppression: lessons from mouse models. Cell Mol Life Sci. 55: 48 – 63.

Avizienyte, E., A.W. Wyke, R.J. Jones, G.W. McLean, M.A. Westhoff, V.G. Brunton, and M.C. Frame. 2002. Src-induced de-regulation of E-cadherin in colon cancer cells requires integrin signalling. Nat. Cell Biol. 4:632–638

Axelrod, D. et al., 1976. Mobility measurement by analysis of fluorescence photobleaching recovery kinetics. Biophys. J., 16, pp. 1055–1069.

Bardeesy, N., DePinho, R. 2002. Pancreatic cancer biology and genetics. Nature Reviews Cancer 2, 897-909

Bilder, D., Li, M. & Perrimon, N. 2000. Cooperative regulation of cell polarity and growth by Drosophila tumor suppressors. Science 289, 113–116.

Birchmeier, W., and Behrens,J. 1994. Cadherin expression in carcinomas: role in the formation of cell junctions and the prevention of invasiveness. Biochim. Biophys. Acta, 1198, pp. 11–26.

Boguslavsky, S., Grosheva, I., Landau, E., Shtutman, M., Cohen M., Arnold, K., Feinstein, E., Geiger, B., and Bershadsky, A. 2007. p120 catenin regulates lamellipodial dynamics and cell adhesion in cooperation with cortactin. Proc. Natl. Acad. Sci. U.S.A., 104, pp. 10882–10887.

Brasch J, Harrison OJ, Honig B, & Shapiro L. 2012. Thinking outside the cell: how cadherins drive adhesion. Trends Cell Biol 22(6):299-310.

Brembeck, F.H., Schwarz-Romond, T., Bakkers, J., Wilhelm, S., Hammerschmidt, M., Birchmeier, W.. 2004. Essential role of BCL9-2 in the switch between beta-catenin's adhesive and transcriptional functions. Genes Dev., 18, pp. 2225–2230.

Brooks SA, Lomax-Browne HJ, Carter TM, Kinch CE, Hall DM. 2010. Molecular interactions in cancer cell metastasis. Acta histochemica, 112, pp. 3-25.

Carrero G, McDonald D, Crawford E, de Vries G, Hendzel MJ. 2003. Using FRAP and mathematical modeling to determine the in vivo kinetics of nuclear proteins. Methods, 29, pp. 14–28.
Cavey M, Rauzi M, Lenne PF, Lecuit T. 2008. A two-tiered mechanism for stabilization and immobilization of E-cadherin. Nature, 453(7196):751-6.

Chen, Y.T., Stewart, D.B., and Nelson, W.J., 1999. Coupling assembly of the E-cadherin/beta-catenin complex to efficient endoplasmic reticulum exit and basal–lateral membrane targeting of E-cadherin in polarized MDCK cells. J. Cell Biol., 144, pp. 687-699.

Chitaev, N.A., and Troyanovsky, S.M., 1998. Adhesive but not lateral E-cadherin complexes require calcium and catenins for their formation. J. Cell Biol., 142, pp. 837–846.

Choi, H.J., Huber, A.H., and Weis., W.I., 2006. Thermodynamics of beta–catenin–ligand interactions: the roles of the N- and C-terminal tails in modulating binding affinity. J. Biol. Chem. 281, pp. 1027–1038.

Christofori, G., and Semb, H., 1999. The role of cell adhesion molecule E-cadherin as a tumour suppressor gene. Trends Biochem Sci., 24, pp. 73–6.

Conacci-Sorrell, M., Zhurinsky, J. and Ben-Ze'ev, A. 2002. The cadherin–catenin adhesion system in signaling and cancer. J. Clin. Invest. 109, pp. 987–991.

Condeelis, J., and Segall, J.E., 2003. Intravital imaging of cell movements in tumours. Nat Rev Cancer, pp. 921–30.

Criscouli, M.L., Nguyen, M., et al., 2005. Tumor metastasis but not tumor growth dependent on Src-mediated vascular permeability. Blood, 105(4), pp. 1508-14.

Daugherty, R., Gottardi, C., 2007. Phospho-regulation of β-Catenin Adhesion and Signaling Functions. Physiology (Bethesda). 2007 Oct;22:303-9

Davis, M.A., Ireton, R.C., and Reynolds, A.B., 2003. A core function for p120-catenin in cadherin turnover. J. Cell Biol., 163, pp. 525–534.

De Beco, S., Gueudry, C., Amblard, F., and Coscoy, S., 2009. Endocytosis is required for E-cadherin redistribution at mature adherens junctions. Proc Natl Acad Sci U.S.A., 106, pp. 7010–7015.

De Beco S, Amblard F, Coscoy S, 2012. New Insights into the Regulation of E-cadherin Distribution by Endocytosis. Jeon, K., (ed) International Review of Cell and Molecular Biology, Vol. 295, Burlington: Academic Press, pp. 63-108.

de Rooij J., Kerstens A., Danuser G., Schwartz M., Waterman-Storer C. 2005. Integrin-dependent actomyosin contraction regulates epithelial cell scattering. J. Cell Biol.;171:153–164.

Desai R, Sarpal, R., Ishiyama, N., Pellikka,M., Ikura, M., Ulrich Tepass, U., 2013. Monomeric alpha-catenin links cadherin to the actin cytoskeleton. Nat Cell Biol 15(3):261-273.

Dow, E., Humbert, O,. 2007. Polarity regulators and the control of epithelial architecture, cell migration and tumorigenesis. Int Rev Cytol 262: 253-302.

Drees, F., Pokutta, S., Yamada, S., Nelson, W.J., and Weis, W.I., 2005. Alpha-catenin is a molecular switch that binds Ecadherin- beta-catenin and regulates actin-filament assembly. Cell, 123, pp. 903–915.

Edidin, M., 1994. Fluorescence photobleaching and recovery, FPR, in the analysis of membrane structure and dynamics. In Mobility and Proximity in Biological Membranes, pp. 109–135, CRC Press

The experimental study of tumour progression. Volumes I-III academic press. London (1954)

Frixen UH1, Behrens J, Sachs M, Eberle G, Voss B, Warda A, Löchner D, Birchmeier W. 1991. E-cadherin mediated cell-cell adhesion prevents invasiveness of human carcinoma cells. J. Cell Biol., 113, pp. 173–85.

Fujita, Y., Krause, G., Scheffner, M., Zechner, D., Leddy, H.E.M., Behrens, J., Sommer, T., and Birchmeier, W., 2002. Hakai, a c-Cbl-like protein, ubiquitinates and induces endocytosis of the E-cadherin complex. Nat. Cell Biol., 4, pp. 222–231.

Fukata, M., Kuroda, S., Nakagawa, M., Kawajiri, A., Itoh, N., Shoji, I., Matsuura, Y., Yonehara, S., Fujisawa, H., Kikuchi, A., Kaibuchi, K., 1999. Cdc42 and Rac1 regulate the interaction of IQGAP1 with beta-catenin. J. Biol. Chem. 274, pp. 26044–26050.

Gaida M, Steffen T, Günther F, Tschaharganeh D, Felix K, Bergmann F, Schirmacher P, Hänsch GM. 2012. Polymorphonuclear neutrophils promote dyshesion of tumor cells and elastase-mediated degradation of E-cadherin in pancreatic tumors. Eur J Immunol 42(12):3369-3380.

Gillies RJ, Gatenby RA. 2007. Hypoxia and adaptive landscapes in the evolution of carcinogenesis. Cancer Metastasis Rev 26: 311–317.

Gooding JM, Yap KL, Ikura M. 2004. The cadherin-catenin complex as a focal point of cell adhesion and signalling: new insights from three-dimensional structures. Bioessays;26(5):497-511.

Gumbiner, B.M., 2000. Regulation of cadherin adhesive activity. J. Cell Biol., 148, pp. 399–404.

Hakkinen, K.M., Harunaga, J.S., Doyle, A.D., Yamada, K.M., 2011. Direct comparisons of the morphology, migration, cell adhesions, and actin cytoskeleton of fibroblasts in four different three-dimensional extracellular matrices. Tissue Eng. A 17 (5–6), 713–724

Hanahan, D. and Weinberg, R.A., 2000. The hallmarks of cancer. Cell, 2000, 100(1), pp. 57-70.

Hanahan, D., and Weinberg, R.A., 2011. Hallmarks of cancer: the next generation. Cell, 144(5), pp 646-74.

T. Harris (ed.) 2012. Adherens Junctions: From Molecular Mechanisms to Tissue Development and Disease. Subcellular Biochemistry 60.

Harrison, O.J., Corps, E.M., Kilshaw, P.J. 2005. Cadherin adhesion depends on a salt bridge at the N-terminus. J. Cell Sci. 118, pp. 4123–4130.

Harrison, O.J., Bahna, F., Katsamba, P.S., Jin, X., Brasch, J., Vendome, J., Ahlsen, G., Carroll, K.J., Price, S.R., Honig, B., and Shapiro, L. 2010. Two-step adhesive binding by classical cadherins. Nat. Struct. Mol. Biol., 17, pp. 348–357.

Harrison, O.J., Jin, X., Hong, S., Bahna, F., Ahlsen, G., Brasch, J., Wu, Y., Vendome, J., Felsovalyi, K., Hampton, C.M., Troyanovsky, R.B., Ben-Shaul, A., Frank, J., Troyanovsky, S.M., Shapiro, L., and Honig, B., 2011. The extracellular architecture of adherens junctions revealed by crystal structures of type I cadherins. Structure, 19, pp. 244–256.

Hartsock A., Nelson J. 2008. Adherens and tight junctions: Structure, function and connections to the actin cytoskeleton. Biochimica et Biophysica Acta 1778, 660–69

Häussinger, D., Ahrens, T., Aberle, T., Engel, J., Stetefeld, J., and Grzesiek, S.. 2004. Proteolytic E-cadherin activation followed by solution NMR and X-ray crystallography. EMBO J., 23, pp. 1699–1708.

Hezel AF, Kimmelman AC, Stanger BZ, Bardeesy N, Depinho RA. 2006. Genetics and biology of pancreatic ductal adenocarcinoma. Genes Dev. 20(10):1218-49

Helwani, F.M., Kovacs, E.M., Paterson, A.D., Verma, S., Ali, R.G., Fanning, A.S., Weed, S.A., and Yap, A.S.. 2004. Cortactin is necessary for E-cadherinmediated contact formation and actin reorganization. J. Cell Biol. 164, pp. 899–910.

Hidalgo, C., Hooper, S., Chaudhry, S., Williamson, P., Harrington, K., Leitinger, B., Sahai E.. 2010. Collective cell migration requires suppression of actomyosin at cell-cell contacts mediated by DDR1 and the cell polarity regulators Par3 and Par6. Nat. Cell Biol. 2011;13:49–58

Hingorani SR, Petricoin EF, Maitra A, Rajapakse V, King C, Jacobetz MA, Ross S, Conrads TP, Veenstra TD, Hitt BA, Kawaguchi Y, Johann D, Liotta LA, Crawford HC, Putt ME, Jacks T, Wright CV, Hruban RH, Lowy AM, Tuveson DA. 2003. Preinvasive and invasive ductal pancreatic cancer and its early detection in the mouse. Cancer Cell, 4, pp. 437–450.

Hingorani, S., Wang L, Multani AS, Combs C, Deramaudt TB, Hruban RH, Rustgi AK, Chang S, Tuveson DA., . 2005. Trp53R172H and KrasG12D cooperate to promote chromosomal instability and widely metastatic pancreatic ductal adenocarcinoma in mice. Cancer Cell 7:469–483.

Hollestelle A, Peeters JK, Smid M, Timmermans M, Verhoog LC, Westenend PJ, Heine AA, Chan A, Sieuwerts AM, Wiemer EA, Klijn JG, van der Spek PJ, Foekens JA, Schutte M, den Bakker MA, Martens JW. 2013. Loss of E-cadherin is not a necessity for epithelial to mesenchymal transition in human breast cancer. Breast Cancer Res Treat. 2013 Feb;138(1):47-57.

Hong, S., Troyanovsky, R.B., and Troyanovsky, S.M. 2011. Cadherin exits the junction by switching its adhesive bond. J. Cell Biol., 192, pp. 1073–1083.

Hong, S., Troyanovsky, R.B., and Troyanovsky, S.M., 2010. Spontaneous assembly and active disassembly balance adherens junction homeostasis. Proc Natl Acad Sci USA, 107, pp. 3528–3533.

Hong S, Troyanovsky RB, Troyanovsky SM . 2013. Binding to F-actin guides cadherin cluster assembly, stability, and movement. J Cell Biol 201: 131-143

Hoschuetzky, H., Aberle, H., and Kemler, R., 1994. Beta-catenin mediates the interaction of the cadherin–catenin complex with epidermal growth factor receptor. J. Cell Biol., 127, pp. 1375–1380.

Hruban, R.H., Goggins, M., Parsons, J., and Kern, S.E., 2000. Progression model for pancreatic cancer. Clin. Cancer Res., 6, pp. 2969–2972.

Huber, A.H., Nelson, W.J., and Weis, W.I., 1997. Three-dimensional structure of the armadillo repeat region of beta-catenin. Cell, 90, pp. 871–882.

Huber, A.H., and Weis, W.I., 2001, The structure of the beta-catenin/E-cadherin complex and the molecular basis of diverse ligand recognition by beta catenin, Cell, 105, pp. 391–402.

Huber MA, Kraut N, Beug H. 2005. Molecular requirements for epithelial-mesenchymal transition during tumor progression. Curr Opin Cell Biol, 17:548–58.

Humbert, P., Russell, S. & Richardson, H. Dlg, 2003. Scribble and Lgl in cell polarity, cell proliferation and cancer. BioEssays 25, 542–553

Huveneers S, de Rooij J. 2013. Mechanosensitive systems at the cadherin-F-actin interface. J Cell Sci.;126:403–13.

Ito, S., Nakanishi, .H, Ikehara, Y., Kato, T., Kasai, Y., Ito, K., Akiyama, S., Nakao, A., and Tatematsu, M., 2001. Realtime observation of micrometastasis formation in the living mouse liver using a green fluorescent protein gene-tagged rat tongue carcinoma. cell line, Int. J. Cancer, 93, pp. 212–217.

Jayo, A., Parsons, M., 2012. Imaging of cell adhesion events in 3D matrix environments. European Journal of Cell Biology 91 824– 833

Jemal A,. Bray, F,. Center, M,. Ferlay, J,. Ward, E,. Forman, D,. 2011. Global cancer statistics. CA, 61, 69–90.

Kametani,Y., and Takeichi, M., 2007. Basal-to-apical cadherin flow at cell junctions. Nat. Cell Biol., 9, pp. 92–98.

Kao, H.P., Abney, J.R. and Verkman, A.S., 1993. Determinants of the translational mobility of a small solute in cell cytoplasm. J. Cell Biol., 120, pp. 175–184.

Kim, S.A., Tai, C.Y., Mok, L.P., Mosser, E.A., and Schuman, E.M. 2011. Calcium-dependent dynamics of cadherin interactions at cell-cell junctions. Proc. Natl. Acad. Sci. USA, 108, pp. 9857–9862.

Kimura H., Hieda M., Cook PR. 2004. Measuring histone and polymerase dynamics in living cells. Methods Enzymol, 375, pp. 381–393.

Kitagawa, M., Natori, M., Murase, S., Hirano, S., Taketani, S., and Suzuki, S.T., 2000. Mutation analysis of cadherin-4 reveals amino acid residues of EC1 important for the structure and function. Biochem Biophys Res. Commun., 271, pp. 358–363.

Kizhatil, K., Davis, J.Q., Davis, L., Hoffman, J., Hogan, B.L., Bennett, V., 2007. Ankyrin-G is a molecular partner of E-cadherin in epithelial cells and early embryos. J. Biol. Chem., 282:26552-61

Klaus, A., Birchmeier, W.. 2008. Wnt signalling and its impact on development and cancer. Nat. Rev. Cancer 8, 387–398.

Klingelhöfer, J., Laur, O.Y., Troyanovsky, R.B., and Troyanovsky, S.M., 2002. Dynamic interplay between adhesive and lateral E-cadherin dimers. Mol. Cell Biol., 22, pp. 7449–7458.

Klonis N., Rug M., Harper I., Wickham M., Cowman A., Tilley L. 2002. Fluorescence photobleaching analysis for the study of cellular dynamics. Eur. Biophys. J., 31, pp. 36–51.

Kobielak, A., Pasolli, H.A. and Fuchs, E., 2004. Mammalian formin-1 participates in adherens junctions and polymerization of linear actin cables. Nat. Cell Biol., 6, pp. 21 –30.

Kusumi A, Sako Y, Yamamoto M. 1993. confined lateral diffusion of membrane receptors as studied by single particle tracking (nanovid microscopy). Effects of calcium-induced differentiation in cultured epithelial cells. Biophys J. Nov;65(5):2021-40

Kusumi, A. and Sako, Y. 1996. Cell surface organization by the membrane skeleton. Curr Opin Cell Biol, 8, 566-74.

Kusumi, A., Suzuki, K., and Koyasako, K., 1999. Mobility and cytoskeletal interactions of cell adhesion receptors. Curr Opin Cell Biol., 11, pp. 582–590.

Kusumi A, Nakada C, Ritchie K, Murase K, Suzuki K, Murakoshi H, Kasai RS, Kondo J, Fujiwara T. . 2005. Paradigm shift of the plasma membrane concept from the two-dimensional continuum fluid to the partitioned fluid: high-speed single-molecule tracking of membrane molecules. Annu Rev Biophys Biomol Struct 34:351-378.

Kwiatkowski, A.V., S.L. Maiden, S. Pokutta, H.J. Choi, J.M. Benjamin, A.M. Lynch, W.J. Nelson, W.I. Weis, J. Hardin. 2010. In vitro and in vivo reconstitution of the cadherin-catenin-actin complex from Caenorhabditis elegans. Proc. Natl. Acad. Sci. USA. 107:14591–14596.

Lang, GA., Iwakuma, T., Suh, YA., Liu, G., Rao, VA., Parant, JM. 2004. Gain of function of a p53 hot spot mutation in a mouse model of Li- Fraumeni syndrome. Cell. 119: 861 – 72.

Laur, O.Y., Klingelhöfer, J., Troyanovsky, R.B., and Troyanovsky, S.M., 2002. Both the dimerization and immunochemical properties of E-cadherin EC1 domain depend on Trp(156) residue. Arch. Biochem. Biophys., 400, pp. 141–147.

Li, L, Hartley, R., Reiss, B., Sun, Y., Pu J., Wu, D., Lin, F., Hoang, T., Yamada, S., Jiang, J., Zhao, M., 2012. E-cadherin plays an essential role in collective directional migration of large epithelial sheets. Cell Mol Life Sci. Aug 2012; 69(16): 2779–2789.

Lickert, H., Bauer, A., Kemler, R., and Stappert, J., 2000. Casein kinase II phosphorylation of E-cadherin increases E-cadherin/beta-catenin interaction and strengthens cell–cell adhesion. J. Biol. Chem., 275, pp. 5090–5095.

Lilien, J., Balsamo, J., Arregui, C., and Xu, G., 2002. Turn-off, drop-out: functional state switching of cadherins. Dev. Dyn., 224, pp.18–29.

Iino R, Koyama I, & Kusumi A . 2001. Single molecule imaging of green fluorescent proteins in living cells: E-cadherin forms oligomers on the free cell surface. Biophys J 80(6):2667-2677

Liotta, L.A., and Kohn, E.C., 2001. The microenvironment of the tumor- host interface. Nature, 411, pp. 375–9.

Lippincott-Schwartz, J., Altan-Bonnet, N. and Patterson, G.H., 2003. Photobleaching and photoactivation: following protein dynamics in living cells. Nat. Cell Biol. Suppl., S7–S14.

Lippincott-Schwartz, J., Snapp, E., and Kenworthy, A., 2001. Studying protein dynamics in living cells. Nature Rev. Mol. Cell Biol., 2, pp. 444–456.

Martin, T.A., Goyal, A., Watkins, G., and Jiang, W.G., 2005. Expression of the transcription factors snail, slug, and twist and their clinical significance in human breast cancer. Ann. Surg. Oncol., 12, pp. 488–496.

McCrea, P.D., and Gumbiner, B.M., 1991. Purification of a 92-kDa cytoplasmic protein tightly associated with the cell–cell adhesion molecule E-cadherin (uvomorulin). Characterization and extractability of the protein complex from the cell cytostructure. J. Biol. Chem., 266, 4514–4520.

McCrea, P.D., Turck, C.W., and Gumbiner, B., 1991. A homolog of the armadillo protein in Drosophila (plakoglobin) associated with E-cadherin. Science, 254, pp. 1359–1361.

McNeill, H., Ryan, T.A., Smith, S.J., and Nelson, W.J., 1993. Spatial and temporal dissection of immediate and early events following cadherin-mediated epithelial cell adhesion. J. Cell Biol., 120, pp. 1217-1226.

Meng, W., and Takeichi, M., 2009. Adherens junction: molecular architecture and regulation. Cold Spring Harb Perspect Biol 1:a002899

Morton JP, Timpson P, Karim SA, Ridgway RA, Athineos D, Doyle B, Jamieson NB, Oien KA, Lowy AM, Brunton VG, Frame MC, Evans TR, Sansom OJ. 2010. Mutant p53 drives metastasis and overcomes growth arrest/senescence in pancreatic cancer. Proceedings of the National Academy of Sciences of the United States of America.;107(1):246–251.

Morton JP, Karim SA, Graham K, Timpson P, Jamieson N, Athineos D, Doyle B, McKay C, Heung MY, Oien KA, Frame MC, Evans TR, Sansom OJ, Brunton VG. 2010-2. Dasatinib Inhibits the Development of Metastases in a Mouse Model of Pancreatic Ductal Adenocarcinoma. Gastroenterology.139(1):292-303

Muller PA, Vousden KH, Norman JC. 2011. P53 and its mutants in tumor cell migration and invasion. J Cell Biol. 192: 209 – 18.

Nagafuchi, A., Shirayoshi, Y., Okazaki, K., Yasuda, K., and Takeichi, M., 1987. Transformation of cell adhesion properties by exogenously introduced E-cadherin cDNA. Nature, 329, pp. 341-343.

Nagar, B., Overduin, M., Ikura, M., and Rini, J.M., 1996. Structural basis of calcium-induced E-cadherin rigidification and dimerization. Nature, 380, pp. 360–364.

Nanes BA, Chiasson-MacKenzie C, Lowery AM, Ishiyama N, Faundez V, Ikura M, Vincent PA, Kowalczyk AP. 2012. p120-catenin binding masks an endocytic signal conserved in classical cadherins. J Cell Biol 199(2): 365-80.

Naumov, G.N., Wilson, S.M., MacDonald, I.C., Schmidt, E.E., Morris, V.L., Groom, A.C., Hoffman, R.M. and Chambers, A.F., 1999. Cellular expression of green fluorescent protein, coupled with high-resolution in vivo videomicroscopy, to monitor steps in tumor metastasis. J. Cell Sci., 112, pp. 1835–1842.

Nelson, W.J., and Nusse, R., 2004. Convergence of Wnt, beta-catenin, and cadherin pathways. Science, 303, 1483–1487.

Niessen C., 2007. Tight Junctions/Adherens Junctions: Basic Structure and Function. Journal of Investigative Dermatology, 127, 2525–32

Nobis M., Carragher NO., McGhee EJ., Morton JP., Sansom OJ., Anderson KI., Timpson P. 2013. Advanced intravital subcellular imaging reveals vital three-dimensional signalling events driving cancer cell behaviour and drug responses in live tissue. FEBS Journal 280 5177–97

Nose, A., Tsuji, K., and Takeichi, M., 1990. Localization of specificity determining sites in cadherin cell adhesion molecules. Cell, 61, pp. 147–155.

Nowell, PC. 1976. The clonal evolution of tumor cell populations. Science. 194(4260):23-8.

Orford, K., Crockett, C., Jensen, J.P., Weissman, A.M., and Byers, S.W., 1997. Serine phosphorylation-regulated ubiquitination and degradation of beta-catenin. J. Biol. Chem., 272, pp. 24735–24738.

Olive K., Tuveson, D., 2006. The Use of Targeted Mouse Models for Preclinical Testing of Novel Cancer Therapeutics. Clin Cancer Res September 15, 12; 5277

Olive K., Tuveson D., Ruhe Z., Yin B., Willis N., Bronson R. 2004. Mutant p53 gain of function in two mouse models of Li-Fraumeni syndrome. Cell. 119: 847 – 60.

Ozaki C, Obata S, Yamanaka H, Tominaga S, & Suzuki ST . 2010. The extracellular domains of E- and N-cadherin determine the scattered punctate localization in epithelial cells and the cytoplasmic domains modulate the localization. J Biochem 147(3):415-425.

Pappas, D.J., D.L. Rimm. 2006. Direct interaction of the C-terminal domain of alpha-catenin and F-actin is necessary for stabilized cell-cell adhesion. Cell Commun. Adhes. 13:151–170.

Patel, S.D., Ciatto, C., Chen, C.P., Bahna, F., Rajebhosale, M., Arkus, N., Schieren, I., Jessell, T.M., Honig, B., Price, S.R., and Shapiro, L., 2006. Type II cadherin ectodomain structures: implications for classical cadherin specificity. Cell, 124, pp. 1255–1268.

Pathak A, Kumar S. 2013. Transforming potential and matrix stiffness co-regulate confinement sensitivity of tumor cell migration. Integr Biol (Camb). 5(8):1067-75.

Phair, R.D. and Misteli, T., 2001. Kinetic modeling approaches to in vivo imaging. Nature Rev. Mol. Cell Biol., 2, 898–907.

Phair RD., Scaffidi P., Elbi C., Vecerová J., Dey A., Ozato K., Brown DT., Hager G., Bustin M., Misteli T. 2004. Global nature of dynamic protein–chromatin interactions in vivo: three-dimensional genome scanning and dynamic interaction networks of chromatin proteins, Mol. Cell. Biol., 24, pp. 6393–6402.

Piedra, J., Miravet, S., Castano, J., Palmer, H.G., Heisterkamp, N., Garcia de Herreros, A., and

Dunach, M., 2003. p120 Catenin-associated Fer and Fyn tyrosine kinases regulate beta-catenin Tyr-142 phosphorylation and beta-catenin–alpha-catenin Interaction. Mol. Cell. Biol., 23, pp. 2287–2297.

Pokutta, S., and Weis, W.I.. 2000. Structure of the dimerization and beta-cateninbinding region of alpha-catenin. Mol. Cell., 5, pp. 533–543.

Pokutta, S., Herrenknecht, K., Kemler, R., and Engel, J., 1994. Conformational changes of the recombinant extracellular domain of E-cadherin upon calcium binding. Eur. J. Biochem., 223, pp. 1019-1026.

Polyak, K., and Weinberg, R.A., 2009. Transitions between epithelial and mesenchymal states: acquisition of malignant and stem cell traits. Nat. Rev. Cancer, 9, pp. 265–273.

Poo, M. and Cone, R.A., 1974. Lateral diffusion of rhodopsin in the photoreceptor membrane. Nature, 247, pp.438–441.

Price, S.R., De Marco Garcia, N.V., Ranscht, B., and Jessell, T.M., 2002. Regulation of motor neuron pool sorting by differential expression of type II cadherins. Cell, 109, pp. 205–216.

Radisky, D. 2005. Epithelial-mesenchymal transition. Journal of Cell Science 118, 4325-4326

Rakshit, S., Zhang, Y.X., Manibog, K., Shafraz, O., Sivasankar., S.. 2012. Ideal, catch and slip bonds in cadherin adhesion, Proc. Natl. Acad. Sci. USA, 109, 18815-18820
Reits, E.A. and Neefjes, J.J., 2001. From fixed to FRAP: measuring protein mobility and activity in living cells. Nat. Cell Biol., 3, pp. 145–147.

Reynolds, A.B., Herbert, L., Cleveland, J.L., Berg, S.T., and Gaut, J.R., 1992. p120, a novel substrate of protein tyrosine kinase receptors and of p60v-src, is related to cadherin-binding factors-catenin, plakoglobin and armadillo. Oncogene., 7, pp. 2439–2445.

Rhee, J., Mahfooz, N.S., Arregui, C., Lilien, J., Balsamo, J., and
Van Berkum, M.F.. 2002. Activation of the repulsive receptor Roundabout inhibits N-cadherin-mediated cell adhesion. Nat. Cell Biol., 4, pp. 798–805.

Rimm D.L., Koslov E.R., Kebriaei P., Cianci, C.D., and Morrow, J.S., 1995. Alpha1(E)-catenin is an actin-binding and bundling protein mediating the attachment of F-actin to the membrane adhesion complex. Proc. Natl. Acad. Sci. USA, 92, pp. 8813–8817.

Rorth P. 2009. Collective Cell Migration. Annual Review of Cell and Developmental Biology 25: 407–429.

Roura, S., Miravet, S., Piedra, J., Garcia de Herreros, A., and Dunach, M., 1999. Regulation of E-cadherin/Catenin association by tyrosine phosphorylation. J. Biol. Chem., 274, pp. 36734–36740.

Royer C, Lu X. 2011. Epithelial cell polarity: a major gatekeeper against cancer? Cell Death Differ.;18:1470–1477.

Sahai, E., 2007.Illuminating the metastatic process. Nat.Rev. Cancer, 7, pp. 737–49.

Sako, Y., Nagafuchi, A., Tsukita, S., Takeichi, M., Kusumi, A. 1998. Cytoplasmic regulation of the movement of E-cadherin on the free cell surface as studied by optical tweezers and single particle tracking: corralling and tethering by the membrane skeleton. J Cell Biol. 140; 5, p1227-40

Saxton, M.J., 1999. Lateral diffusion of lipids and proteins. Curr. Top. Membr., 48, pp. 229–282.

Scarpa A, Capelli P, Mukai K, Zamboni G, Oda T, Iacono C, Hirohashi S. 1993. Pancreatic adenocarcinomas frequently show p53 gene mutations. Am J Pathol.;142:1534–1543.

Serrels A, Timpson P, Canel M, Schwarz JP, Carragher NO, Frame MC, Brunton VG, Anderson K. 2009. Real-time study of E-cadherin and membrane dynamics in living animals: implications for

disease modeling and drug development. Cancer Res 69(7):2714-2719.

Shapiro, L., Fannon, A.M., Kwong, PD., Thompson, A., Lehmann, M.S., Grübel, G., Legrand, J.F., Als Nielsen, J., Colman, D.R., and Hendrickson, W.A., 1995. Structural basis of cell-cell adhesion by cadherins. Nature, 374, 327–337.

Smith HA, Kang Y. 2013. The metastasis-promoting roles of tumor-associated immune cells. Journal of Molecular Medicine.;91(4):411–429

Sprague, B., Pego, R., Stavreva, D., and McNally, J., 2004. Analysis of binding reaction by fluorescence recovery after photobleaching. Biophysical J., 86, pp. 3473-3495.

Sprague, BL., McNally, JG., 2005. FRAP analysis of binding: proper and fitting. Trends Cell Biol 15(2):84-91.

Stehbens, S.J., Paterson, A.D., Crampton, M.S., Shewan, A.M., Ferguson, C., Akhmanova, A., Parton, R.G., and Yap, A.S., 2006. Dynamic microtubules regulate the local concentration of E-cadherin at cell-cell contacts. J. Cell Sci., 119, pp. 1801–1811.

Steinberg, M. S. and M. Takeichi . 1994. Experimental specification of cell sorting, tissue spreading, and specific spatial patterning by quantitative differences in cadherin expression. Proc Natl Acad Sci U S A 91(1): 206-9

Takahashi K, Nakanishi H, Miyahara M, Mandai K, Satoh K, Satoh A, Nishioka H, Aoki J, Nomoto A, Mizoguchi A, Takai Y , 1999. Nectin/PRR: an immunoglobulin-like cell adhesion molecule recruited to cadherin-based adherens junctions through interaction with Afadin, a PDZ domain-containing protein. J Cell Biol 145:539–549

Takai Y, Ikeda W, Ogita H, Rikitake Y. 2008. The immunoglobulin-like cell adhesion molecule nectin and its associated protein afadin. Annu Rev Cell Dev Biol 24:309–342

Takeichi M., 1990. Cadherins: A Molecular Family Important in Selective Cell-Cell Adhesion. Annu Rev of Biochem, 59: 237-52

Takeichi, M., 1995. Morphogenetic roles of classic cadherins. Curr. Opin. Cell Biol., 7, pp. 619–627.

Tao, Y.S., Edwards, R.A., Tubb, B., Wang, S., Bryan, J., and McCrea, P.D., 1996. Beta-Catenin associates with the actin-bundling protein fascin in a noncadherin complex. J. Cell Biol., 134, pp.1271-1281.

Thiery JP. 2002. Epithelial-mesenchymal transitions in tumour progression. Nat Rev Cancer. 2(6):442-54.

Thoreson, M.A., Anastasiadis, P.Z., Daniel, J.M., Ireton, R.C., Wheelock, M.J., Johnson, K.R., Hummingbird, D.K. and Reynolds. A.B., 2000. Selective uncoupling of p120(ctn) from E-cadherin disrupts strong adhesion. J. Cell Biol., 148, pp. 189–202.

Thoumine, O., Lambert, M., Mège, R.M., and Choquet, D., 2006. Regulation of N-cadherin dynamics at neuronal contacts by ligand binding and cytoskeletal coupling. Mol. Biol. Cell, 17, pp. 862–875.

Timpson, P., McGhee, E.J., and Anderson, K.I., 2011. Imaging molecular dynamics in vivo - from cell biology to animal models. J. Cell Sci., 124, pp. 2877–2890.

Timpson P, Mcghee E, Erami Z, Nobis M, Quinn J, Edward M, Anderson K. 2011. Organotypic Collagen I Assay: A Malleable Platform to Assess Cell Behaviour in a 3-Dimensional Context. J. Vis. Exp. (56), e3089

Tomschy, A., Fauser, C., Landwehr, R., and Engel, J., 1996. Homophilic adhesion of E-cadherin occurs by a co-operative two-step interaction of N-terminal domains. EMBO J., 15, pp. 3507-3514.
Troyanovsky, R.B., Sokolov, E., and Troyanovsky, S.M., 2003. Adhesive and lateral E-cadherin

dimers are mediated by the same interface. Mol. Cell Biol., 23, pp. 7965–7972.

Troyanovsky, S., 2005. Cadherin dimers in cell-cell adhesion. Eur. J. Cell Biol., 84, 225-233.

Troyanovsky, R.B., Sokolov, E.P., and Troyanovsky, S.M., 2006. Endocytosis of cadherin from intracellular junctions is the driving force for cadherin adhesive dimer disassembly. Mol. Biol. Cell 17, 3484–3493.

Vaezi, A., Bauer, C., Vasioukhin, V., and Fuchs, E., 2002. Actin cable dynamics and Rho/Rock orchestrate a polarized cytoskeletal architecture in the early steps of assembling a stratified epithelium. Dev. Cell, 3, pp. 367–381.

Vasioukhin, V., Bauer, C., Yin, M., Fuchs, E., 2000. Directed actin polymerization is the driving force for epithelial cell-cell adhesion. Cell 100, 209–219.

Vasioukhin, V., and Fuchs, E., 2001. Actin dynamics and cell-cell adhesion in epithelia. Curr. Opin. Cell Biol., 13, pp. 76–84.

Vendome, J., Posy, S., Jin, X., Bahna, F., Ahlsen, G., Shapiro, L., and Honig, B., 2011. Molecular design principles underlying β-strand swapping in the adhesive dimerization of cadherins. Nat. Struct. Mol. Biol., 18, pp. 693-700.

Verkman, A.S., 2002. Solute and macromolecule diffusion in cellular aqueous compartments. Trends Biochem. Sci., 27, pp. 27–33.

Vunnam, N., Flint, J., Balbo, A., Schuck, P., and Pedigo, S., 2011. Dimeric states of neural- and epithelialcadherins are distinguished by the rate of disassembly. Biochemistry, 50, pp. 2951–2961.

Warshaw, A.L., and Fernández-del Castillo, C., 1992. Pancreatic carcinoma. N. Engl. J. Med., 326, pp. 455–465.

Weinberg, R.A., 2007. The Nature of Cancer, in The Biology of Cancer. Garland Science, p. 24.

Weiss, M., and Nilsson, T., 2004. In a mirror dimly: tracing the movements of molecules in living cells. Trends Cell Biol., 14, pp. 267–272.

Weisz L., Oren M., Rotter V. 2007. Transcription regulation by mutant p53. Oncogene 26:2202–2211.

Wodartz A. and Näthke I. 2007. Cell polarity in development and cancer. Nat Cell Biol 9: 1016-1024

Wu, Y., Jin, X., Harrison, O., Shapiro, L., Honig, B.H., Ben-Shaul, A., 2010. Cooperativity between trans and cis interactions in cadherin-mediated junction formation. Proc. Natl. Acad. Sci. USA, 107, pp. 17592–17597.

Yamada, S., Pokutta, S., Drees, F., Weis, WI., and Nelson, WJ., 2005. Deconstructing the cadherin-cateninactin complex. Cell, pp. 123, pp. 889–901.

Yap, A.S., Niessen, C.M., and Gumbiner, B.M., 1998-1. The juxtamembrane region of the cadherin cytoplasmic tail supports lateral clustering, adhesive strengthening, and interaction with p120 ctn. J. Cell Biol. 141, p.p. 779–789.

Yap, A.S., 1998-2. The morphogenetic role of cadherin cell adhesion molecules in human cancer: a thematic review. Cancer Invest., 16, pp. 252–261.

Yu X., Vazquez A., Levine A., Carpizo D.. 2012. Allele-specific p53 mutant reactivation. Cancer Cell. 21: 614 – 25.

Zhang, Y., Sivasankar, S., Nelson, W.J., and Chu, S., 2009. Resolving cadherin interactions and binding cooperativity at the single-molecule level. Proc. Natl. Acad. Sci. USA, 106, pp. 109-114.